460

SMALL CRAFT HARBOUR BRANCH
DEPARTMENT OF FISHERIES AND OCEANS

A STUDY OF THE STABILITY OF BERM BREAKWATERS

HYDRAULIC MODEL TEST RESULTS

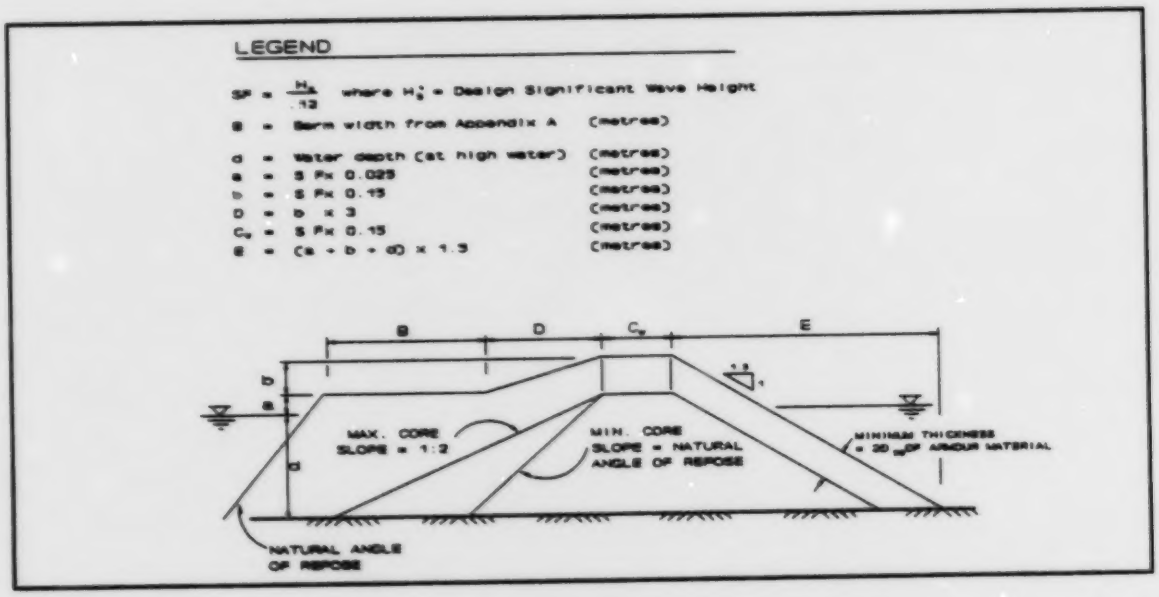
LEGEND
SF = $\frac{H_s}{.12}$ where H_s = Design Significant Wave Height
B = Berm width from Appendix A (metres)
d = Water depth (at high water) (metres)
a = B Fx 0.025 (metres)
b = B Fx 0.15 (metres)
D = b x 3 (metres)
C_w = B Fx 0.15 (metres)
E = Ca + b + d0 x 1.5 (metres)
B
D
C_w
E
b
a
d
1:2
MAX. CORE SLOPE = 1:2
MIN. CORE SLOPE = NATURAL ANGLE OF REPOSE
MINIMUM THICKNESS = 2D n OF ARMOUR MATERIAL
NATURAL ANGLE OF REPOSE

OCTOBER, 1991

A STUDY OF THE STABILITY OF BERM BREAKWATERS

REPORT # 1 - HYDRAULIC MODEL TEST RESULTS

SMALL CRAFT HARBOURS BRANCH
DEPARTMENT OF FISHERIES AND OCEANS

October, 1991

QUEEN'S UNIVERSITY COASTAL ENGINEERING LABORATORY

92-05954/

TABLE OF CONTENTS

1.0	Introduction	1
	1.1 Introduction	1
	1.2 Background	1
	1.3 Study Purpose	4
2.0	Review of Concept	6
3.0	Study Background	14
	3.1 Dimensional Analysis	14
	3.2 Two Dimensional Testing Programme	16
	3.2.1 Introduction	16
	3.2.2 Materials	16
	3.2.3 Experimental Equipment and Instrumentation	19
	3.2.3.1 Wave Flume	19
	3.2.3.2 Water Level Transducers	19
	3.2.3.3 Data Aquisition	19
	3.2.3.4 Profiler	19
	3.2.4 Test Methodology	20
	3.3 Test Programme	23
	3.4 Two Dimensional Test Results	28
	3.4.1 General Observations During Testing	28
	3.4.2 Reduction and Analysis of Data	28
	3.4.2.1 Effect of Wave Height	29
	3.4.2.2 Effect of Uniformity of Stones	29
	3.4.2.3 Influence of Rounded Stones	30
	3.4.2.4 Effect of Wave Groupiness	31
	3.4.3.5 Effect of Wave Steepness	34
	3.4.2.6 Effect of Spectral Peak Period	35
	3.4.2.7 Effect of Average Wave Period	36
	3.4.2.8 Effect of Storm Duration	37
	3.5 Conclusions	

4.0 Three Dimensional Testing Programme 38

4.1 Testing Programme 38
4.1.1 Facilities 38
4.1.2 Materials 38
4.1.3 Wave Climate 38
4.1.4 Test Programme 41

4.2 Test Results 45
4.2.1 Series 1 45

5.0 Data Analysis 47

5.1 Two Dimensional Tests 47
5.1.1 Regression Analysis 47
5.1.1.1 Length of Toe Erosion 47
5.1.1.2 Volume of Stones 52
5.1.1.3 Berm 53
5.1.2 Sensitivity of Model 54
5.1.3 Comparison with Model Results 55
5.1.4 Comparison with Prototype Results 55

6.0 Conclusions 57

6.1 Two Dimensional Tests 57
6.2 Three Dimensional Tests 59

7.0 References

1.1 INTRODUCTION

This report describes the results of a research programme undertaken by the Small Craft Harbours Branch of the Department of Fisheries and Oceans in conjunction with the Queen's University Coastal Engineering Research Laboratory (QCERL). The study, which is aimed at producing a set of guidelines for the design of naturally armouring or berm breakwaters and shore protection structures was being completed under Supply and Services Canada File Number 055FF.FP802-8-2824 and Contract Number FP802-2824/01-SS. Mr. M. Mulcahy, Director of Harbour Maintenance, SCH, is the acting scientific authority for the client.

The investigation at QCERL was undertaken by graduate students in the Department of Civil Engineering at Queen's University under the supervision of Dr. K.R. Hall.

The study was commenced during the month of February, 1989 with a completion date of July 1, 1991. The results of the research will be applied to the development of a design manual for naturally armouring breakwaters. In addition, specific skills were developed by the graduate students which may provide further benefits to SCH at a later date.

1.2 BACKGROUND

In recent years, the failure of many large conventional type breakwater structures has led to a careful examination of the physical processes of wave-structure interaction. Although naturally armouring structures, which gain their stability as a consequence of profile readjustment due to wave action, have been around in various forms for hundreds of years, the high incidence of failure of conventional structures has led to their increased use in the past decade.

The interaction of an incident wave with a rubblemound breakwater results in complex flow patterns involving unsteady non-uniform flow (Hall (1987)). In most cases, it is desirable to construct a breakwater which works in harmony with the flow field; that is to construct a structure with a geometry and armour stone weight gradation which results in natural profile readjustment and subsequent minimization of the applied hydrodynamic loadings.

As a naturally armouring breakwater can be described as a mound of rock,often comprised of a wide range of stone sizes, which undergoes reshaping as a result of wave-structure interaction. As a consequence of this wave action, a stable profile is developed. Two major processes occur in the development of the stable profile. First, the overall geometry of the structure responds to the nature of the hydrodynamic loadings. Material is sorted and redistributed into a profile which acts to minimise the applied forces by altering the flow field kinematics. Secondly, this natural sorting leads to consolidation (densification) of the armour layer as stones that move eventually find voids into which they nest.

This type of structure has been used extensively in the past decade and it has been found that these structures are significantly less expensive than more conventional breakwaters designed in accordance with guidelines given in design manuals such as the US Army Corps of Engineers Shore Protection Manual. The armour stones required are smaller than those required by conventional stability formulae and a much wider gradation can be used. This allows for the

design to be based on the actual quarry output rather than some pre-conceived specification for stone for which a quarry must be found. Experimental studies have indicated that the reshaped breakwater profile can be closely predicted for the design wave conditions and the available material properties. This profile can be used as an initial design. Currently model studies are used to optimize the design and minimise the cost.

The concept of a naturally armouring breakwater, on which the applied forces are minimised, has been further supported from the results of a review of breakwaters constructed during the 19th century, breakwater failures and prototype experience with natural profile breakwaters gained in the past decade [Hall (1987)].

The final stable profile developed as a result of wave action will be influenced by a number of variables including the gradation of stones used in the armour layer, the shape of the stones and the angle of wave approach. When a wide gradation of armour stones is used, a natural sorting of stones occurs. In addition, interlocking between stones is developed since stones of a given size tend to roll about the surface until they find voids into which they nest. This allows maximum interlocking between stones to be achieved.

The shape of the stone influences its rolling resistance, its frictional resistance and also influences the magnitude of the applied hydrodynamic forces. Both the stone gradation and the stone shape affect the porosity and permeability of the structure. This has been shown to affect the stability of the structure, by modifying the external and internal flow field kinematics.

The structure also tends to reach its equilibrium profile at different rates for differing wave conditions. Therefore simulation of possible wave conditions during the passing of the design storm is desirable in model tests.

The angle of wave approach affects the magnitude of the applied hydrodynamic forces and therefore influences the relative distance moved by each particle in the direction of the applied force. For very lightweight material, the path of a particle is affected such that motions perpendicular to the longitudinal axis of the breakwater may be decreased while motions in the direction of the longitudinal axis are increased.

These structures develop their stability due to an increase in the total volume of voids of the armour layer (compared with conventional structures) and due to natural sorting of stones which results in profile adjustment and the development of an armoured profile.

The high total volume of voids of the armour provides a suitable medium through which the incoming wave energy can be dissipated. In a conventional breakwater, the flow is channelled up through the armour stone layer, which is usually only two units thick, and consequently the individual drag force acting on each stone is very high due to a relatively high velocity field in the armour layer. In a naturally armoured concept, the incoming wave can spread its energy over a larger mass and area, thereby reducing the velocity field which results in a reduction in the forces acting on individual stones. Because the forces are smaller, smaller sized armour stones can be used. The stability of the armour layer is a function of the stone gradation selected and the thickness of the armour layer over the core. As the stone sizes decrease to the

point where individual stones are hydraulically unstable, the breakwater derives its stability through another mechanism which is described below.

Movement of the stones and consolidation of the structure increases the armour layer's stability and resistance to wave action. The profile of the structure is adjusted so that the applied hydrodynamic forces are reduced. The movement of stones also results in a sorting and nesting of the armour stones. As a result, the interlocking between individual stones is maximised. The natural sorting, or armouring involves a significant amount of motion of stones in the surface layers of armour.

It is important to recognise that the motion observed and the reshaping of the profile do not constitute a failure. On the contrary, these processes create a surface layer of armour stones which is more resistant to wave attack than loosely placed stones that are many times the weight of the stones used in this concept. The overall stability of the structure is improved once the nesting of stones has occurred.

The performance of an armoured breakwater when exposed to wave conditions exceeding the design conditions is significantly better than the performance of conventional designs. A conventional design will lose its armour protection relatively quickly when design conditions are exceeded and this may lead to breaching of the breakwater. Damage to the mass armoured design takes place at a much slower rate because the incident wave energy is dissipated over the armour layer and the energy available to remove material from the upper section of the structure is considerably reduced.

This type of structure has been used extensively over the last two decades in Australia, Brazil, Canada and Iceland. In most cases, cost savings of 60 to 70 percent of the cost of a conventional multilayer design were achieved. The concept has the advantage of utilizing the total yield of the locally available quarry. The available material is usually determined before the structure is designed (using trial blasting and geotechnical investigation). The structure is then optimized for the given design conditions (wave height, wave period and water depth). The geometry of the structure is determined to minimise placed quantities. Material is not simply placed in a mound at the natural angle of repose.

Further support for proposing widespread use of naturally armouring breakwaters can be developed by recalling the nature of the applied hydrodynamic forces and analysing the results of prototype surveys and hydraulic model studies. A number of generalized trends, which are common to most model and prototype experiences are given below:

(i) Flatter slopes develop in areas where the hydrodynamic forces are maximum on conventional structures; that is, in the area just below the still water level. Slope readjustment reduces the magnitude of the forces in this area. This results in the ability to use smaller stones.

(ii) Below certain elevations, no significant profile adjustment occurs, indicating an area in which the hydrodynamic forces are relatively small. Smaller size stones can be used in this area.

(iii) In the area above the still water level, the hydrodynamic forces lessen as the elevation increases, therefore a return to steeper slopes may be achieved in this area (for a given stone size). Alternatively,if the stone size is reduced, flatter slopes will prevail in this area as well as in the area identified in (i).

By observing the trends described above, one can conclude that a stable breakwater can be achieved by utilising a wide range in armour stone sizes, departing from a conventional design. Due to the complex nature of wave-structure interaction, the intensity of the applied forces varies with location on the structure. Armour stability can be achieved by various methods. In most cases, the most economical design is one in which the available material is placed to the geometry dictated by the applied forces. The most obvious way of achieving this goal is to deposit material in sufficient quantities and let the waves move the material (natural sorting) to the final slopes and depths required to achieve stability.

Alternatively, by understanding the general trends and by conducting the proper investigations, the geometry of a stable structure for a given material and wave climate can be determined and the structure could be constructed as close as possible to the approximate stable profile, thereby reducing the amount of readjustment necessary and the time required to achieve the stable profile. However, by constructing a breakwater in this manner, the additional stability due to the natural armouring that occurs as a result of stone motion induced by wave attack would not be developed.

1.3 STUDY PURPOSE

The concept of a naturally armouring breakwater has been discussed. It is evident that there are a number of variables which govern the design of these structures. However, several key design parameters can be identified which have a very significant effect on the stability of naturally armouring breakwaters. These are the wave climate (wave height and period), the armour stone gradation, angle of wave approach and the design storm profile.

At present, the hydraulic stability must be determined with the support of hydraulic model studies. A number of trial and error solutions must be assessed before the final design is narrowed in on. This often results in a lengthy, costly model program. Additionally, each breakwater at each site will probably be constructed with a different gradation of armour stone (it should be since the idea of the concept is to maximize use of locally available material and most quarries have varying characteristics). This results in the requirement of "hand" picking the modelling stones to match the estimated prototype gradation (again a costly procedure). If during construction, it is found that the actual prototype gradation varies significantly from the estimated gradation used in the hydraulic model studies, additional tests are required to properly assess the influence of this change on the final design.

The research study presented in this report is intended to eliminate most of the initial trial and error tests and to provide a basis for assessing the influences of changes in breakwater material specifications on breakwater stability, which may arise following initiation of construction. This was achieved by undertaking an extensive series of hydraulic model studies in which stone gradation, stone shape, wave climate, the relative angle of wave attack with respect to the

structure and design storm profile was varied over a wide range, encompassing many possible design scenarios. In the proceeding chapters, data measured in these tests are analyzed and subsequently design guidelines are prepared.

These guidelines can be used in the following manner:

(1) For a new breakwater site, the characteristics of the locally available quarry should be estimated (trial blasting or geotechnical investigation). For the wave conditions which occur at the site, a preliminary design can be selected from the guidelines.

(2) The preliminary design can be adjusted along the length of the structure to take into account variations in depth and/or wave conditions (will assist in minimizing the cost of the structure).

(3) The influence of the angle of wave attack can be assessed using the guidelines. This is particularly important if there is uncertainty over the dominant wave directions or if there is a large range of wave exposure. Modification of the preliminary design is possible using the guideline.

(4) The preliminary design developed in (1), (2) and (3) can now be tested using a hydraulic model. By using steps (1), (2) and (3) a considerable modelling effort has been saved.

(5) During construction, if it is found that the preliminary estimate of the quarry yield was not realistic,modification to the final design can be made based on information presented in the guideline eliminating the need for re-initiating the modelling program.

(6) Volume estimates can be prepared for any breakwater site based on a preliminary design of the structure using the guidelines. These volume estimates should be very realistic since major alterations to the preliminary design should not be required.

2.0 REVIEW OF CONCEPT

The concept of a naturally armouring breakwater, on which the applied forces are minimised, can be supported by undertaking a review of breakwaters constructed during the 19th century, breakwater failures and by reviewing prototype experience with these types of breakwaters gained in the past decade.

A vast amount of historical data is available which provides information regarding the long term performance of breakwater structures. Many of the early breakwater structures were constructed by simply dumping quarried stone, which was available at the job site, into the sea. Enough material was placed for the breakwater to eventually develop a stable profile. The action of the waves would redistribute and sort the stones into a stable rubblemound configuration.

Stability can be defined as either static or dynamic. Typically, in the past 50 years breakwaters have been designed to be statically stable; that is, no changes to the profile are expected after the structure is built. Alternatively, a dynamically stable structure is one which develops a stable profile following a period of wave attack at a given threshold level. A dynamically stable profile does not imply that individual particles are immovable, but rather that there is no net movement on the structure. Some particles may move around a median position.

The bulk of the research into dynamically stable systems has been undertaken for sand and gravel beaches [Kemp (1960), Watts (1964), Van Hijum (1976), Gourlay (1980), etc]. However, examination of existing breakwater structures can provide valuable data regarding the development of stable profiles of breakwaters subject to wave attack. Hall et al. (1983) and Baird and Hall (1984) presented the results of investigations conducted to produce stable breakwater designs which maximise the use of locally available quarry material.

Many rubblemound breakwaters built during the 19th century were designed to allow wave action to mould the structure into its final shape. Table 2.1 provides a summary of some of these early rubblemound structures, indicating the final wave-adjusted slopes. Many of these structures are now into their second century of service. Figure 2.1 compares the relative geometries of these structures.

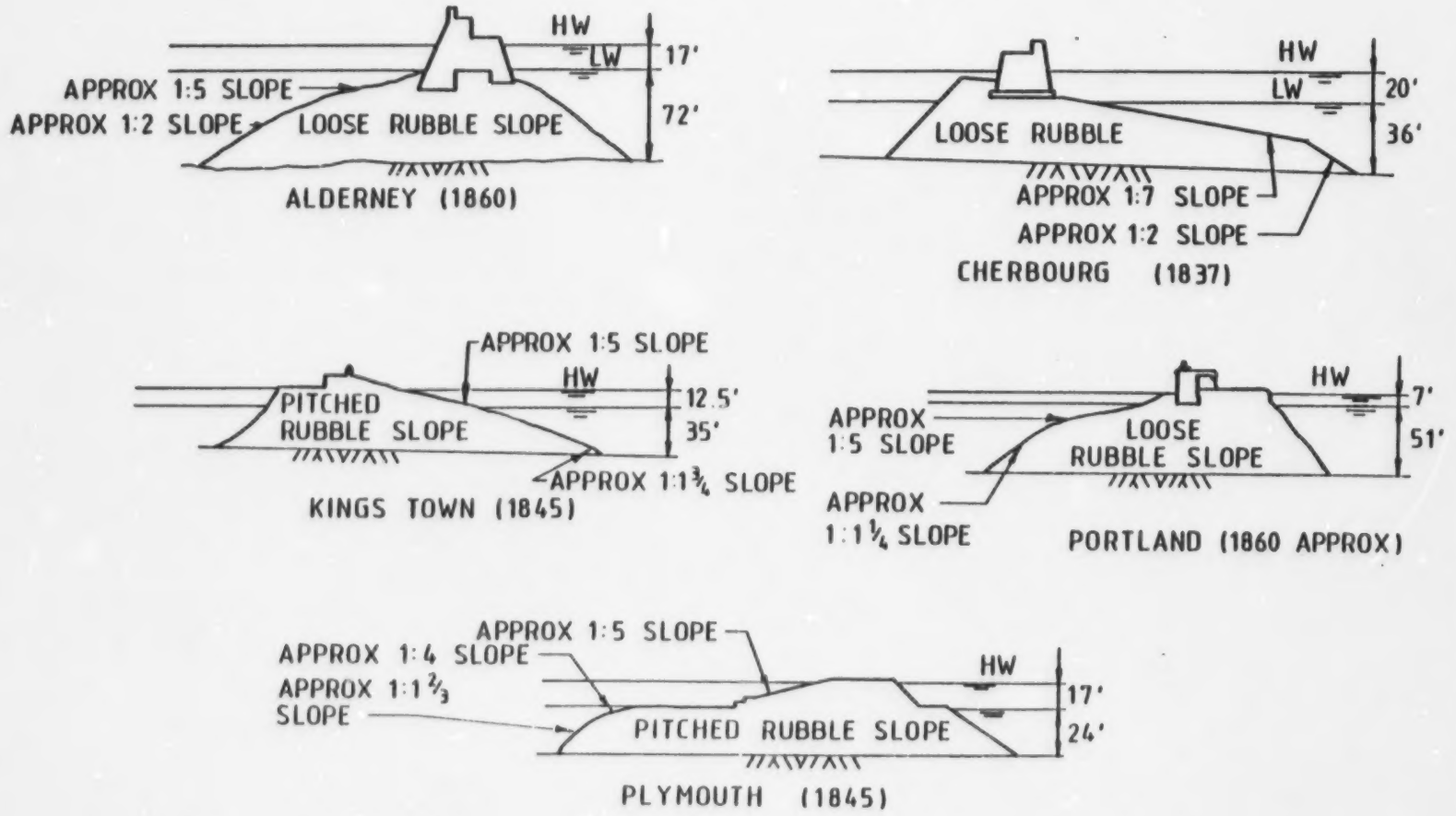

FIGURE **2.1** SUMMARY OF HISTORICAL BREAKWATERS

Table 2.1 Summary of 19th Century Rubblemound Breakwaters

Breakwater	Nature of Construction	General Slopes			
		From Bottom to Near Low Water	Near Low Water	Up to High Water	Above High Water
Portrush	Loose rubble	1.75 to 1	6 to 1	3 to 1	1.3 to 1
Plymouth	Loose rubble below Hw pitched slopes above	1.67 to 1	4 to 1	5 to 1	5 to 1
Portland	Loose rubble below Hw, plumb wall above Hw	1.25 to 1	5 to 1	5 to 1	5 to 1
Cherbourg	Loose rubble	2 to 1	7 to 1	7 to 1	1.2 to 1
Alderney	Loose rubble	2 to 1	5 to 1	Plumb wall	
Kingston	Pitched slopes of rubble	1.75 to 1	5 to 1	5 to 1	5 to 1
Holyhead	Loose rubble	1 to 1	6 to 1	6 to 1	
Cette	Loose rubble with plumb wall	1.5 to 1	3.5 to 1	Plumb wall	

A number of authors have conducted studies aimed at assessing profile development of sand beaches, till shorelines and rubblemound breakwater structures. These studies have been conducted in laboratories and in the field. the results of the major investigations which have direct application to rubblemound breakwater design are described below.

Popov (1960) undertook a model investigation to determine the characteristics of stable profile development on the shorelines of earth dams and reservoirs. He noted that the developed profiles were a function of the wave height and period, grain size diameter and fluid viscosity. Popov characterised the stable slopes into five distinct zones, shown in Figure 2.2.

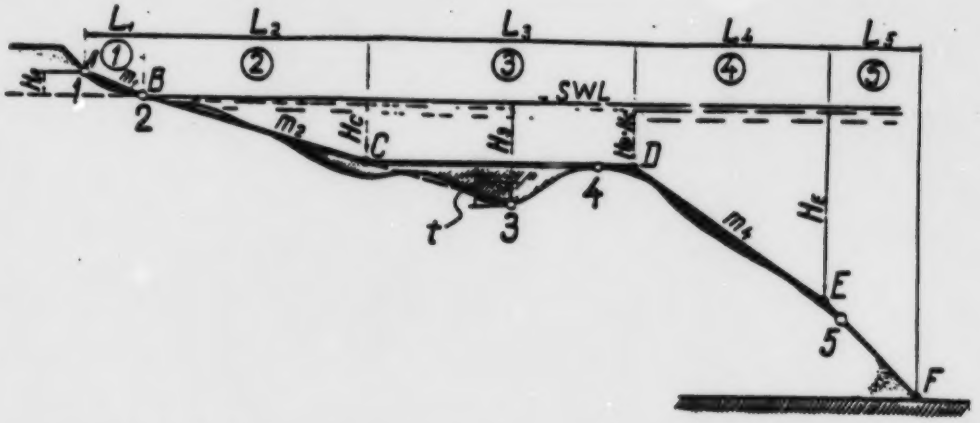

FIGURE 2.2 DEFINITION OF A STABLE PROFILE
(After POPOV, 1960)

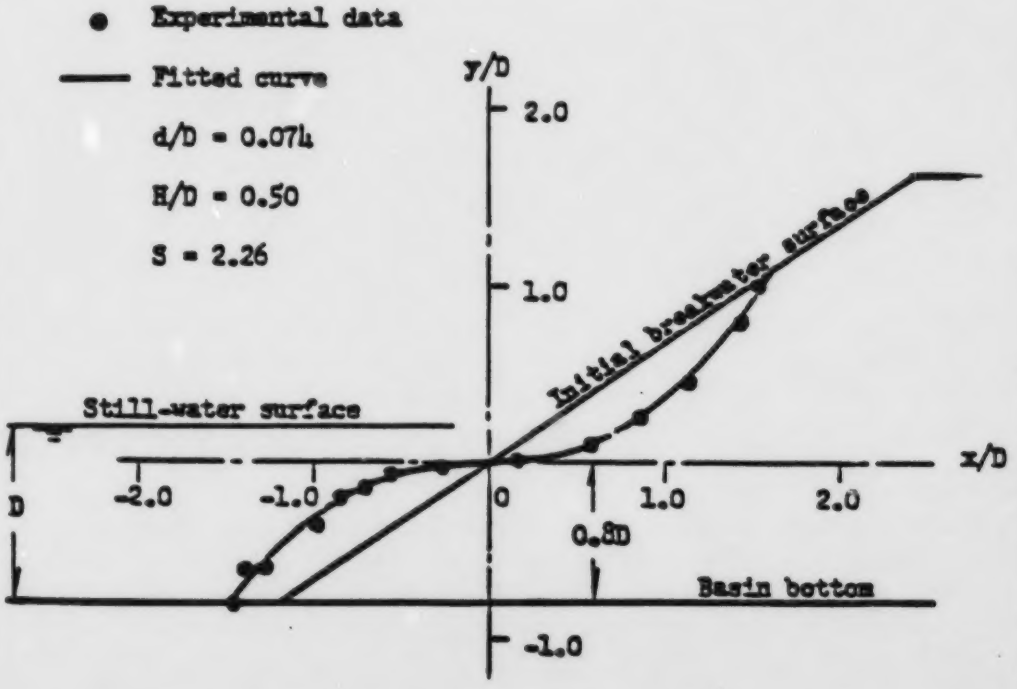

FIGURE 2.3 STABLE PROFILE FOR CONCRETE CUBES
(After PRIEST et al, 1964)

Priest et al. (1964) described the results of a model investigation in which the profiles developed as a result of wave action were measured for several breakwaters constructed with armour stones and concrete cubes. Results of their tests are summarised in Figure 2.3. They found that the profiles could be described by the equation:

$$Y/D = m\left(\frac{X}{D}\right)^n$$

where m = coefficient
n = exponent
X = horizontal dimension
Y = vertical dimension
D = still water depth

In their test program, the structures were initially constructed with a front slope of 1:1.5. No initial overtopping was allowed. They found that m and n were a function of a dimensionless grain diameter, d/D, (where d = average grain size), and the relative density of the material. They proposed the following equation for m and n:

$$m \text{ or } n = A \log\frac{d}{D} + B$$

where B = constant

In their tests they observed that once a stable section was formed, there was no longer movement of material, except for very lightweight material within a small zone slightly below the still water level. Hall et al. (1983), Baird and Hall (1984) and Hall (1985) also concluded from the results of laboratory experiments that movement ceased once the stable profile was developed. The profile that had developed during early exposure to the design wave condition did not alter after a given period of time. Ahrens (1975) reported that stones which were moved by wave action tend to find stable positions which reduce the void space within the armour layer. This suggests a natural consolidation process, which is described later.

Priest et al. (1964) found that an increase in the armour stone size resulted in a decrease in the volume of material moved. The same trends were found by Hall et al. (1983) although a more complex relationship was observed which involved the relative gradation of stones.

Priest et al. found that by using concrete cubes having the same weight as stones, a decrease in the volume of material moved was observed. This suggests that the shape of the armour unit has an influence on the profile development.

Kogami (1978) gave a relationship between two parameters used to describe the profiles observed during an experimental investigation of stone covered sand-mastic breakwaters. Figure 2.4(a) shows the characterisation of the slope as given by Kogami. The relationship between the depth of the beach, d_c, and the deepwater wave steepness, H/L_o, is given in Figure 2.4(b). Kogami found the action of stones in three regions to be distinct. In zone (a), the stones were rapidly eroded by wave action. Readjustment of the slope to a flatter value resulted in a decrease in the velocity of the wave uprush. Therefore the movement of stones eventually ceased and a stable profile was reached. In zone (b), the stone motion was found to be oscillatory with some profile redevelopment occurring. Stones from section (a) were deposited into section (c) where they were stable.

Moutzouris (1978) classified the profiles of breakwaters observed in hydraulic model tests into four distinct zones according to the type of wave action experienced by each. These zones are shown in Figure 2.5. Moutzouris stated that zone 1, which can be vertical, is an inert zone, that is, no significant change occurs in this zone. Zone 2 is characterised by flatter slopes and occurs in an area of wave instability, where breaking is initiated. The third zone is characterised by a horizontal section. Moutzouris stated that a water layer was formed in this zone resulting in a damming of the shock pressures resulting from the impact of the breaking waves. He stated that this zone was situated at or slightly below the still water level and was usually larger than the maximum length of the breaking zone for the largest design waves. The fourth zone was situated above the still water level and was characterised by steep slopes developed to retard wave runup.

Foster (1969) described the results of a model investigation undertaken to develop a design for a breakwater structure in Tasmania, Australia. The structure was built of quarry run obtained from over-burden and dumped at its natural angle of repose and allowed to be shaped by wave action. The material was comprised of stones weighting up to 10 tonnes maximum,but with only 5 percent greater than 2 tonnes; and 8 percent less than 2 kg. Prototype surveys undertaken 10 years following completion of the structure indicated slopes of the order of 1 in10 through the waterline.

Van Hijum and Pilarczyk (1982) investigated the development of equilibrium profiles for coarse materials. They compared the results of regular and irregular wave tests and concluded that the resulting profiles were the same if the irregular waves were characterised by a wave height and wave period which was 15 percent higher than the deepwater significant wave height and significant wave period respectively.

The profile formation was found to be a function of a number of external parameters including the wave characteristics (height, period, celerity), wave angle, viscosity, specific gravity, grain diameter, grain shape and top elevation of the beach. The shape of the equilibrium profile was not influenced by the initial profile.

They found that the grain size distribution was not constant along the equilibrium profile. At the beach crest, the diameter was found to increase with time initially, and then decrease. At the still water line, no relation between the grain diameter and the wave characteristics was found. The diameter tended to fluctuate around the initial values. An increase in the median diameter was found between the still water level and the profile step. The depth of foreshore

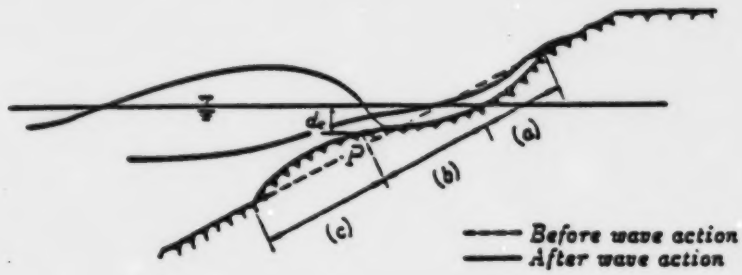

FIGURE 2.4 a STABLE RUBBLEMOUND BREAKWATER CONFIGURATION
(After KOGAMI, 1978)

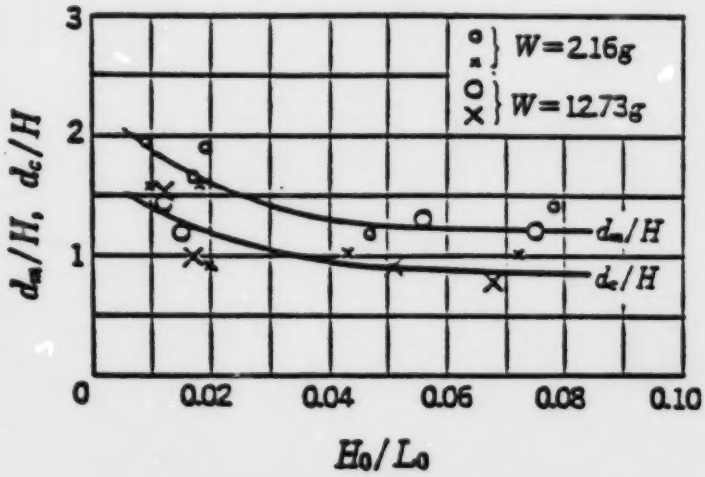

FIGURE 2.4 b VARIATION OF DIMENSIONLESS CRITICAL STABILITY DEPTH WITH WAVE STEEPNESS
(After KOGAMI, 1978)

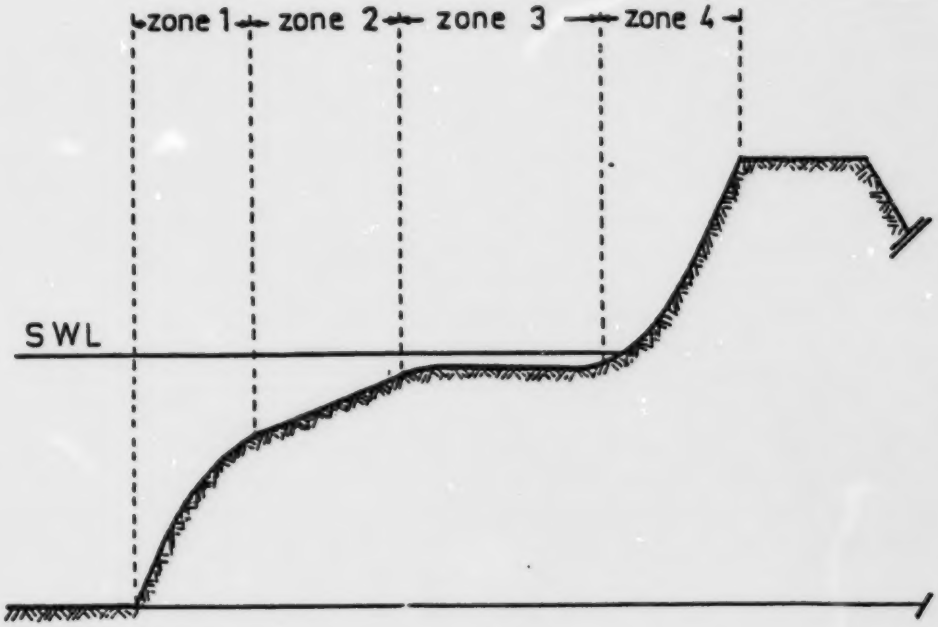

FIGURE **2.5** PROPOSED STABLE PROFILE FOR A RUBBLEMOUND BREAKWATER (MOUTZOURIS, 1978)

was found to have no influence on the equilibrium profile.

Naheer and Buslov (1983) presented two cases in which the geometrical properties of rubblemounds was investigated. The first case involved a hydraulic model study of a structure designed on the basis of a naturally armoured profile. The main armour consisted of 9-12 tonne stone. The second case involved prototype monitoring of a damaged tetrapod breakwater at Ashdod, Isreal. Profiles measured on the prototype structure revealed that the original structure (1:1.33 slope) had been transformed into a naturally armoured profile. It was noted that compaction of the slope due to readjustment of the broken tetrapod pieces resulted in an increase in stability during the reshaping process. This supports data gathered by Hall et al. (1983) where nesting of individual stones within the surface layer of armour resulted in considerable compaction of the armour layer. The degree of compaction was found to be a function of the gradation of armour stone. Evidence of this consolidation suggests that the increase in stability that is associated with the adjustment of the breakwater profile can not be replicated simply by artificial shaping (constructing the breakwater to its final profile) as suggested by Naheer and Buslov's laboratory model. Processes such as natural sorting of stones and compaction of the armour layer will not be reproduced.

Ahrens (1984) provided the results of a study undertaken to investigate 'reef type' breakwaters, which were defined by Ahrens as a homogeneous pile of stones sufficient to resist wave attack. Profiles were measured before and after testing. The final profile represented an equilibrium profile. Ahrens noted that most of the stone motion occurred during the first 10-15 minutes of testing. This is consistent with the observations of Hall et al. (1983). Ahrens observed that waves appeared to be absorbed into the structure before they could break into it. This was due to the porous nature of the structure.

Ahrens investigated the influence of irregular waves on the performance of the reef type structure. The stability of the structures was assessed on the basis of a modified stability number, N_s^*, proposed by Graveson et al. (1980), where:

$$N_s^* = \frac{\left(H_s^2 L_p\right)^{1/3}}{\left(w_{50}/w_r\right)^{1/3}(S_r - 1)}$$

Where
- N_s^* = spectral stability number
- H_s = significant wave height
- L_p = deep water wave length at peak frequency
- w_{50} = median stone weight
- w_r = unit weight of stone
- S_r = relative density of stone

The spectral stability number takes into account the period of the peak energy density of the spectrum. Ahrens noted that it was convenient to relate the damage to the zero moment wave height due to the statistical stability of the parameter and because of its relation to the area

under the spectrum. However, it was commonly observed that larger waves in the distribution moved most of the stone. Ahrens concluded that the severity of irregular wave attack is better measured by the parameter $H_s^2 L_p$ than H_s^3.

Ahrens found that the threshold of stone movement occurred at a value of N_s^* of 7. For $N_s^3 < 6$ little or no stone movement occurred; whereas, for N_s^* values in excess of 8, significant damage occurred.

Hall et al. (1983) and Baird and Hall (1984) described a similar type of breakwater concept which has been utilised recently. Table 2.2 summarises the wave climate, stone gradation and water depth for some of the installations of this 'berm' type breakwater. The berm breakwater is in fact one particular type of naturally armouring breakwater, which provides good constructability. In most cases, cost savings of 60 to 70 percent of the cost of a conventional multilayer design were achieved. The concept has the advantage of utilising the total yield of the locally available quarry. The available material is determined before the structure is designed (using trial blasting and geotechnical investigation). The structure is then optimised for the given design conditions (wave height, wave period, water depth). The geometry of the structure is determined to minimise placed quantities. The material is not simply placed in a mound at the natural angle of repose.

Table 2.2 Examples of Prototype 'Berm' Type Breakwaters

Location	Depth (m)	Design Wave Height (m)	Armour Stone Gradation
Aracaju, Brazil	5.5	4	0.5 to 4 t
Helguvik Bay, Iceland	22	6(oblique)	1.7 to 7 t
Codroy, Canada	8	7*	0.5 to 4 t
Racine, Wisconsin, USA	8	6.5*	0.3 to 3 t
North Bay, Canada	3	2.0*	0.002 to 0.7 t
Cap Chat, Canada	5	4.0*	0.3 to 8 t

* indicates depth limited wave conditions

The type of structure proposed by Hall et al. (1983) and Baird and Hall (1984) develops its stability due to an increase in the total volume of voids of the armour layer (over conventional structures) and due to a natural sorting of stones which results in profile adjustment and the development of an armoured profile. These phenomena can be described as follows:

(i) The high total volume of voids of the berm provides a suitable medium through which the incoming wave energy can be dissipated. In a conventional breakwater, the flow is

channelled up through the armour stone layer, which is usually only two units thick, and consequently the individual drag force acting on each stone is very high due to a relatively high velocity field in the armour layer [see Figure 2.6]. In the berm concept, the incoming wave can spread its energy over a larger mass and area, thereby reducing the velocity field which results in a reduction in the forces acting on individual stones [Figure 2.6]. Because the forces are smaller, smaller sized armour stones can be used. The stability of the armour layer is a function of the stone gradation selected and the width of the horizontal berm (i.e. minimum thickness of armour over the core). As the stone sizes decrease to the point where individual stones are hydraulically unstable, the breakwater derives its stability through another mechanism which is described below in (ii).

(ii) Movement of the stones and consolidation of the berm increases the armour layer's stability and resistance to wave action. The profile of the berm is adjusted so that the applied hydrodynamic forces are reduced. The movement of stones also results in a sorting and nesting of the armour stones leading to an increase in the shear strength of the berm. As a result of armour stones nesting, the interlocking between individual stones is maximised. The natural sorting, or armouring process, involves a significant amount of motion of stones in the surface layers of the armour.

It is important to recognise that the motion observed and the reshaping of the profile do not constitute a failure. On the contrary, these processes create a surface layer of armour stones that is more resistant to wave attack than loosely placed stones that are many times the weight of the stones used in the berm concept. The overall stability of the structure is improved once the nesting of stones has occurred.

Although the final shape of the cross-section may be similar to the naturally armoured profiles reported by other investigators [Naheer and Buslov (1983), Bruun and Johanneson (1974)], there are several differences. The berm does not change profile below a certain depth. Stones are not rolled out of the top of the berm and carried down to the seabed. The berm is consolidated because the stones in the surface layers of armour that move eventually find voids into which the nest. Also, the profile of the berm is quite regular through the water line, typically of the order of 1:5, where as naturally armoured profiles reported by other investigators tend to have a degree of curvature to them in the region of the waterline (and thus have been described as "S" shaped profiles in some publications).

A number of studies directly applicable to determining the stable breakwater profile for a given wave climate, stone size, relative stone gradation, and initial breakwater geometry have been summarised. A comparison of some of these profiles is presented in Figure 2.7. The plot shows dimensionless X and Y co-ordinates referenced to the intersection of the stable profile and the mean water level. The profiles were made dimensionless by multiplying the X and Y offsets by $(M/\rho)^{1/3}$, where

M = average armour mass
ρ = density of the individual armour units

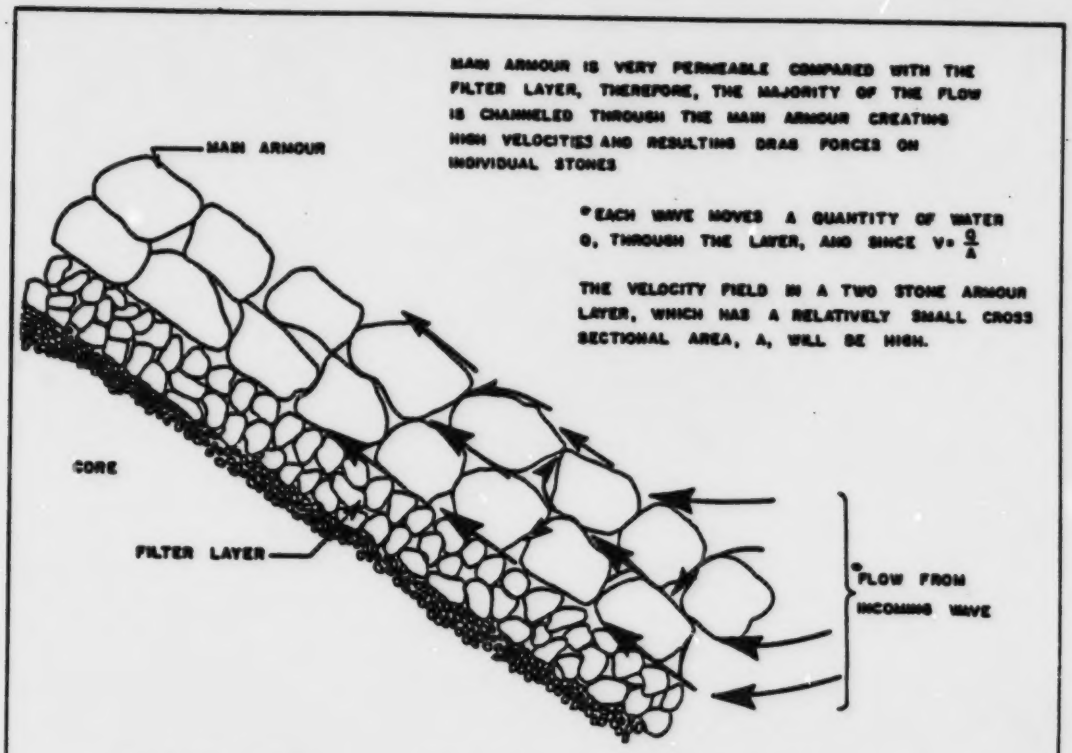
MAIN ARMOUR IS VERY PERMEABLE COMPARED WITH THE FILTER LAYER, THEREFORE, THE MAJORITY OF THE FLOW IS CHANNELED THROUGH THE MAIN ARMOUR CREATING HIGH VELOCITIES AND RESULTING DRAG FORCES ON INDIVIDUAL STONES
MAIN ARMOUR
*EACH WAVE MOVES A QUANTITY OF WATER Q, THROUGH THE LAYER, AND SINCE V= Q/A
THE VELOCITY FIELD IN A TWO STONE ARMOUR LAYER, WHICH HAS A RELATIVELY SMALL CROSS SECTIONAL AREA, A, WILL BE HIGH.
CORE
FILTER LAYER
*FLOW FROM INCOMING WAVE

FIGURE 2.6a FLOW IN A CONVENTIONAL TWO STONE AMOUR LAYER

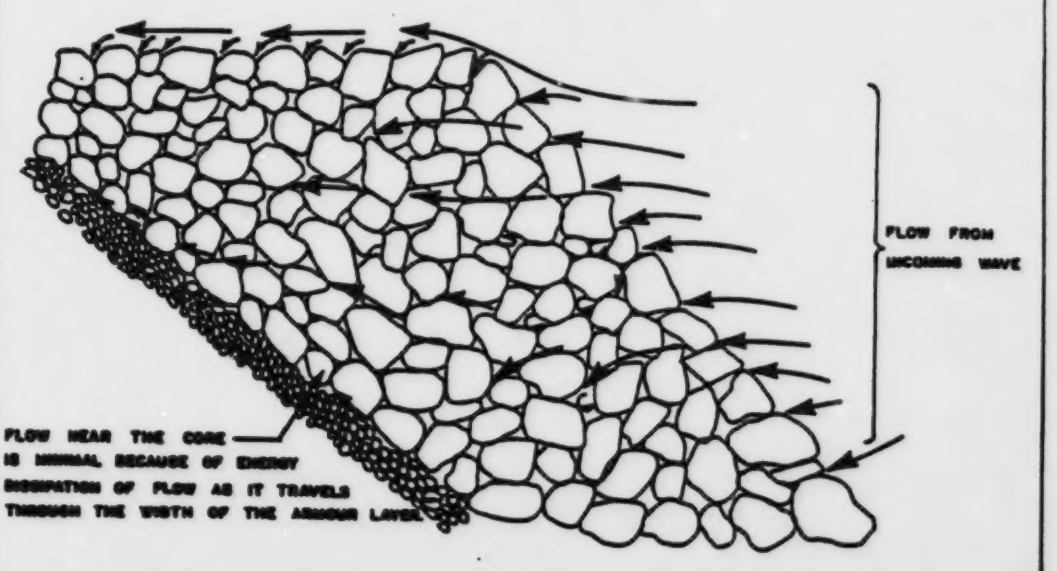
FLOW FROM AN INCOMING WAVE, Q, CAN DISSIPATE OVER A LARGE CROSS SECTIONAL AREA, A, OF HIGH PERMEABILITY.
FLOW FROM INCOMING WAVE
FLOW NEAR THE CORE IS MINIMAL BECAUSE OF ENERGY DISSIPATION OF FLOW AS IT TRAVELS THROUGH THE WIDTH OF THE ARMOUR LAYER

FIGURE 2.6b FLOW IN A MASS ARMOURED DESIGN

The resulting dimensionless profiles exhibit a distinct similarity, even though the profiles range from clay size particles to massive armour stones placed in a variety of initial geometries and subjected to a wide variation in incident wave climate.

From the results presented in Figure 2.7 and recalling the nature of the applied hydrodynamic forces, a number of general trends listed below may be deduced. These trends allow for further support to be developed for proposing the widespread use of naturally armouring rubblemound breakwaters.

(i) Flatter slopes develop in areas where the hydrodynamic forces are maximum on conventional structures; that is, in the area just below the still water level. The slope readjustment reduces the magnitude of the forces in this area. This results in the ability to use smaller stones.

(ii) Below a certain elevation, no significant profile adjustment occurs, indicating an area in which the hydrodynamic forces are relatively small. Smaller size stones can be used in this area.

(iii) In the area above the still water level, the hydrodynamic forces lessen as the elevation increases; therefore a return to steeper slopes may be achieved in this are (for a given stone size). Alternatively, if the stone size is reduced, flatter slopes will prevail in this area identified in (i).

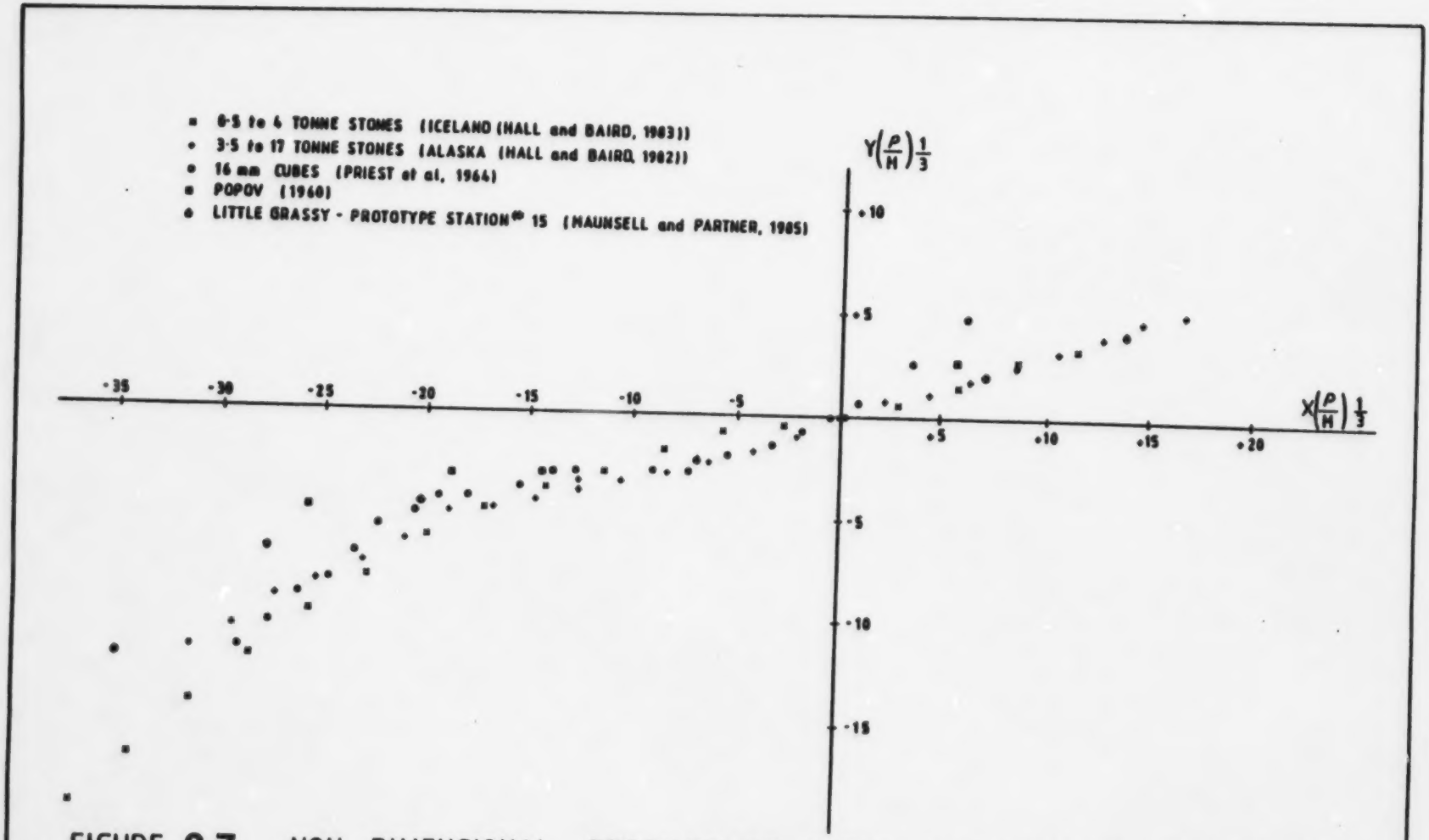

FIGURE **2.7** NON DIMENSIONAL PROFILES OF NATURALLY ARMOURING STRUCTURES

3.0 STUDY BACKGROUND

In order to study the stability of berm breakwaters, it is important to study the reshaping of the structure (having certain intrinsic resistance to deformation)under certain applied loads.

Although the problem is simple to define, there is as yet no theory developed to describe the formation of a dynamically stable profile given the external wave conditions.

In this section, the various parameters that constitute the load (disturbing force) and strength (stabilising force) will be studied. Such parameters will be identified to see if they are important factors in determining the overall stability of berm breakwaters. Parameters that are important contributors to the stability and reshaping of berm breakwaters will be singled out and studied in subsequent tests described later.

3.1 DIMENSIONAL ANALYSIS

A dimensional analysis was carried out to derive the dimensionless parameters to be studied in this research. Consider any property, Z, resulting from wave-breakwater interaction in the model or prototype; such property may be described in its most general form by the following relationship:

$$Z = \Phi\left(H_s,\ T_p,\ GF,\ N_R,\ D_{50},\ \frac{D_{85}}{D_{15}},\ w_w,\ w_r,\ d,\nu,\ g,\ P_R\right) \qquad [1]$$

where, $\Phi(...)$ denotes Z is a function of the variables in the brackets, H_s is the significant wave height, T_p is the spectral wave period, GF is the groupiness factor, N_R is the relative number of waves attacking the structure (number of attacking waves/3000) ν is the kinematic viscosity of water, P_R is the percentage of rounded stones in the armour, w_w is the unit weight of water, w_r is the unit weight of rock, d is the water depth and D_{50}, D_{85} and D_{15} refer to specific grain size within the armour stone gradation.

The variables in the brackets are factors that affect the reshaping process, for example, H_s, T_p and GF are variables that characterize wave loading, N_R measures the effect of variation of number of waves attacking, D_{50}, D_{85}/D_{15}, w_r and P_R measures the characteristics of the material interacting with waves. In particular D_{85}/D_{15} defines the shape of the gradation curve and P_R defines the relative proportion of rounded stones to angular stones. D_{50} is a characteristic dimension chosen to represent the absolute size of the stones and is commonly used by other researchers to describe armour stones sizes; therefore, utilization of D_{50} facilitates easy comparison with the research results of others.

Using D_{50}, g and w as repeaters [1] may be written in dimensionless form as

$$\Pi_z = \Phi_z\left(\frac{H_s}{D_{50}}, \frac{gT_p^2}{D_{50}}, GF, N_R, \frac{D_{85}}{D_{15}}, \frac{w_r}{w_w}, \frac{d}{D_{50}}, \frac{\sqrt{gD_{50}}\,D_{50}}{\nu}, P_R\right) \qquad [2]$$

where Π_z is a dimensionless parameter involving Z, and $\Phi_Z(...)$ denotes Π_Z is a function of the dimensionless variables in the brackets. The model will be tested based on Froude scaling and therefore similarity of $(g^{1/2}D_{50}{}^{3/2})/\nu)$ between model and prototype was ignored. In line with current understanding, effects due to viscosity can be minimized by using stones of such a size to ensure that $g^{1/2}D_{50}{}^{3/2}/\nu > 3 \times 10^4$. This was the case with all armour gradations used in this testing programme. Variation of d was not studied. Dividing H_sD_{50} by $gT_p{}^2/D_{50}$ gives $H_s/(gT_p{}^2)$ or more commonly, the wave steepness, H_s/L_o. The stability number $H_s/((S_r\text{-}1)D_{50})$, can be formed by dividing the dimensionless parameter H_s/D_{50} by $(S_r\text{-}1)$ giving another dimensionless parameter. This parameter has been used by many researchers, and thus [2] becomes

$$\Pi_z = \Phi_z\left(\frac{H^s}{S_r\text{-}1)D_{50}}, \frac{H_s}{L_o}, GF, N_R, \frac{D_{85}}{D_{15}}, S_r, P_R\right) \qquad [3]$$

where Π_Z is a dimensionless parameter involving Z, and Φ_Z' (..) denotes Π_z as a function of the dimensionless variables in the brackets. By making g/D_{50} constant in the study, T_p can also be studies independently so that the effect of wave period is studied directly. The parameters that were studied were therefore $H_s/((S_s\text{-}1)D_{50})$, H_s/L_o, T_p, GF, N_R, D_{85}/D_{15} and P_R. Three parameters describing various aspects of the initial structure or the profile after reshaping were chosen as dependent parameters, (Z in equation 1). The three parameters, illustrated in figure 3.1, are the volume of armour stone on the front slope after reshaping, (A), the width of berm eroded, (B), and the width of the toe following reshaping, (L). These parameters are of practical and theoretical importance; perhaps the most important of all is the volume of stones on the front slope following reshaping. In calculating this volume only armour on the front slope was considered; the volume of armour on the back slope was not included in the calculation since wave overtopping was not allowed during the tests and thus there was no reshaping of the backslope. A good idea of the quantity of stones required at an early stage in the design process allows the designer and the contractor to determine the adequacy of potential quarries. As a result of compaction by waves, the volume occupied by the breakwater is slightly smaller than that occupied during construction, typically varying from 0 to 2%, but is dependent on the magnitude of waves. The compaction factor (see figure 3.2) is defined using the total volume of stones initially placed, (A_o), and the volume of stones measured following each segment of wave attack, A. Figure 3.2 defines the parameters A, L and B for the case when 3000 waves of certain wave height will just cause the erosion of the berm to the toe of the 1.:3 slope. The compaction factor A/A_o measured during the experiments is shown in figure 3.2 and was found

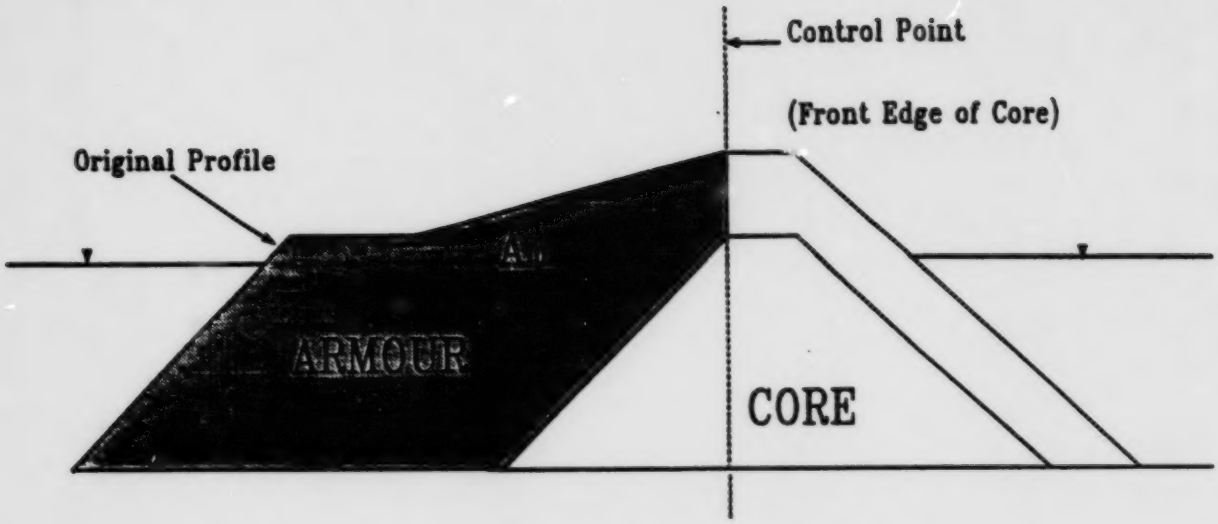

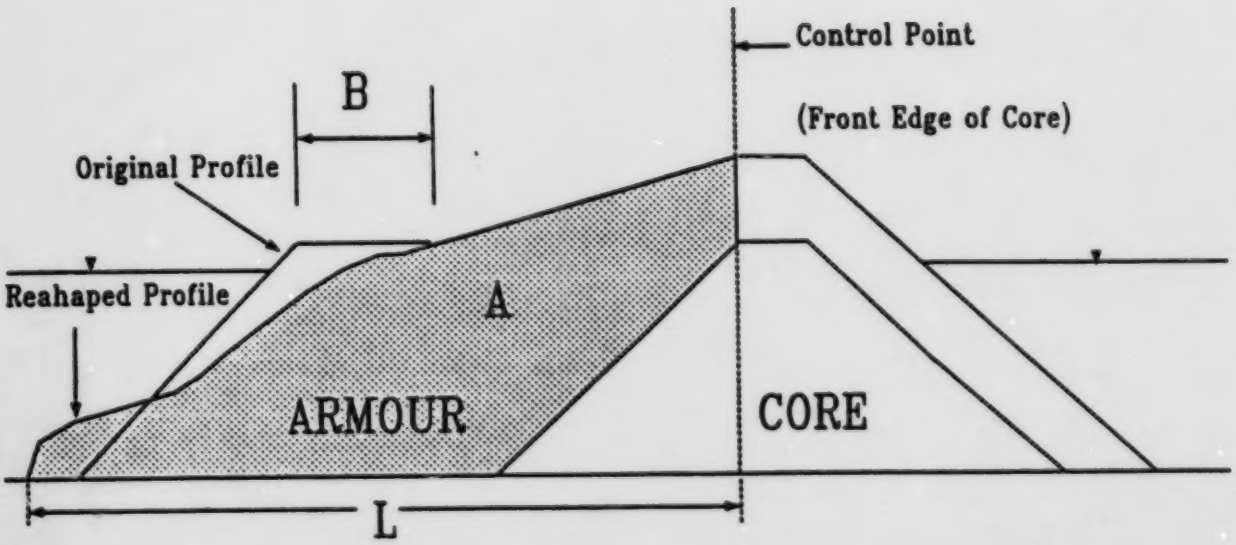

Figure 3.1 Definition of parameters

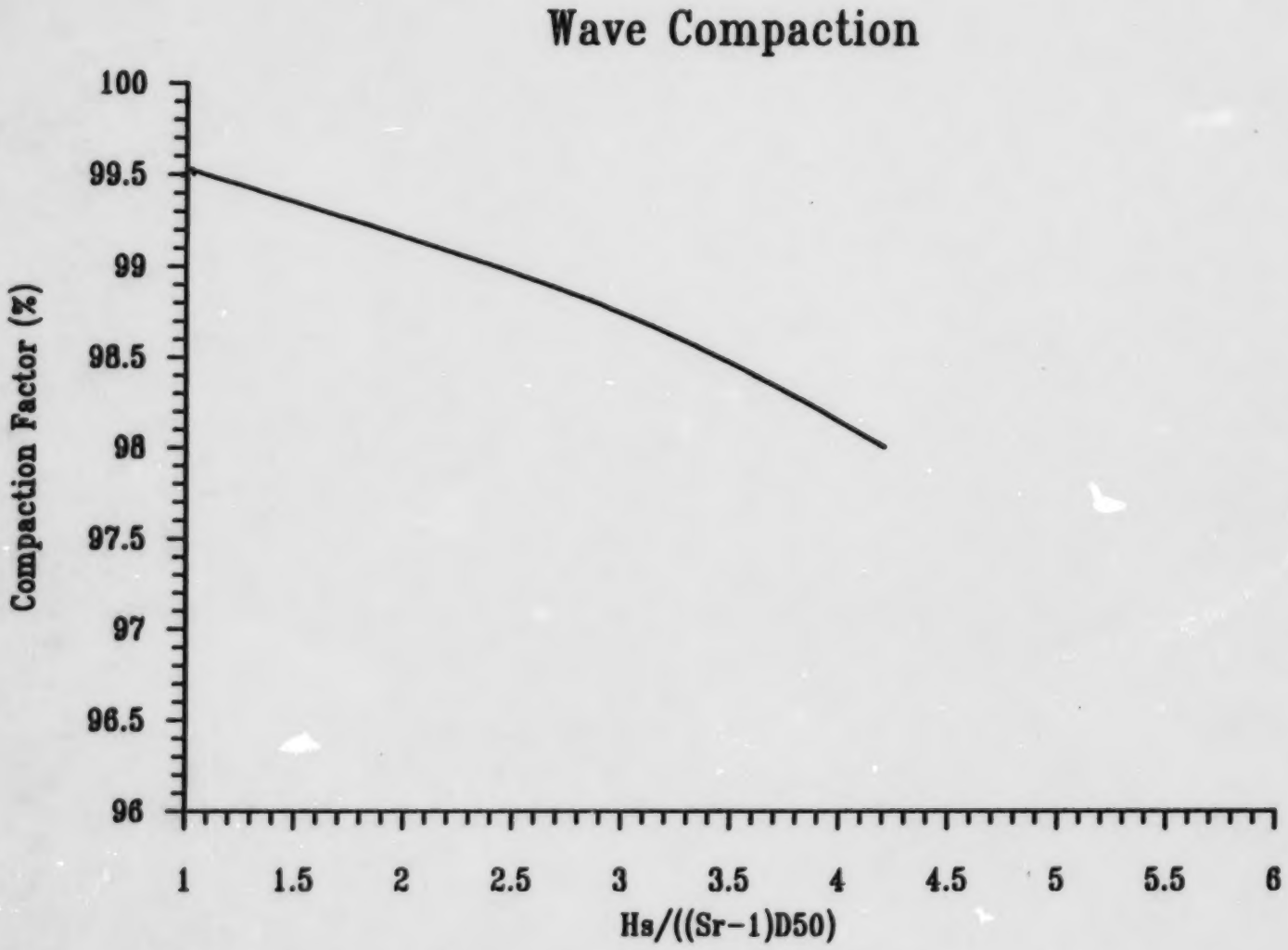

Figure 3.2 Compaction factor A/A_0 as a function of instability number (from experimental results)

to vary slightly as a function of $H_s/((S_r-1)D_{50})$.

From the present series of tests, the compaction due to waves was not found to be significant and for practical purposes, the effect can be ignored so that for design purposes A_o is equal to A. Figure 3.3 indicates the parameters L, A and B if the erosion of the initial berm does not reach the toe of the 1:3 slope; in this case the reshaped profile is shifted towards the toe of the 1:3 slope (or, equivalently, subtracting the cross-hatched area from calculations involving A and L). Thus A is the dotted area and L is the sum of two lengths L' and L" as shown in the figure. B is the width of berm actually eroded.

The toe width is of importance in that it allows the designer to determine the extent to which the toe will reshape and depart from its original position. Suitable navigational buoys would need to be placed to mark the extent of the reshaped breakwater so that boaters would not move too close to it and become grounded. In the planning stage, such information is necessary to determine the area where boats can be moored and where the fairway will be. It is also useful is assessing whether the reshaped breakwater will encroach onto adjacent property.

The width of berm eroded is important since it gives the designer an indication of the width of the berm required to ensure stability. Thus the designer need not provide a wider berm than necessary nor to incur the undesirable consequence of providing an insufficient width of berm which would result in the crest of the structure being attacked by waves and potentially being damaged. In general, the width of berm eroded is related to the area following reshaping and within construction error and possible variations of the angle of repose of the armour under water, the relationship is unique.

The influences of the variables on the right hand side of equation [3] on the dependent parameters discussed above were assessed during the testing programme. In subsequent analysis, these dependent parameters will be made dimensionless by dividing by D_{50} or D_{50}^2 as appropriate. Unless otherwise specified, the values used will be those corresponding to the attack of 3000 waves. The parameters used in subsequent discussions will therefore be L/D_{50}, A/D_{50}^2 and B/D_{50}.

3.2 TWO DIMENSIONAL TESTING PROGRAMME

3.2.1 Introduction

A comprehensive set of experimental studies were undertaken using the facilities of the Coastal Engineering Research Laboratory of Queen's University, Kingston, Canada. The studies were undertaken primarily to investigate the mechanism of reshaping of berm breakwaters and to evaluate the specific influence of the various parameters that may affect the reshaping process. These parameters include wave height, wave period, wave groupiness, duration of each segment of the design storm, the gradation of the armour stones, and the percentage of rounded stones occurring in the gradation.

The studies were undertaken in a 1.4 m wide channel in a 2 m wide wave flume in which a rubble mound breakwater with a permeable core was subjected to irregular wave attack. The

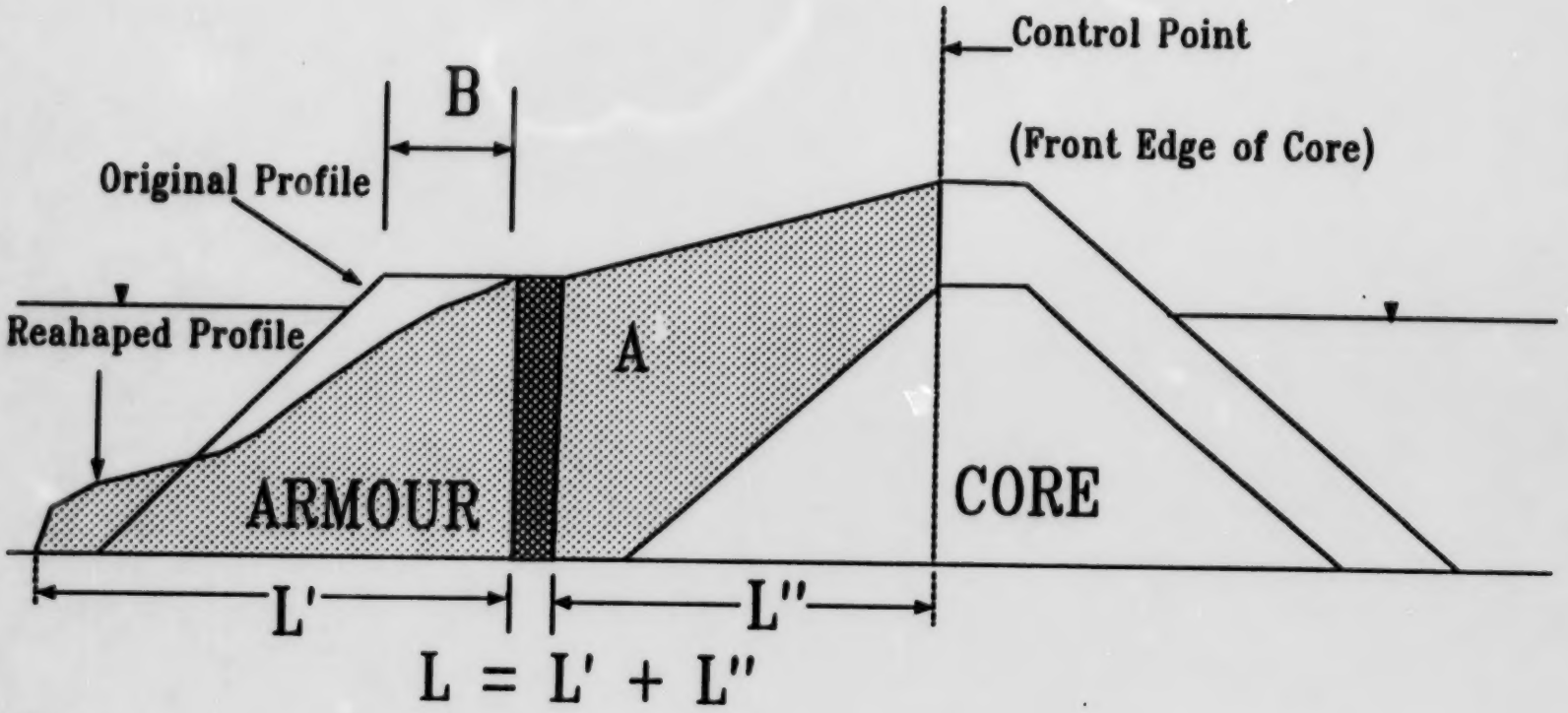

Notes:

1. A = ▨

Figure 3.3 Definition of parameters, for case where erosion of berm does not reach the toe of the 1:3 slope

test section was installed about 40 m from the wave paddle and was placed on a concrete platform 0.4 m high. A gentle slope of approximately 1:15 was used as a transition from the flume bottom to the platform. Energy absorbing material was placed at the end of the flume opposite the wave paddle to absorb wave energy from the side channels and thus minimize reflection (a schematic layout of the flume is shown in figure 3.4).

3.2.2 Materials

The rubble mound structure consisted of a core having a D_{50} of 1.2 cm and an armour layer having a D_{50} of 1.9 cm. Four different gradations of the armour stones were used with D_{85}/D_{15} ratios ranging from 1.4 to 5.4 (figure 3.5 illustrates the grading curves for each of the gradations and figure 3.6 shows the same grading curves but expressed in weight and scaled up at a geometric scale of 1:40). Figure 3.7 shows typical trial blast curve taken from actual quarries together with gradation 2 armour. Details of the armour are also given in Table 3.1. All four gradations contained 30% rounded and 70% angular stones.

Two other gradations of armour stones with a D_{50} of 1.9 cm and a D_{85}/D_{15} ratio of 1.9 but with different percentages of round stones (0% and 15%) were also used in the tests, so that three degrees of roundness were evaluated. Table 3.2 provides a comparison of the gradations having a variable degree of roundness.

The grading curve of the core material is shown in figure 3.8

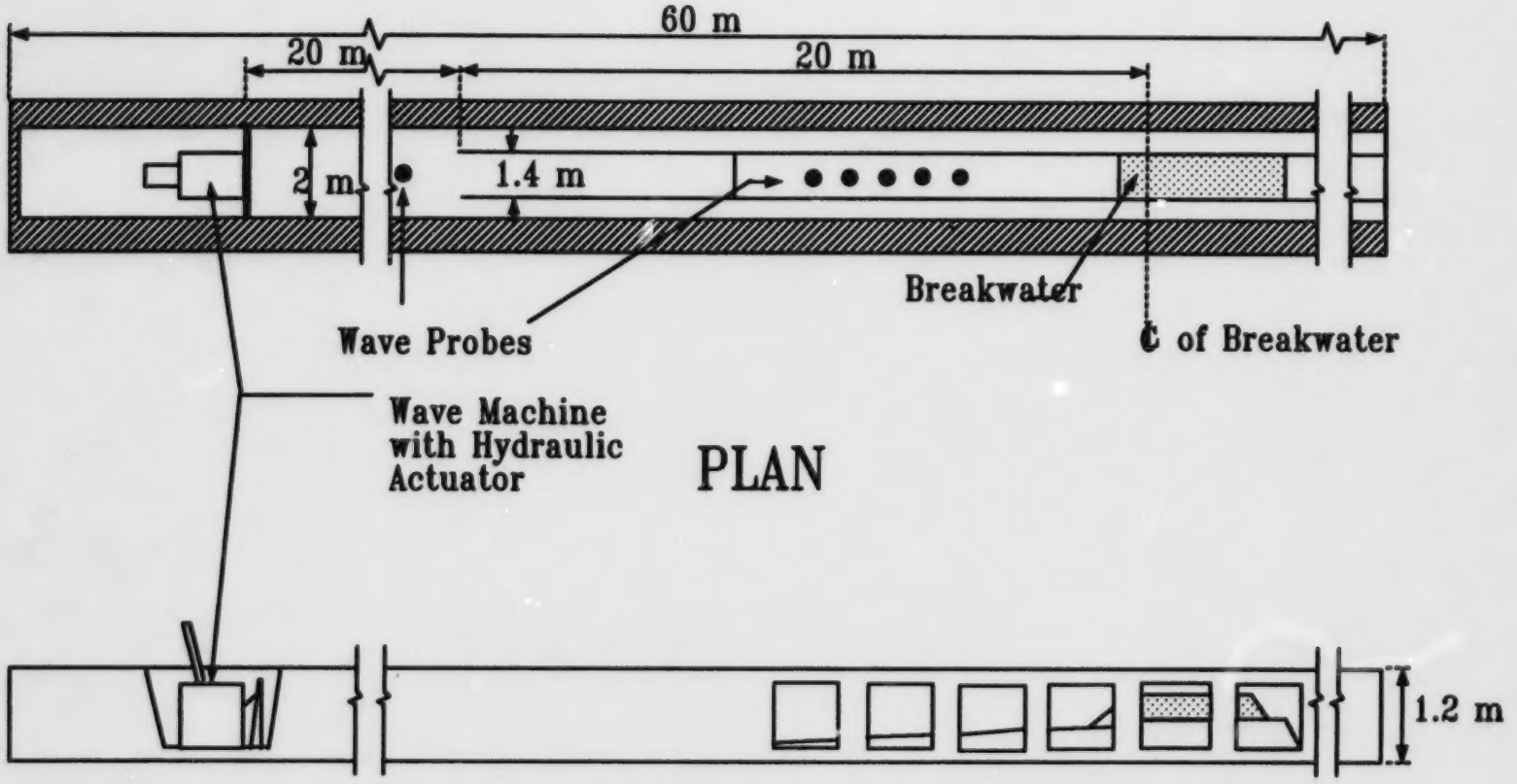

FIGURE 3.4 Layout of flume

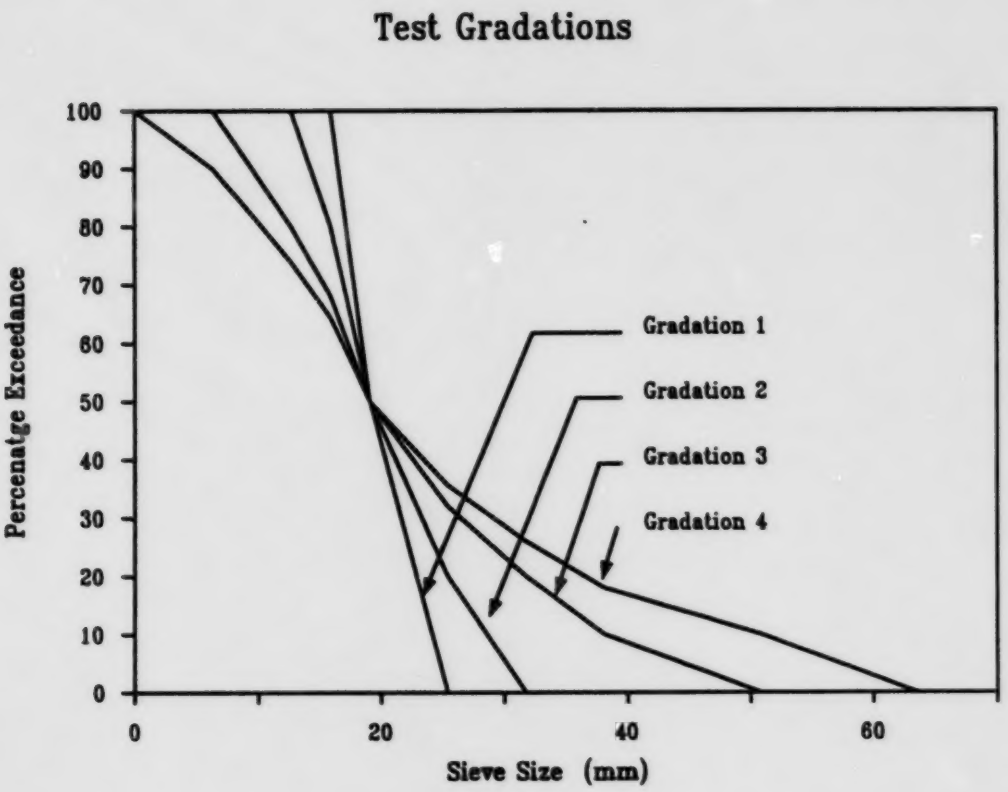

FIGURE 3.5 Test gradations

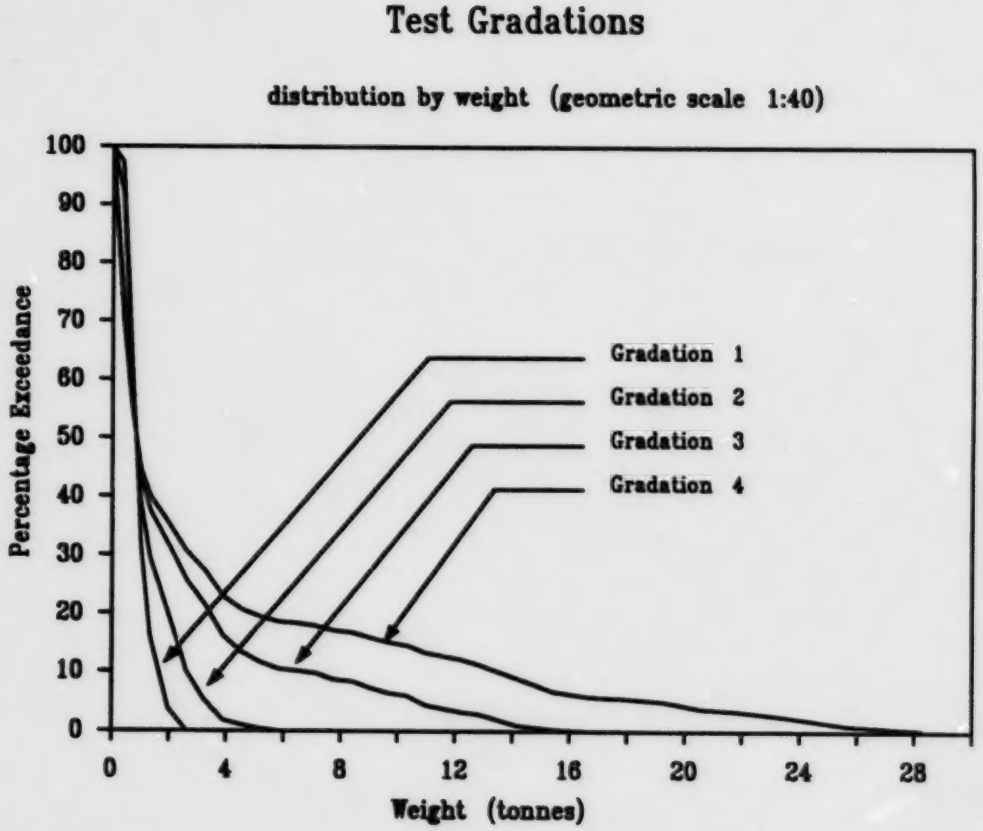

FIGURE 3.6 Test gradations in weight (geometric scale 1:40)

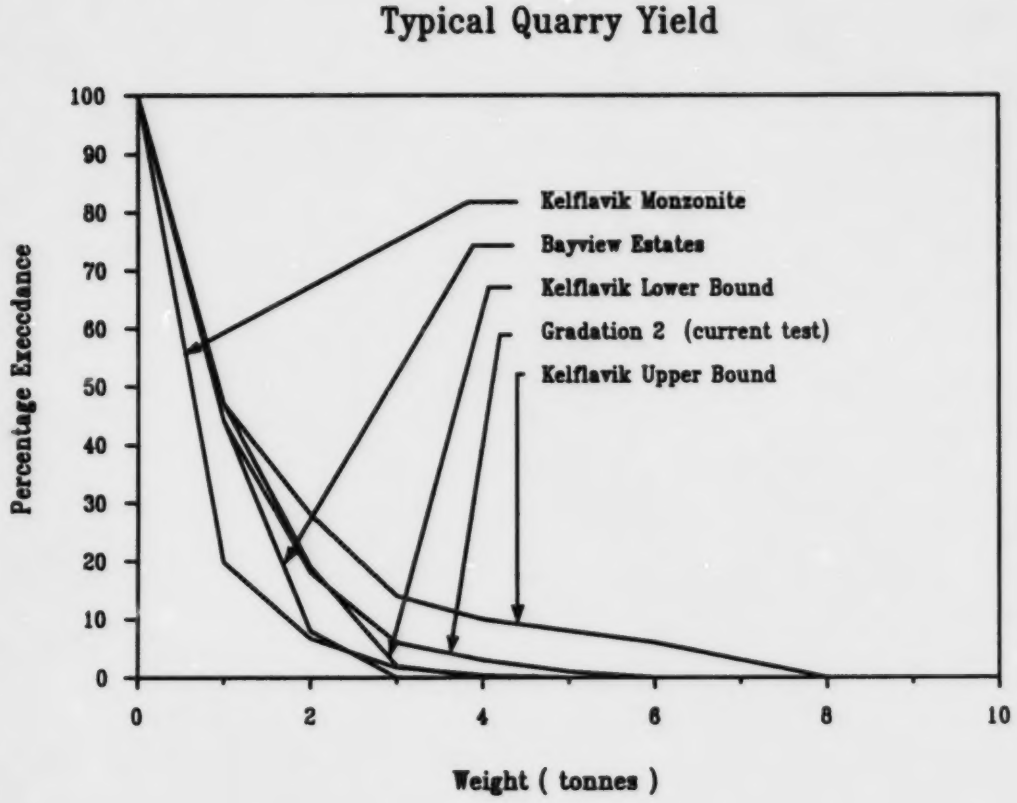

FIGURE 3.7 Typical quarry yield

Core Material

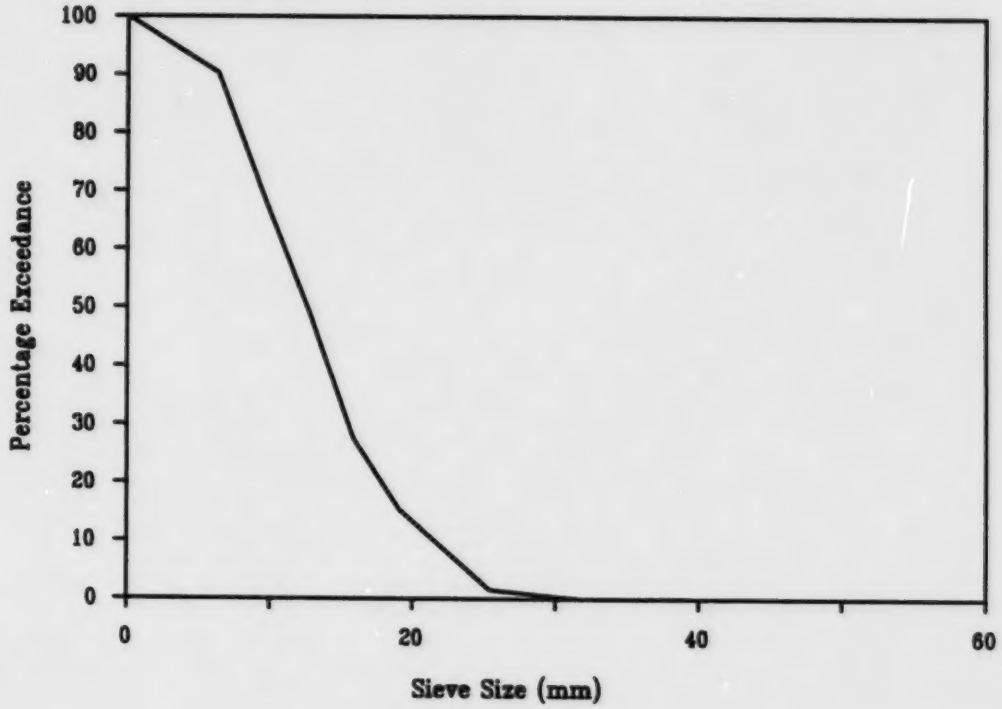

FIGURE 3.8 Gradation of core material

Table 3.1 Details of Armour Stones, Gradations 1,2,3 and 4

Gradation	1	2	3	4
D_{85}/D_{15}	1.35	1.9	3	5.4
W_{85}/W_{15}	2.5	6.9	27	160
D_{50} (cm)	1.9	1.9	1.9	1.9
W_{50} (g)	13	13	13	13
W_{max} (g)	30	60	250	460
D_{max} (cm)	2.5	3.2	5.1	6.3

Notes (1) D = equivalent diameter

(2) W = stone mass

Table 3.2 Details of Armour Stones, Gradations 2, 2A and 2B

Gradation	1	2A	2B
D_{85}/D_{15}	1.9	1.9	5.4
W_{85}/W_{15}	6.9	6.9	6.9
D_{50} (cm)	1.9	1.9	1.9
W_{50} (gm)	13	13	13
W_{max} (gm)	60	60	60
D_{max} (cm)	3.2	3.2	3.2
% rounded, P_R	30	0	15

3.2.3 Experimental Equipment and Instrumentation

3.2.3.1 Wave Flume

The flume is 60 m long, 1.2 m deep and 2.0 m wide with 6 panels for viewing the test breakwater. A 1.4 m wide channel was partitioned in the middle of the flume. A false floor 0.4 m high was built in order to provide sufficient depth of water at the paddle to generate the desired high waves. Irregular waves were generated using a servo controlled hydraulic actuator.

3.2.3.2 Water level transducer

Capacitance-type water level transducers were used to measure the dynamic free surface fluctuations. An array of five wave probes were used in front of the model breakwater and out of the five, three probes were used to resolve the measured wave into incident and reflected waves (see figure 3.4 for their locations).

3.2.3.3 Data acquisition

Data acquisition of the wave probe and profiler signals was accomplished using a Hewlett Packard A/D interface card (HP9100). It was used in its 8 channel differential mode configuration option. The full voltage range of the board was ± 10.24 V.

3.2.3.4 Breakwater profiler

A multi profiler system for automated, accurate profile acquisition was built as part of this research. It was mounted on the flume to measure the profile of the breakwater at predetermined intervals (see figures 3.9 and 3.10). With the multi-profiler system the X and Y values are directly entered into the computer thus eliminating data entry errors. The system is fast and accurate.

Two parallel rails were installed on top of the flume wall perpendicular to the breakwater as in figure 3.10. Spanning the rails were two 2m-wide wheeled carriages which could be moved along the rails. One of the carriages supported a profiling device which was operated as described below. The horizontal position of the carriage along the rails was indicated by a photosensor attached to the instrument carriage which sensed the marks on the location mark strip fixed to the side to the flume wall. The profile of the breakwater was measured by a "profiling arm", which was linked to the computer through a potentiometer. At the bottom end of the profiling arm was a small circular disc having a diameter equal to the D_{50} of the armour so that the profiler are would not sink into the surficial voids. As the carriage was moved along the rail a light would flash whenever the carriage moved over one of the marks. The operator would lower the profiling arm to the level of the breakwater surface and trigger a button sending a signal to the computer. The lowering of the profiler arm would cause the reading across the potentiometer to change which would be recorded by the computer. Thus, the elevation of the breakwater was determined along the transverse profile of the breakwater.

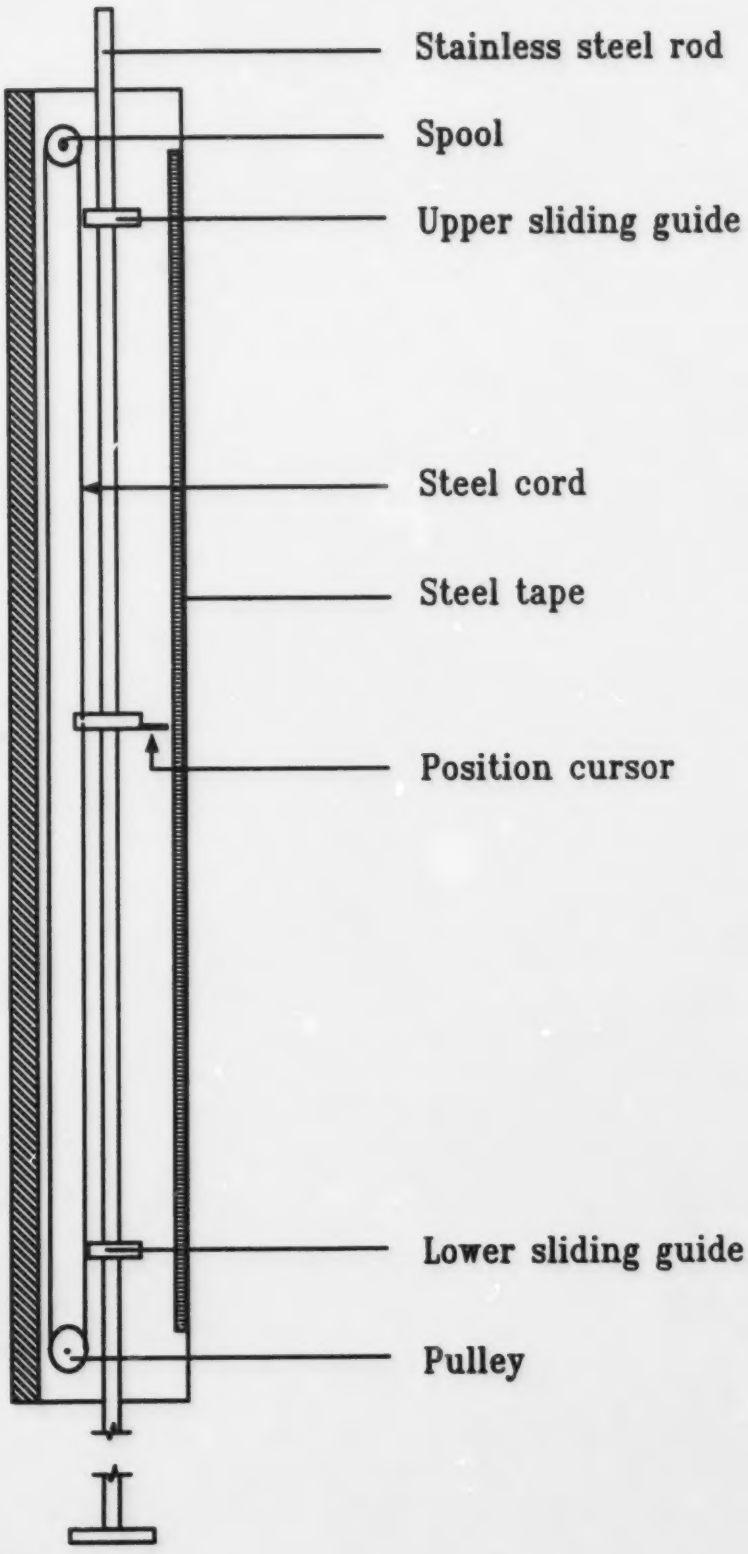

FIGURE 3.9 Profiler

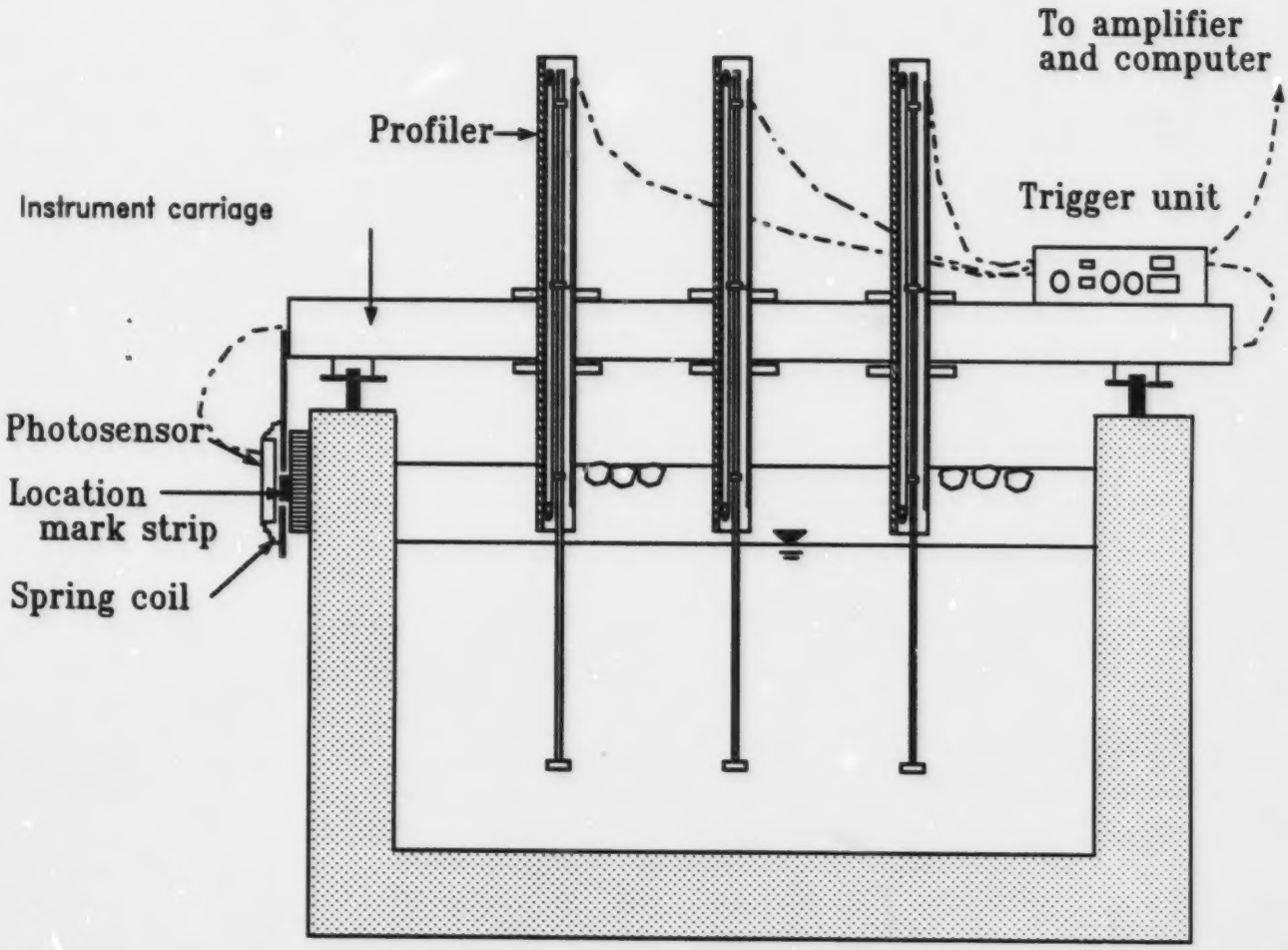

FIGURE 3.10 Layout of profiler and associated equipment

The analogue signals from the potentiometers were digitized using an 11-bit analogue/digital converter interfaced to a Hewlett-packard computer.

3.2.4 Test Methodology

Tests were undertaken on a berm breakwater whose general configuration is shown in figure 3.11. The basic geometry of the test structure was determined based on the large number of berm breakwaters tested at various institutions in Canada and abroad. This configuration has been found to be easy to construct in prototype. Five capacitance type water level transducers were placed just in front of the breakwater to measure the dynamic water level fluctuations. An additional water level transducer was placed immediately in front of the paddle to measure the deep water wave conditions.

Preliminary work was done before the breakwater was built to synthesize, generate and sample the waves and determine the appropriate span settings (settings that control the maximum excursion of the wave paddle) for the wave paddle. All the tests in subsequent experiments were then carried out using the same waves and same span settings. Additionally, the wave records measured during tests with the breakwater in place were separated into incident and reflected components. In most cases, excellent agreement was obtained between results of the reflection analysis and those measured with no structure in the flume. The bounded long wave component resulting from the occurrence of wave groups was removed from the analysis using a software filter.

All tests were conducted with irregular waves synthesized using the GEDAP procedure of the National Research Council of Canada Hydraulic Laboratory. Jonswap spectra were generated having periods of peak energy density, ranging from 1 second to 2 seconds and significant wave heights from 6 cm to 14 cm. Four individual wave climates, each representative of a "design storm", were used and these are described below in Tables 3.3 to 3.6

Each segment of each storm was run for a time equivalent to 3000 waves attacking the structure. Profiles were measured before the test and after each segment of test (see figure 3.12 for a typical profile before and after the test). For certain tests, several intermediate profiles were measured after 500, 1000, 1500 and 2000 waves. To assess the long term reshaping process, some tests were carried out for a duration of 36000 waves with profiles measured every 3000 waves. These tests were used to assess the reshaping of breakwaters as a function of storm segment duration. The berm breakwater was considered to have failed when erosion of the berm progressed landward to the intersection of the horizontal berm with the upper 1:3 slope (see figure 3.11).

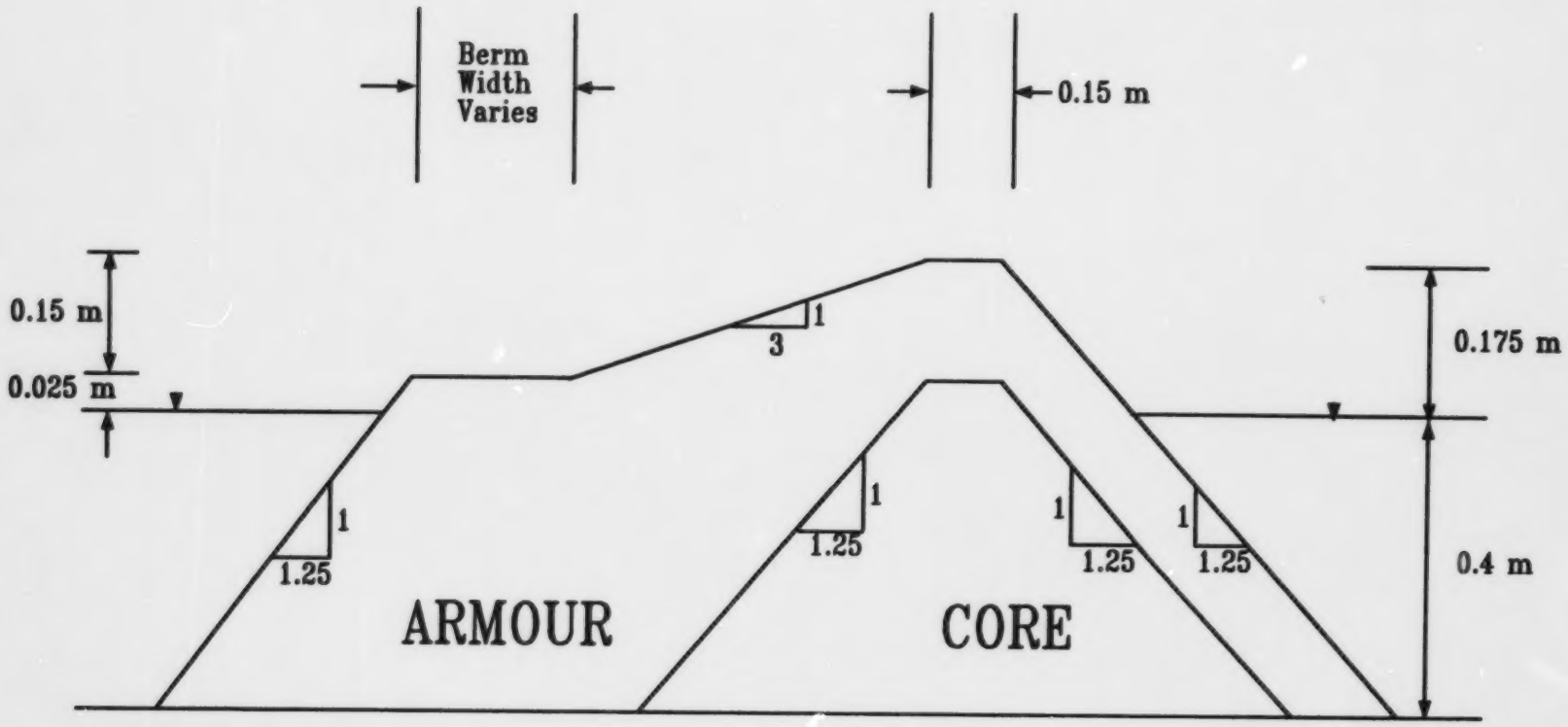

FIGURE 3.11 Layout of test breakwater

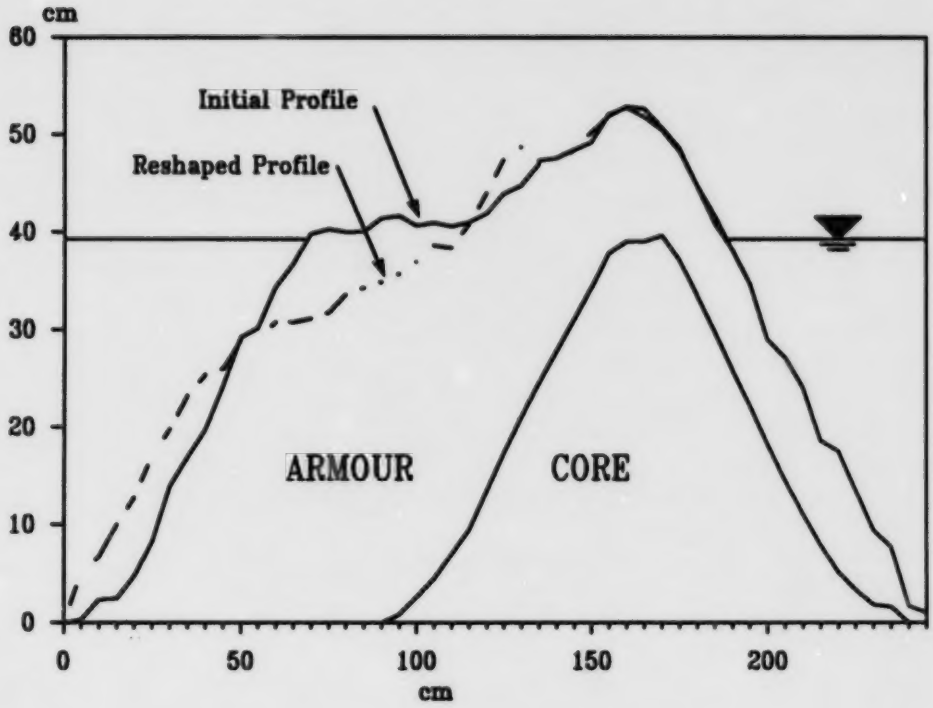

FIGURE 3.12 Reshaping of test breakwater

Table 3.3 Wave Climate 1

H_s(cm)	T_p (sec)	Duration (min)
6	1.0	50
8	1.0	50
10	1.0	50
12	1.2	60
14	1.2	60
12	1.2	60
10	1.0	50
8	1.0	50
6	1.0	50

Table 3.4 Wave climate 2

H_s(cm)	T_p (sec)	Duration (min)
6	1.0	50
8	1.0	50
10	1.2	60
12	1.4	70
14	1.4	70
12	1.4	70
10	1.2	60
8	1.0	50
6	1.0	50

Table 3.5 Wave climate 3

H_s(cm)	T_p (sec)	Duration (min)
6	1.0	50
8	1.2	60
10	1.4	70
12	1.6	80
14	1.8	90
12	1.6	80
10	1.4	70
8	1.2	60
6	1.0	50

Table 3.6 Wave climate 4

H_s(cm)	T_p (sec)	Duration (min)
6	1.2	60
8	1.4	70
10	1.6	80
12	1.8	90
14	2.0	100
12	1.8	90
10	1.6	80
8	1.4	70
6	1.2	60

The following general procedures were followed during each test:

(1) A test was not commenced until the water surface in the flume was completely calm.

(2) Predetermined settings on the hydraulic wave generator were used for all wave conditions.

(3) The same number of samples of water level variations were taken. Sampling would start on the passage of the third wave.

(4) The locations of the water level transducers did not vary from test to test.

(5) Observations were made regarding stone movement resulting from wave attack, both initially and after the breakwater profile reached near equilibrium.

(6) The breakwater was not rebuilt following each segment of wave attack. Rebuilding of the entire breakwater was done following the completion of a test storm and carried out under water, to simulate, as close as possible, prototype construction conditions.

(7) The water level transducers and profiler were calibrated every 3 days and were found to remain stable over the duration of the testing programme.

3.3 TEST PROGRAMME

A total of 52 series of tests were completed in which the following parameters were varied:

- wave climate
- duration of each storm segment
- wave height
- wave period
- wave groupiness
- shape of stones (different percentage of rounded stones)
- uniformity of stones

A summary of the tests carried out in the test programme are shown in tables 3.7 to 3.12. Details of each wave climate were provided in section 3.2.4. The water level was not varied during the test programme. It was assumed that the levels used in these tests was characteristic of maximum design levels for a particular site (that is, a minimum freeboard for the berm elevation in relation to the maximum design water level existed). Previous research has shown that the worst case scenario for reshaping occurs at the maximum water level. In fact, in tidal locations, one or more complete tide cycles will occur during the passage of a storm and consequently reshaping may not be as severe as that indicated in the tests with a constant water level.

Table 3.7 List of tests, gradation 1

Test No.	Wave Climate	Initial Berm Width (cm)
1	1	15
2	1	45
3	1	26
4	1	32
5	1*	32
6	4	32
7	1	41
8	1*	52
9	2*	52
10	3*	52
11	4*	52

Note 1 * only the peak segment of storm was run

Note 2 synthesized groupiness factor = 0.75

Table 3.8 List of tests, gradation 2

Test No.	Wave Climate	Initial Berm Width (cm)	Synthesised Groupiness Factor
12	1*	52	0.75
13	2*	52	0.75
14	2	52	0.75
15	3*	52	0.75
16	4*	52	0.75
17	3	52	0.75
18	1	45	0.75
19	2	45	0.75
20	3	45	0.75
21	4	45	0.75
22	2	49	0.75
23	2*	49	0.25
24	2*	49	0.5
25	2*	49	1.0
26	2*	49	0.75

Note 1 * only the peak segment of storm was run

Table 3.9 List of tests, gradation 3

Test No.	Wave Climate	Initial Berm Width (cm)	Synthesised Groupiness Factor
27	1	38	0.75
28	1*	48	0.75
29	2	62	0.75
30	3	62	0.75
31	1	45	0.75
32	1	48	0.75
33	2	48	0.75
34	3	48	0.75
35	4	48	0.75
36	2*	48	0.75
37	2*	48	0.50
38	2*	48	1.00
39	2*	48	0.25

Note 1 * only the peak segment of storm was run

Table 3.10 List of tests, gradation 4

Test No.	Wave Climate	Initial Berm Width (cm)
40	1	45
41	2	52
42	3	52
43	4	52

Note 1 synthesised groupiness factor = 0.75

Table 3.11 List of tests, gradation 2A

Test No.	Wave Climate	Initial Berm Width (cm)
44	1	58
45	2	58
46	3	58
47	4	58
48	1	50

Note 1. synthesised groupiness factor = 0.75

Table 3.12 List of tests, gradation 2B

Test No.	Wave Climate	Initial Berm Width (cm)
49	1	47
50	2	47
52	3	47
52	4	47

Note 1. synthesised groupiness factor = 0.75

3.4 TWO DIMENSIONAL TEST RESULTS

3.4.1 General Observations During Testing

It was found that the largest portion of berm erosion occurred during the attack of the first few relatively big waves in the wave train. The zone in which movement of stones occurred was located at the seaward edge of the berm. The stones moved by rolling about the slope. On passing of the first few waves, there was little sign of motion of stones in the landward region of the berm; the principal mode of reshaping was by rounding-off of the exposed corner of the berm.

After approximately five to ten big waves, there was very little mass movement, and subsequently, stones moved individually rather than "en masse". With time, the initial berm receded and armour stones were individually removed by the wave forces and deposited at some other location on the slope. With each impinging wave breaking on the berm, stones were removed from the outer edge of he berm and carried by uprush and downrush moving to and fro on the profile formed as a result of erosion. A net migration of stones offshore was observed from the profiles measured following each section of the design storm. The reshaping process was usually too slow to be noticeable to the human eye (apart from the initial "shakedown" of the mound).

3.4.2 Reduction and Analysis of Data

In the following section the influence of each of the test parameters on the three descriptive parameters (L/D_{50}, B/D_{50} and A/D_{50}^2) is presented.

3.4.2.1 Effect of wave height

Toe Width (L)

Figure 3.13 shows a plot of the dimensionless toe width, L/D_{50} against $H_s/((S_r-1)D_{50})$ for all gradations of armour stones. A non-linear relationship exists between the toe width and the wave height; as the wave height increases, the toe width that results increases. This indicates larger quantities of erosion at higher values of wave height.

Plots of L/D_{50} against stability number for each individual armour gradation are shown in figures 3.14 to 3.17.

Volume of Stones (A)

The dimensionless volume of armour stones, A/D_{50}^2, following reshaping is plotted in figure 3.18 for all gradations. It is obvious that there is a clear dependence of volume of armour stones following reshaping on the stability number, with a small gradational bias being exhibited.

Individual plots of A/D_{50}^2 against $H_s/((S_r-1)D_{50})$ for gradations 1, 2, 3 and 4 are shown in figures 3.19 to 3.22.

Width of berm eroded (B)

As expected, the dimensionless width of the berm eroded B/D_{50} was found to have a strong dependence on the wave height. Figure 3.23 shows the relationship for all gradations and indicates a slight gradational bias. Figures 3.24 to 3.27 shown the relationship for gradations 1, 2, 3 and 4.

3.4.2.2 Effect of uniformity of stones

Toe width (L)

Figure 3.28 shows the relationship between L/D_{50} and the stability number for the four gradation of stones having a D_{50} of 1.9 cm, and containing 30% rounded stones. It is seen that gradation 1 is least susceptible to reshaping indicating that the presence of substantial voids in the armour layer contributes to an efficient wave energy dissipation system. As the relative width of the gradation is increased, there are effectively fewer voids in the armour stone matrix. Figure 3.28 shows that the toe width developed increases for gradations 2 and 3. This trend, however, reverses for gradation 4. It is hypothesized that as the maximum stone size in the gradation increases, the influence of a large quantity of stones exceeding a certain upper threshold size begins to dominate over the influence of voids on stability. In gradation 4, a sizeable proportion (20%) of the armour stones exceeds 100 gm in weight. The presence of these large stones no doubt has a considerable influence over the stability of the armour layer.

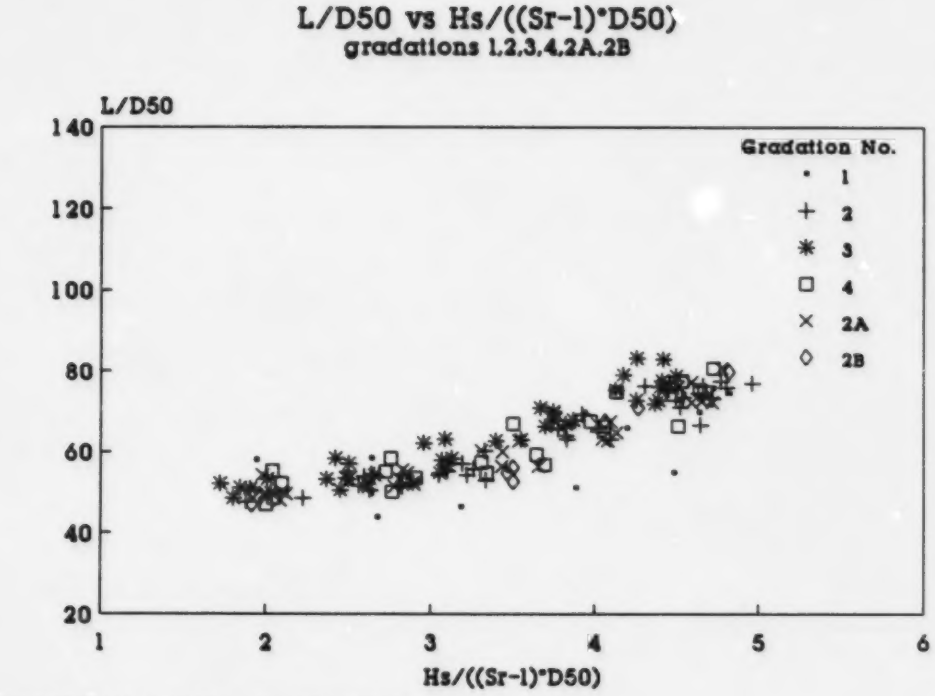

FIGURE 3.13 L/D50 vs Hs/((Sr-1)*D50)

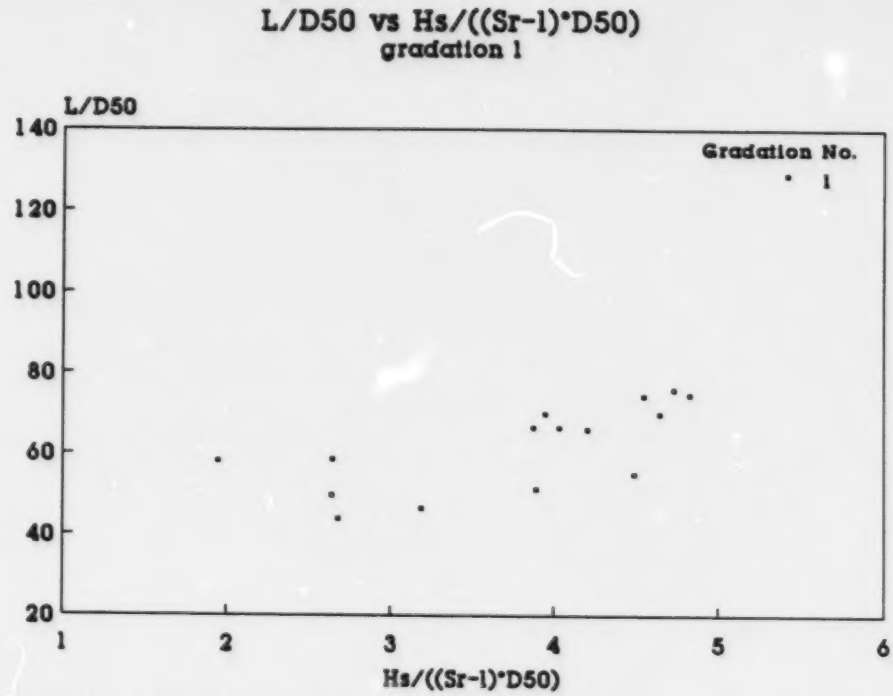

FIGURE 3.14 L/D50 vs Hs/((Sr-1)*D50)

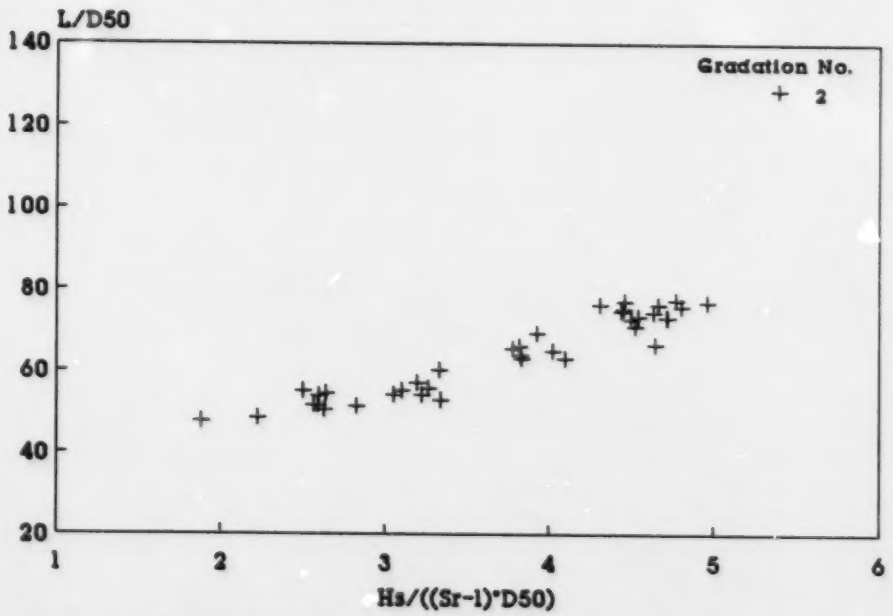

FIGURE 3.15 L/D50 vs Hs/((Sr-1)*D50)

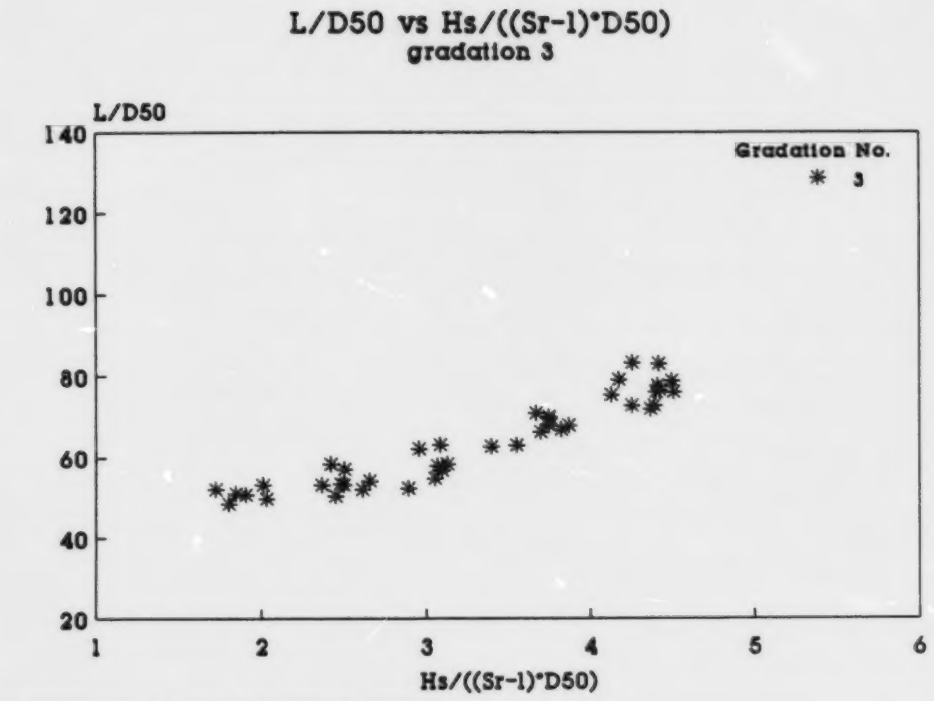

FIGURE 3.16 L/D50 VS Hs/((Sr-1)*D50)

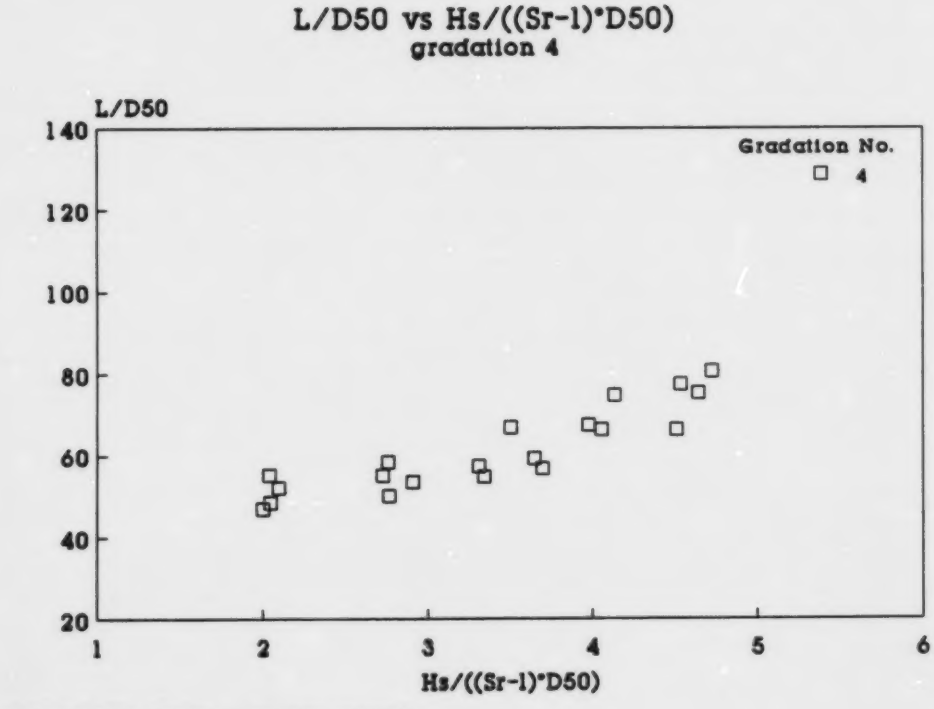

FIGURE 3.17 L/D50 vs Hs/((Sr-1)*D50)

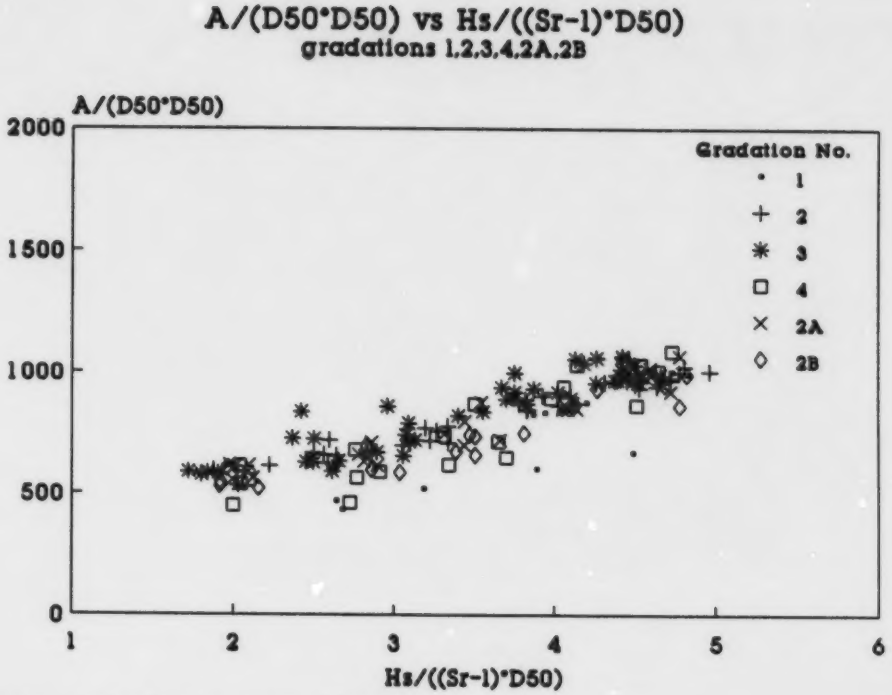

FIG 3.18 A/(D50*D50) vs Hs/((Sr-1)*D50)

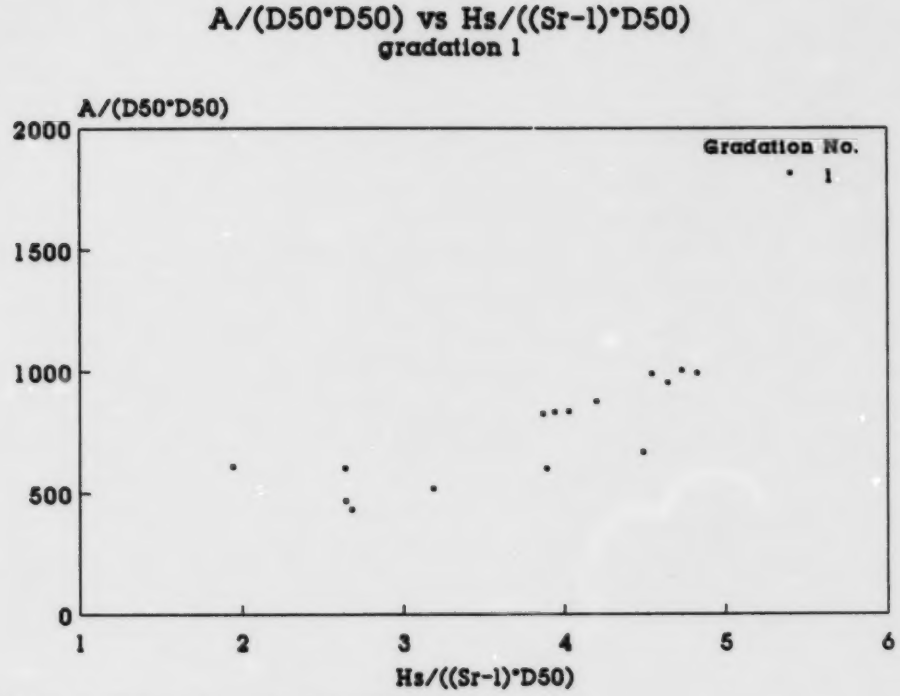

FIG 3.19 A/(D50*D50) vs Hs/((Sr-1)*D50)

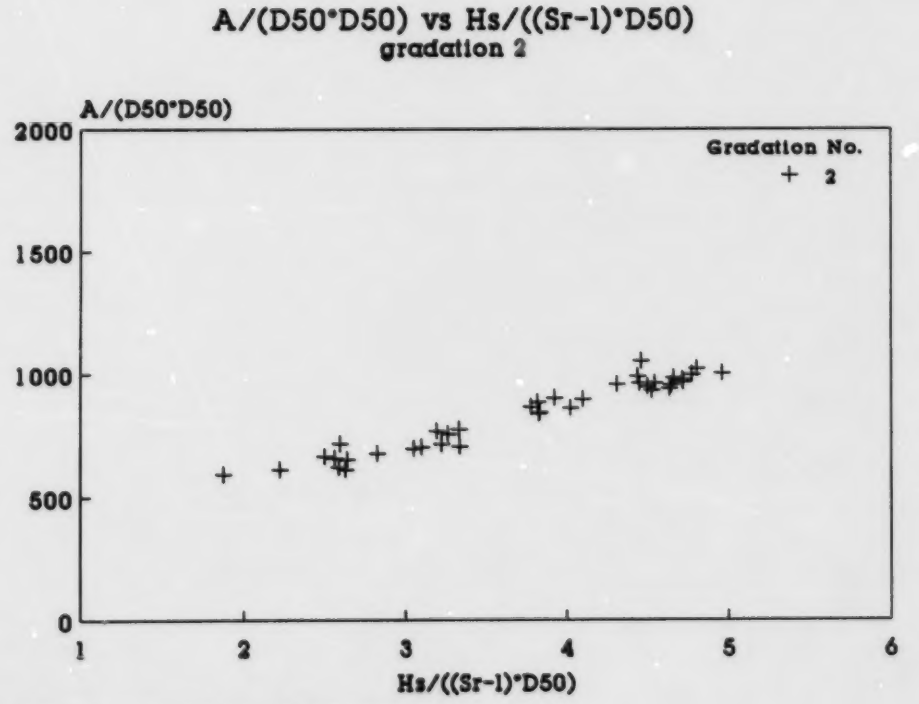

FIG 3.20 A/(D50*D50) vs Hs/((Sr-1)*D50)

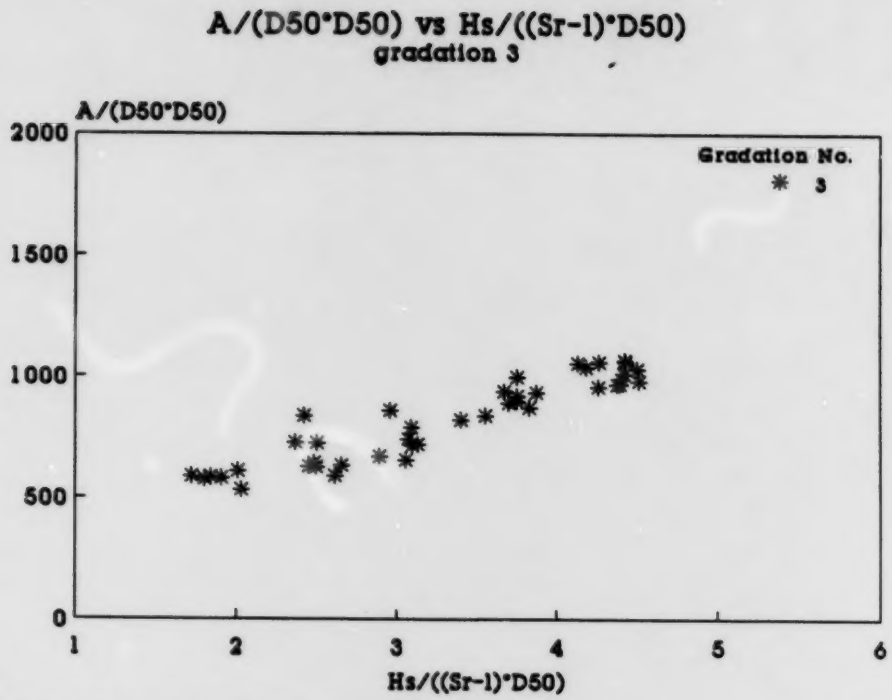

FIG 3.21 A/(D50*D50) vs Hs/((Sr-1)*D50)

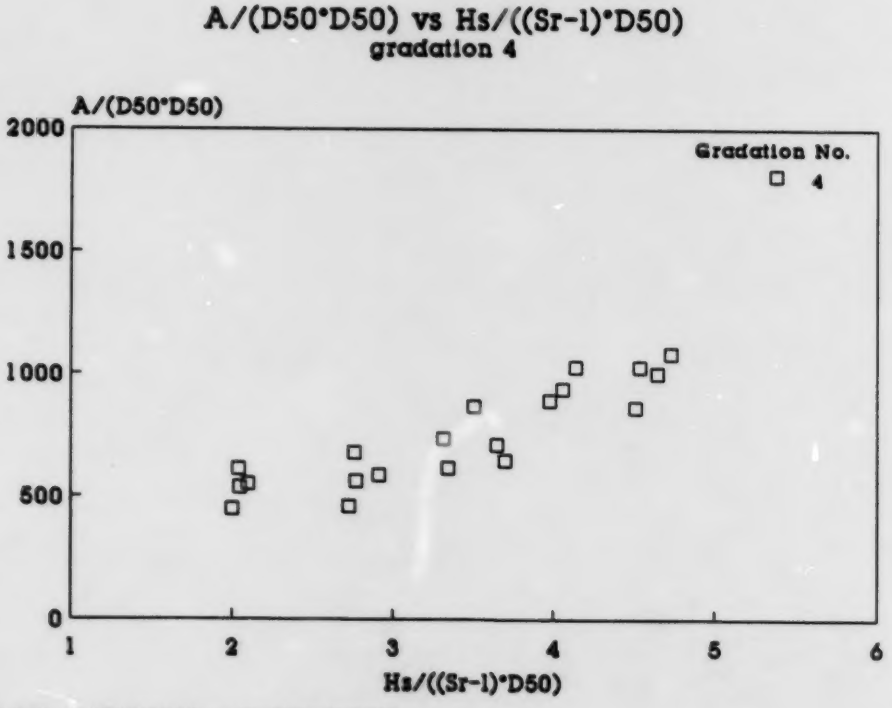

FIG 3.22 A/(D50*D50) vs Hs/((Sr-1)*D50)

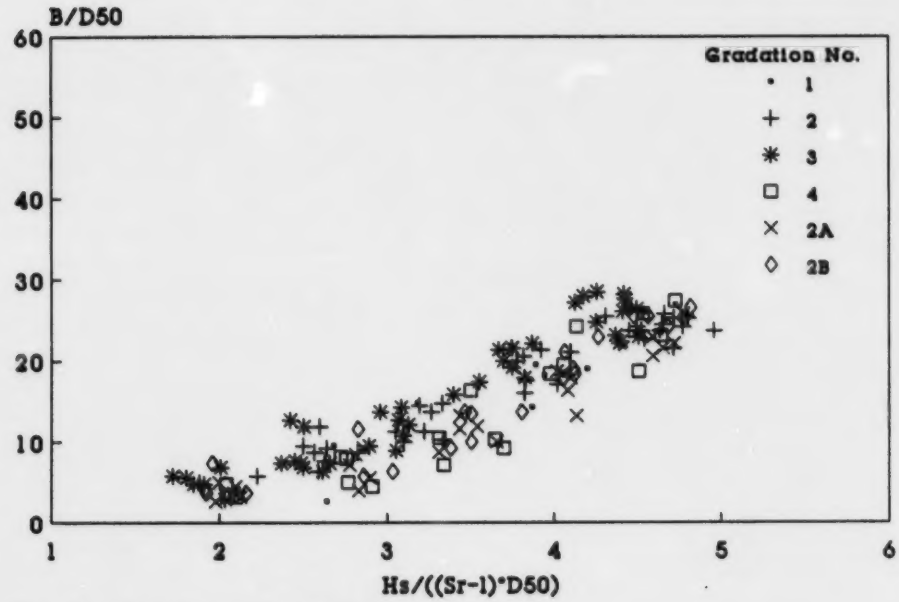

FIGURE 3.23 B/D50 vs Hs/((Sr-1)*D50)

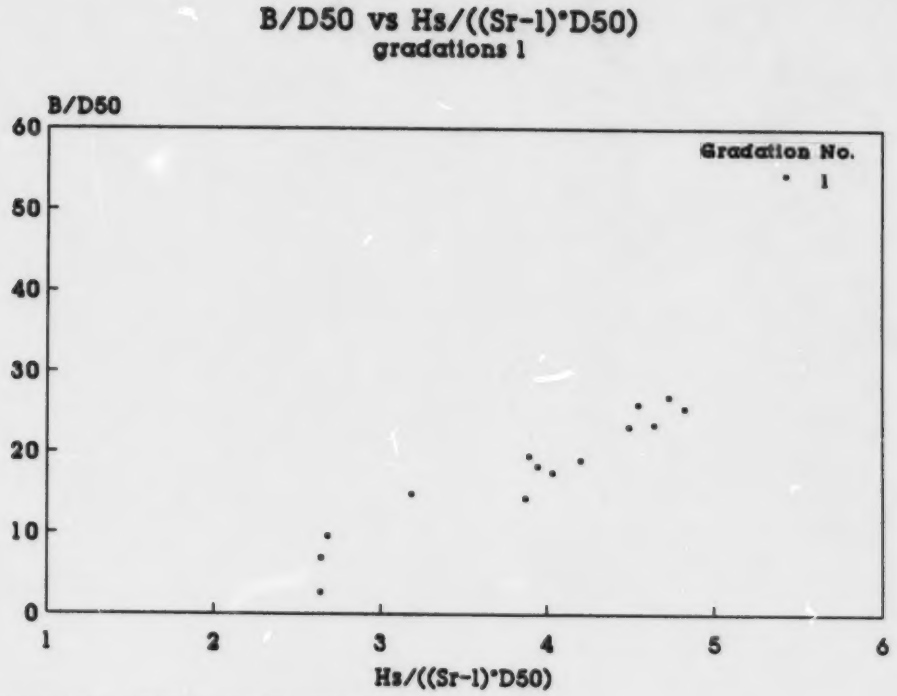

FIGURE 3.24 B/D50 vs Hs/((Sr-1)*D50)

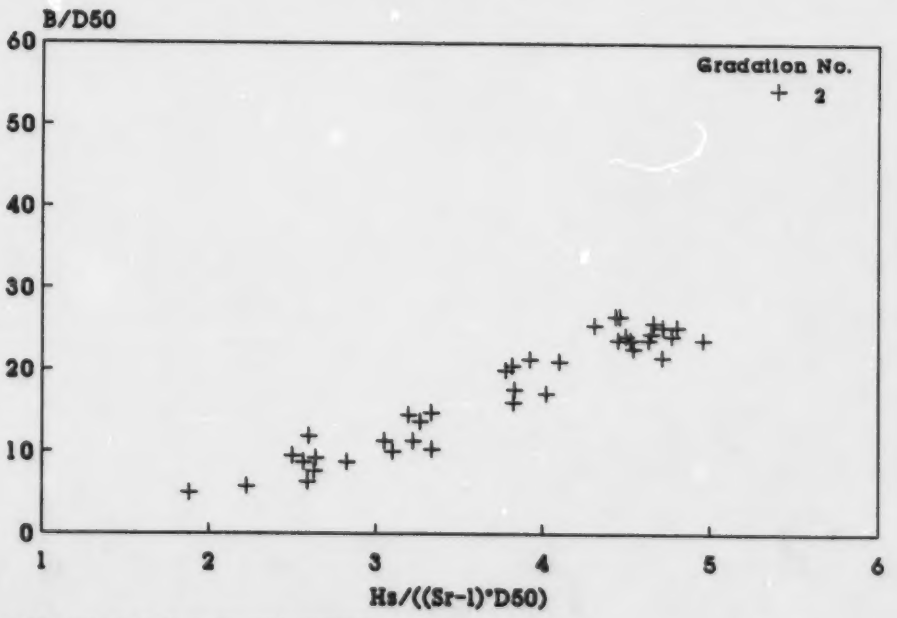

FIGURE 3.25 B/D50 vs Hs/((Sr-1)*D50)

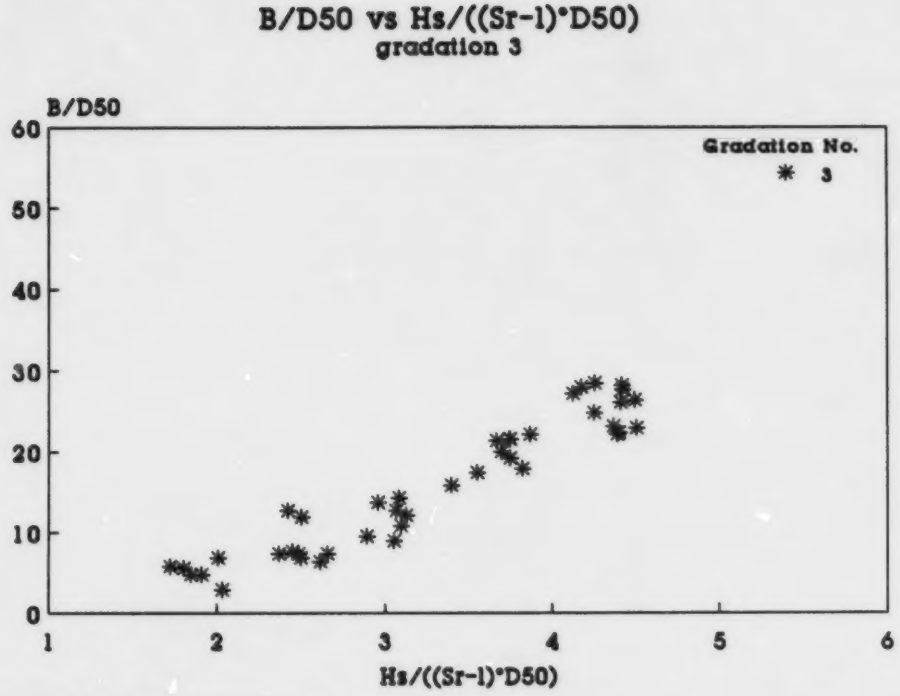

FIGURE 3.26 B/D50 vs Hs/((Sr-1)*D50)

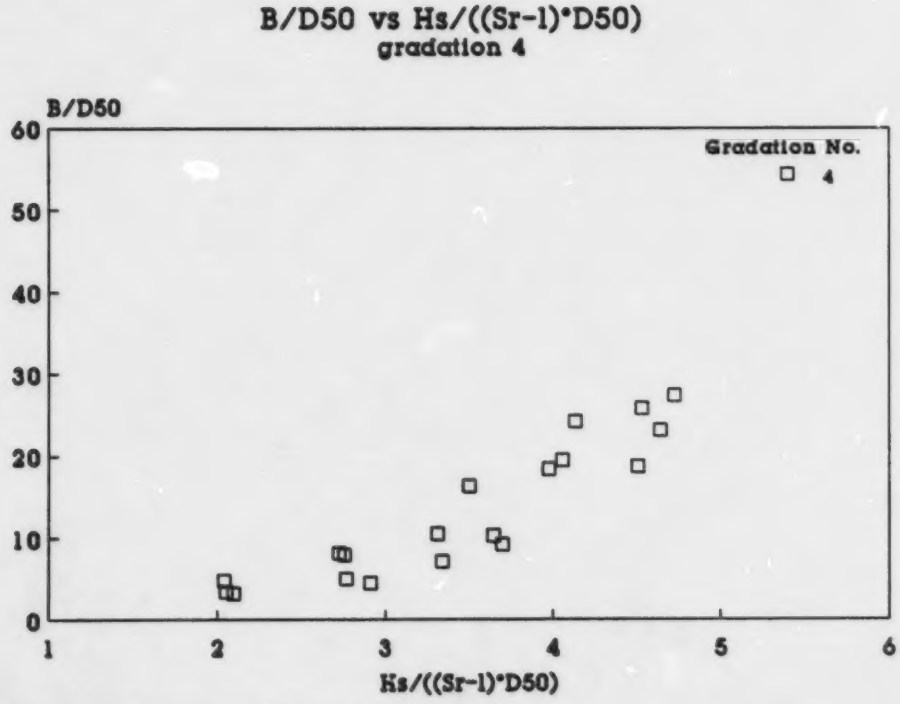

FIGURE 3.27 B/D50 vs Hs/((Sr-1)*D50)

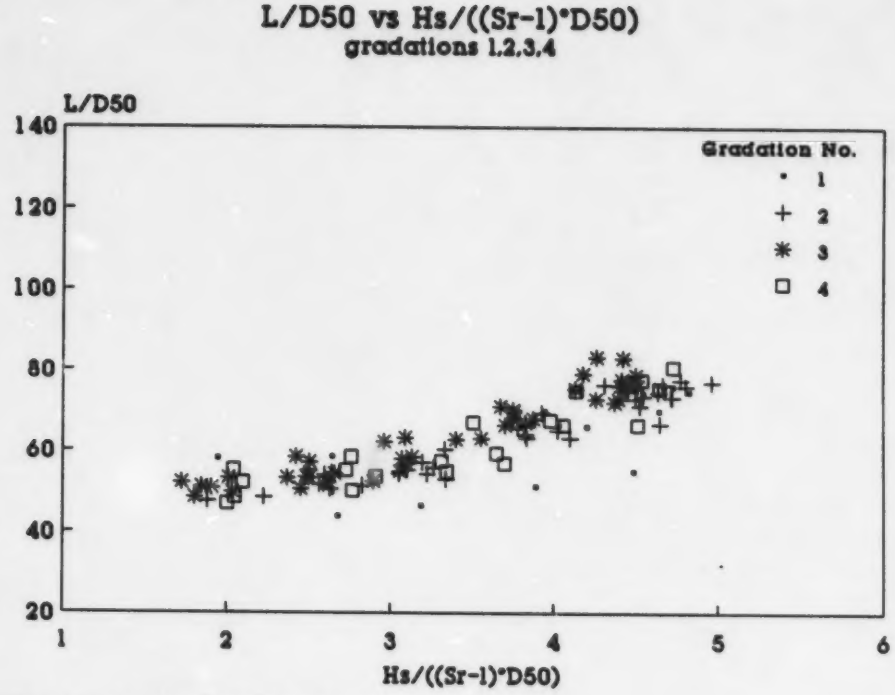

FIGURE 3.28 L/D50 vs Hs/((Sr-1)*D50)

Volume of stones (A)

Figure 3.29 shows plots of A/D_{50}^2 with $H_s/((S_r-1)D_{50})$ as a function of gradation. The same trends described above are observed in this case, namely, the narrowest gradation, having the highest voids ratio is more resistant to reshaping and thus requires a smaller volume of stones in order to reshape into a stable profile.

Width of berm eroded (B)

Figure 3.30 shows values of B/D_{50} plotted against stability number, and illustrates that there is an obvious effect of gradation on the erosion of the berm. Gradations 1 and 4 are more resistant to erosion, other things being constant. Gradation 2 and 3 are less resistant to erosion.

3.4.2.3 Influence of rounded stones in the gradation

The percent of rounded stones will increase with service on a breakwater as a result of chipping and rounding occurring during the motion of stones as the stable profile is developed. The influence of varying the percentage of rounded stones in one of the relative gradations (gradation 2) was assessed. Gradation 2 was selected as it closely approximates the ratio of D_{85}/D_{15} found in many prototype structures. Gradations 2, 2A and 2B contained varying percentages of rounded stone. Gradation 2A represents angular armour stones, gradation 2B represents a more rounded stone matrix with 15% rounded stones, and gradation 2 represents armour material having the highest percentage of rounded stone (30%).

Toe width (L)

In figure 3.31, no significant influence of the percentage of rounded stones in the armour layer on the width of the toe of the breakwater following reshaping was found. Brebner (1978) showed that dolosse armour units were no more hydraulically stable than stones of the same weight in open channel flow. Burcharth and Thompson (1983) indicated that in oscillatory flow, there was no appreciable difference in hydraulic stability between rock armour units and dolosse. In the present case,there is some resemblance to the results of Brebner (1978) and Burcharth and Thompson (1983), in that the stones were removed from the horizontal berm of the breakwater. Such behaviour seems to confirm their results that when the armour units are completely submerged the shape of the armour units do not significantly affect the hydraulic stability.

Volume of stones (A)

Figure 3.32 shows the effect of different percentage of rounded stones on A/D_{50}^2. No distinct trend was observed.

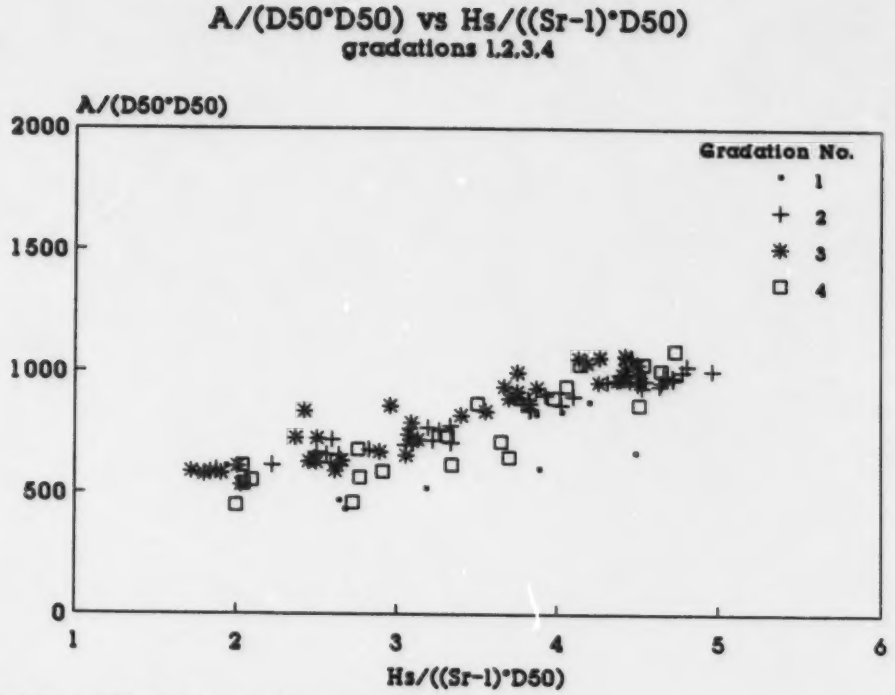

FIG 3.29 A/(D50*D50) vs Hs/((Sr-1)*D50)

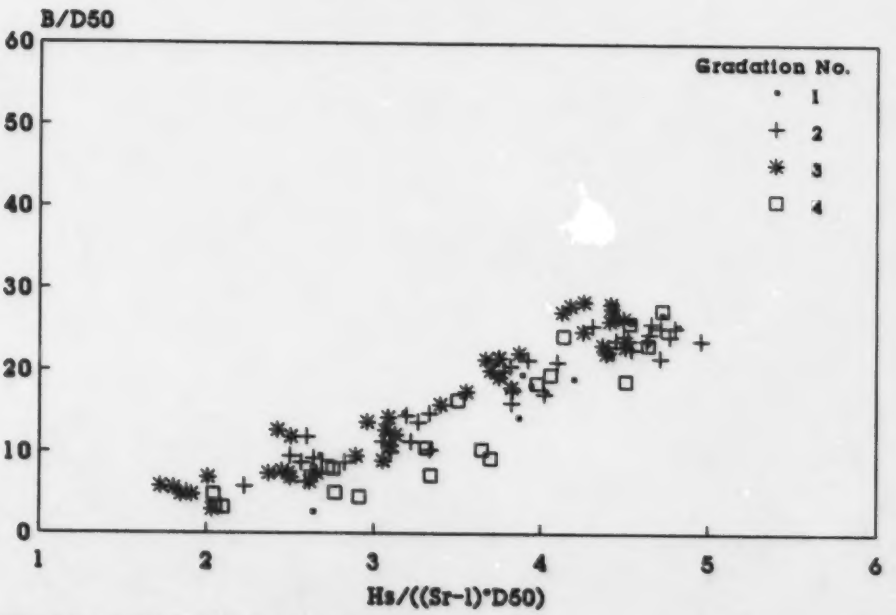

FIGURE 3.30 B/D50 vs Hs/((Sr-1)*D50)

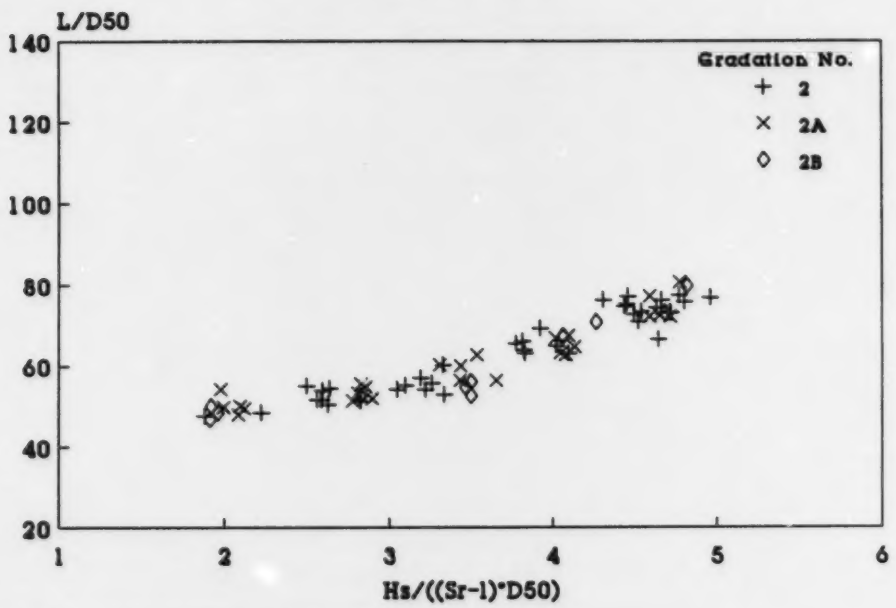

FIGURE 3.31 L/D50 vs Hs/((Sr-1)*D50)

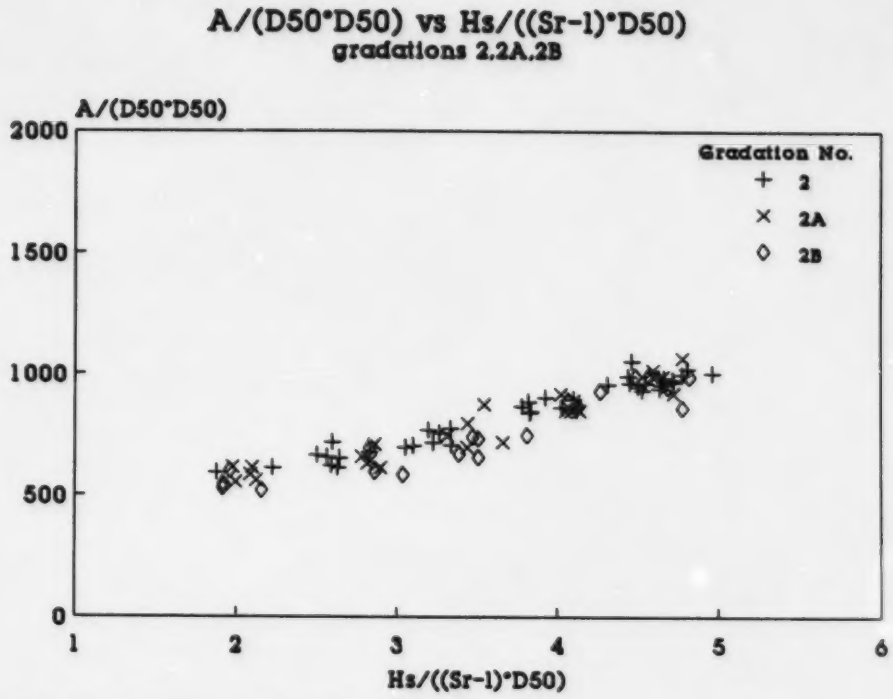

FIG 3.32 A/(D50*D50) vs Hs/((Sr-1)*D50)

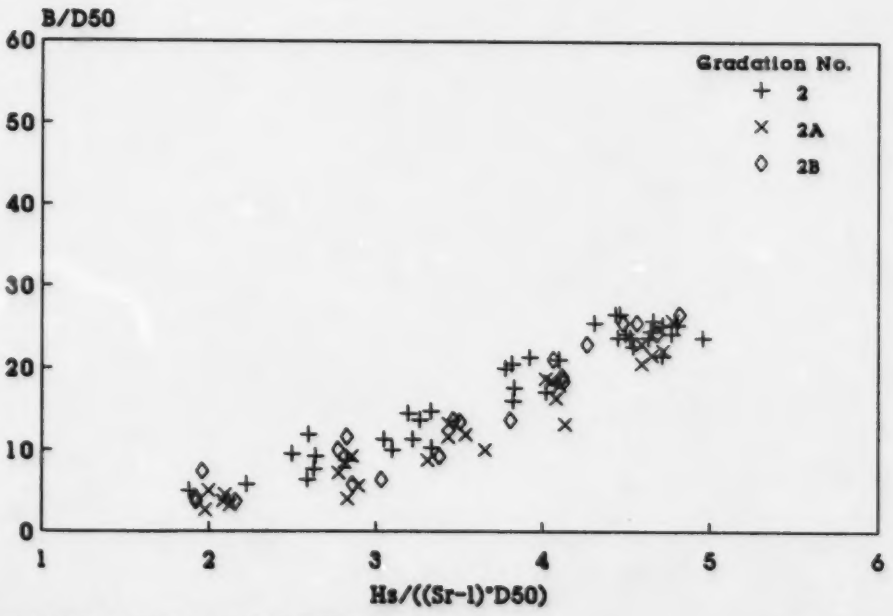

FIGURE 3.33 B/D50 vs Hs/((Sr-1)*D50)

Width of berm eroded (B)

Figure 3.33 shows a plot of the berm width eroded against the instability number for armour stones with different percentages of rounded stones. Gradation 2A stones were found to be more resistant to erosion than gradation 2 stones indicating the proportion of rounded stones in the gradation affects initial movement. A student-t-test indicated that at a significance level of 0.4%, B/D_{50} is dependent on the percentage of rounded stones.

Figure 3.32, shown previously, indicates that the shape of stones does not influence the volume of stones required for reshaping. This apparent anomaly is easily explained by the fact that the results in the previous paragraph indicate that recession of berm is sensitive to the shape of stones. This carries no implication that after the angular stones are moved from the crest of the horizontal berm to areas below the still water level they have the same resistance to erosion; obviously, this is not the case. Figure 3.34 provides a description of the zones of the breakwater in which stone shape appears to be important. The area in the critical zone, when compared with the area under consideration in reshaping (shown dotted) is insignificant, thus explaining this apparent anomaly.

3.4.2.4 Effect of wave groupiness GF

In general, it was found that the reshaping process was not sensitive to the wave groupiness of the incident wave climate. As shown in Tables 4.7 to 4.12, a range of groupiness factor from 0.25 to 1.25 was utilized in the testing programme.

The extent of the variation of GF with $H_s/((S_r-1)D_{50})$ is shown in figure 3.35 A general trend is indicated such that with increasing wave height, the wave groupiness of the measured waves decreases, even though the same target groupiness factor was specified throughout when synthesizing the waves. Furthermore, it is seen that the measured groupiness factor fluctuated considerably within a band of approximately 0.3, or within a limit of ± 15% to ± 25%. The range of the measured groupiness factors are consistent with values measured in prototype.

Close inspection of figure 3.35 indicates that for small wave heights (H_s = 6 cm and $H_s/((S_r-1)D_{50}) \approx 2$), the groupiness factors ranged from 0.8 to 1.15. With increasing wave heights, the groupiness factors ranged from 0.5 to 0.8, lying within a band of about 0.3.

To remove the dependent relationship between wave height and wave groupiness, a dimensionless parameter $GF/(H_s/((S_r-1)D_{50}))$ was chosen for the x-axis. Since wave groupiness and wave height are both "load" parameters, it is reasonable to combine two load parameters to give a new "load" parameter.

The resulting plot of L/D_{50} versus $GF(S_r-1)D_{50}/H_s$ for all six gradations and all wave heights is shown in figure 3.36. To emphasize the effect of rounded stones and effect of gradation on reshaping the same data are plotted on two separate figures, 3.37 and 3.38. In figure 3.37 the effect of gradation is emphasized and in figure 3.38 the effect of rounded stones is emphasized.

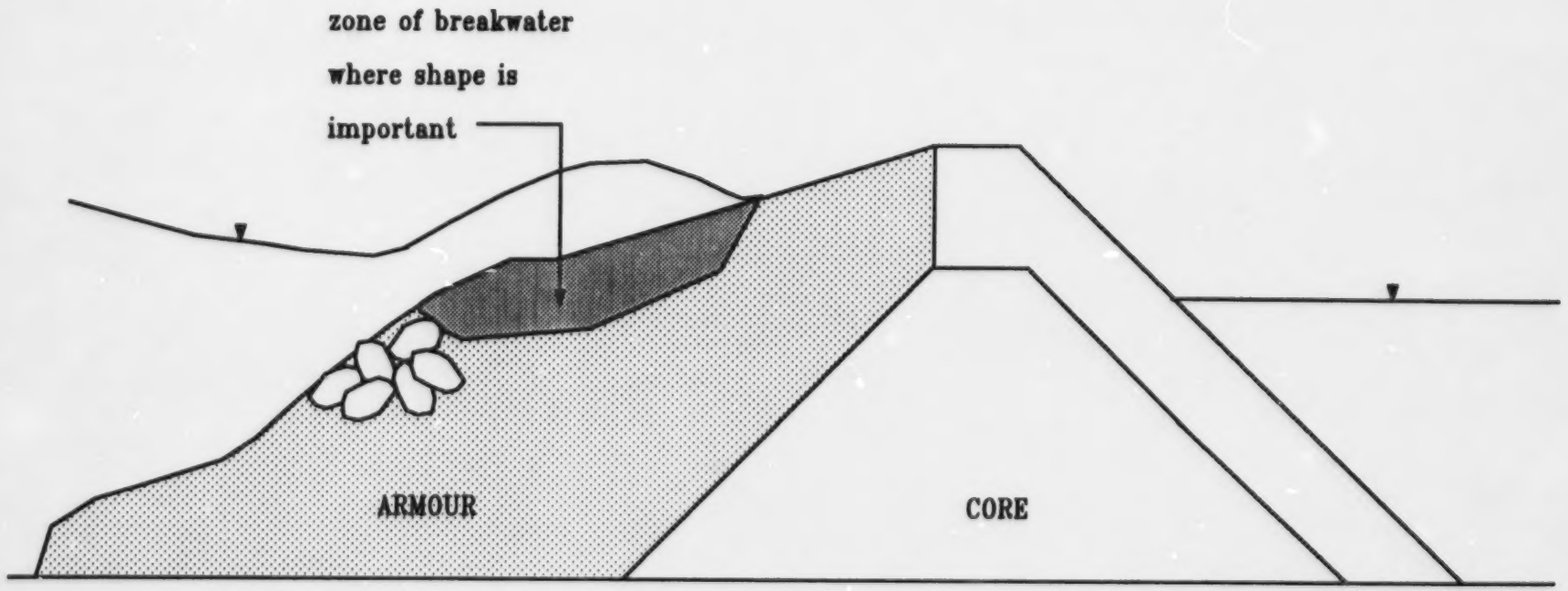

FIGURE 3.34 Zone of breakwater where shape is important

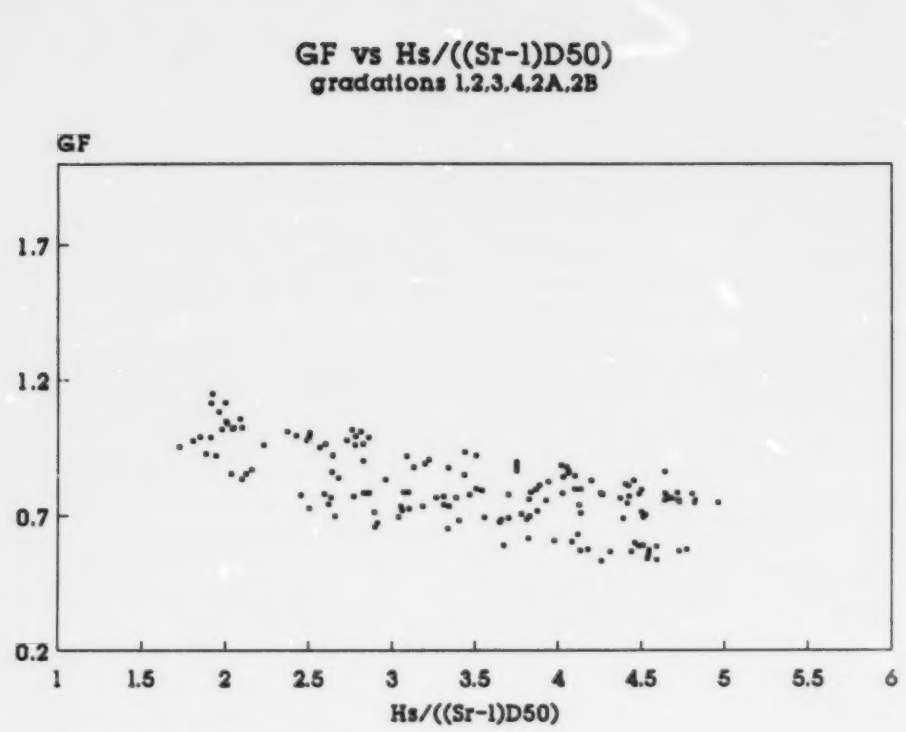

FIGURE 3.35 GF vd Hs/((Sr-1)D50)

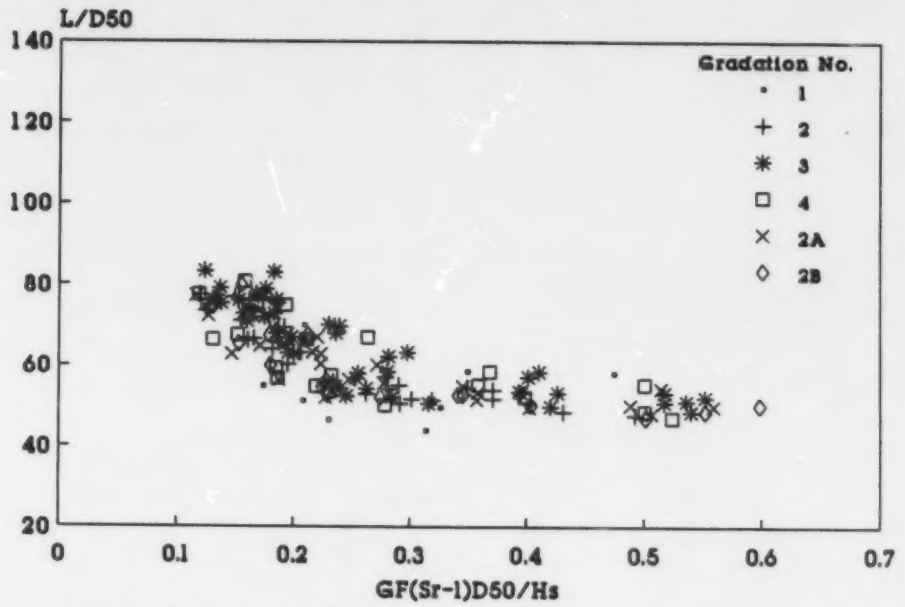

FIGURE 3.36 L/D50 vs GF(Sr-1)D50/Hs

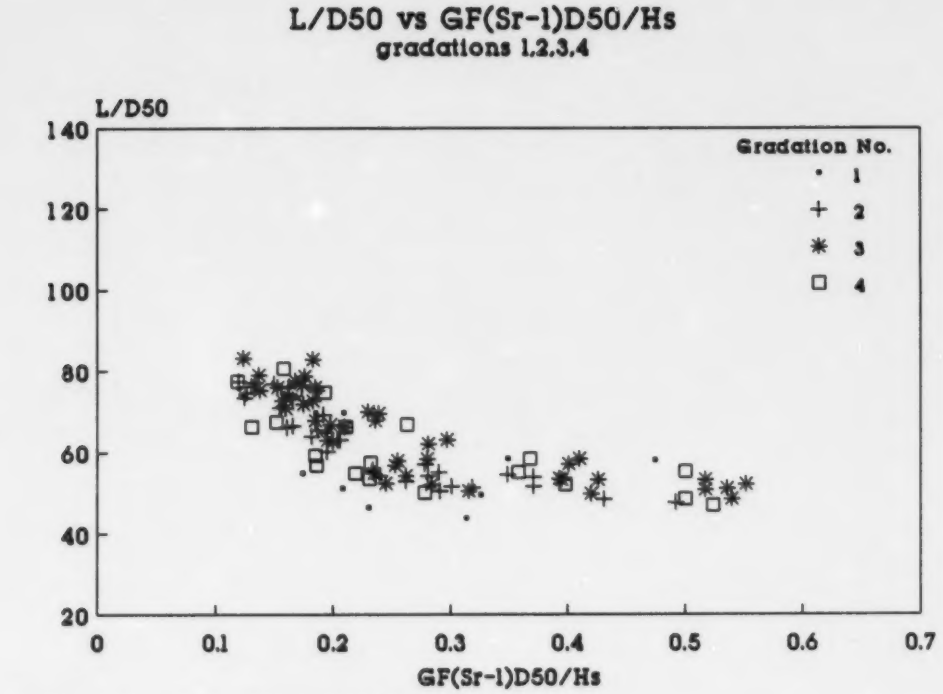

FIGURE 3.37 L/D50 vs GF(Sr-1)D50/Hs

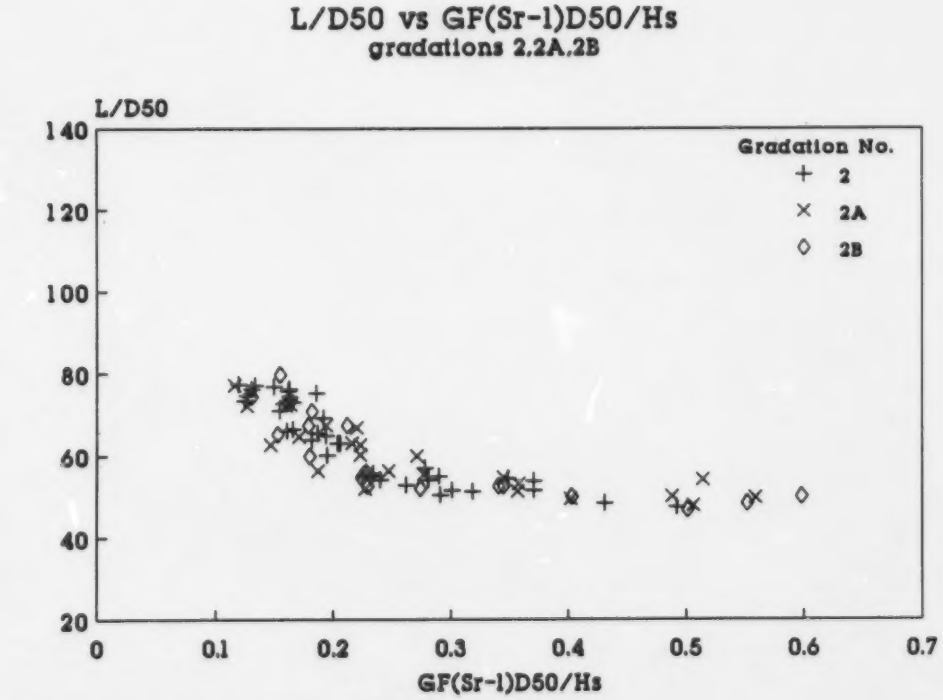

FIGURE 3.38 L/D50 vs GF(Sr-1)D50/Hs

However, presenting data using the combined dimensionless parameter may cause one to lose sight of the physical interpretation. In order to present beyond a doubt any such dependence, a one to one relationship between the dependent parameters (A/D_{50}^2, L/D_{50}, and B/D_{50}) and independent parameters ($H_s/((S_r-1)D_{50})$, GF, wave steepness, wave period T_p, T_{av}, and number of waves) should be assessed.

Consequently, the dependent parameters L/D_{50}, A/D_{50}^2 and B/D_{50} are plotted as a function of GF for constant values of wave height. Figures 3.39 to 3.42 demonstrate that for each gradation and the same wave height, the toe width shows no dependence on wave groupiness. For example, in two of the largest data sets (gradation 2 and 3, 14 cm waves), the difference in maximum and minimum values of L/D_{50} are 15% and 14.6% of the average respectively, deviating from the mean by less than 8%.

Volume of stones (A)

The volume of stones required for reshaping when plotted against groupiness factor is shown in figure 3.43 for gradations 1 to 4 and in figure 3.44 for gradations 2, 2A and 2B respectively. No obvious conclusion can be drawn from these data since the effect of gradation and wave height are sufficiently significant to mask the effect of wave groupiness. The complete set of data was then sorted according to gradation and then wave height. The results for gradations 1, 2,3 and 4 are shown in figures 3.45 to 3.48, respectively. Gradation 1 is a small data set and does not indicate any strong trends. However, gradations 2, 3 and 4 are sufficiently large to give a good indication of the behaviour of the data. It is observed that the volume of stones reshaped is almost independent of the groupiness factor. This is especially true for higher waves (12 cm and 14 cm), indicating that for berm breakwaters, wave groups have no significant effect on the volume of stones required for reshaping. Note that for smaller waves (8 cm and 10 cm), there appears to be a slight increasing trend in A/D_{50}^2 with increasing groupiness factor.

Width of berm eroded. (B)

Figures 3.49 to 3.52 shows the relationship between the width of berm eroded against groupiness factor for gradations, 1, 2, 3 and 4. There is a slight trend showing that for the smaller wave heights, the width of berm eroded is dependent on the wave groups. For example, in figure 3.51 (gradation 3) the 6 cm, 8 cm, and 10 cm waves all show such a trend, whereas for the same breakwater, values of B/D_{50} for 12 and 14 cm waves remains relatively constant over the range of GF.

The influence of grouped waves appears to be important only during or shortly after the stage of incipient motion of the armour units, which originally are in static equilibrium. Once motion is initiated, the armour units start to move "en masse", and wave groupiness is no longer of primary importance. The overall wave energy in the sea state, characterized by wave height, becomes dominant.

In research conducted on statically stable breakwaters, the focus has been concentrated on the stability of individual armour units (individual movement); whereas, in the case of berm

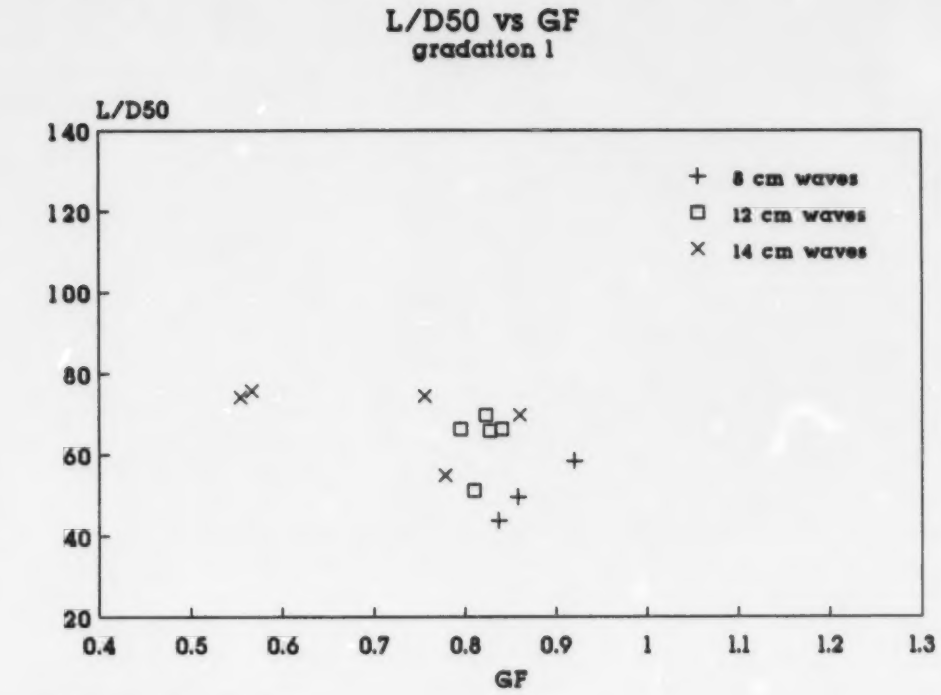

FIGURE 3.39 L/D50 vs GF

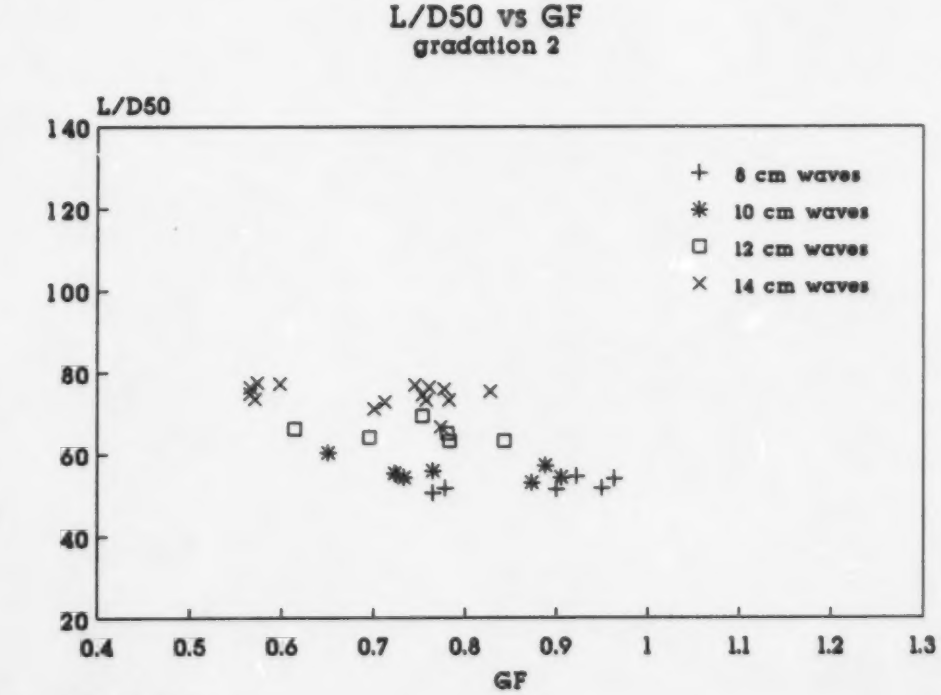

FIGURE 3.40 L/D50 vs GF

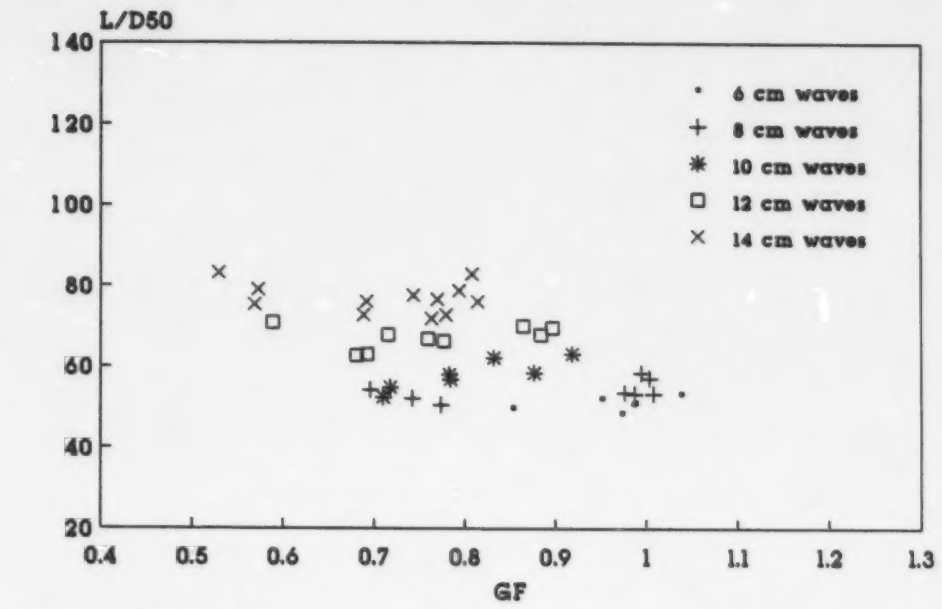

FIGURE 3.41 L/D50 vs GF

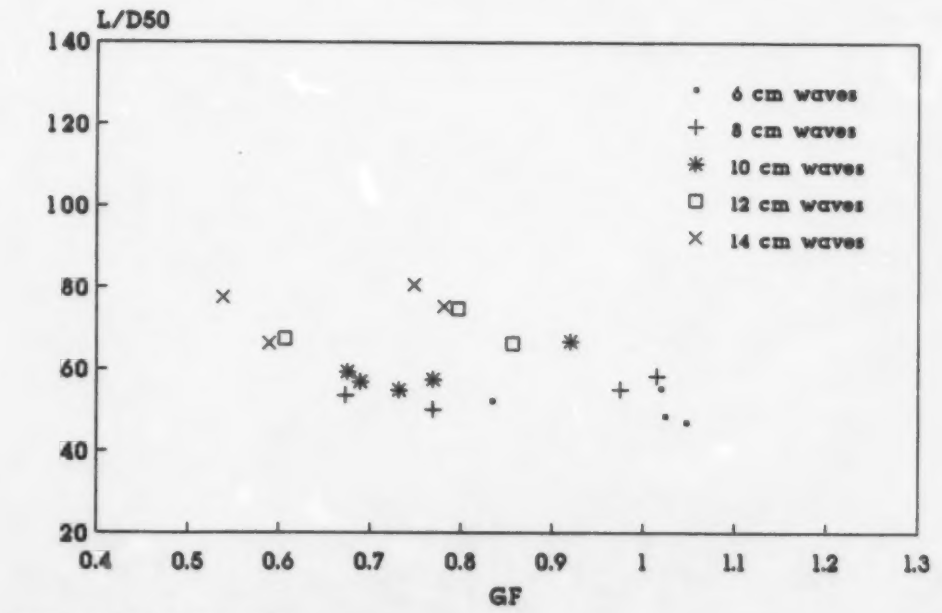

FIGURE 3.42 L/D50 vs GF

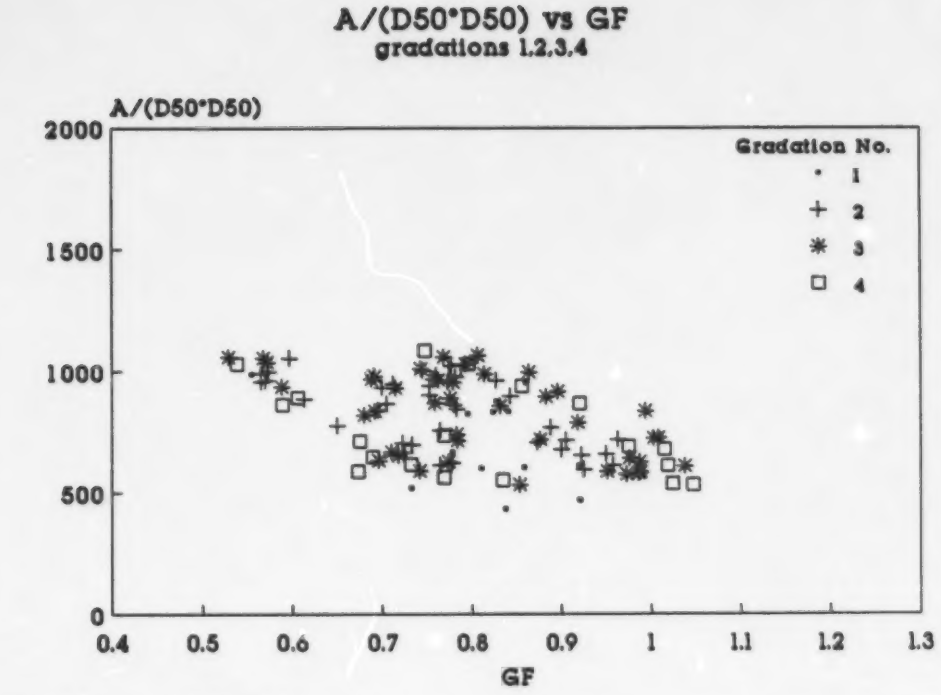

FIGURE 3.43 A/(D50*D50) vs GF

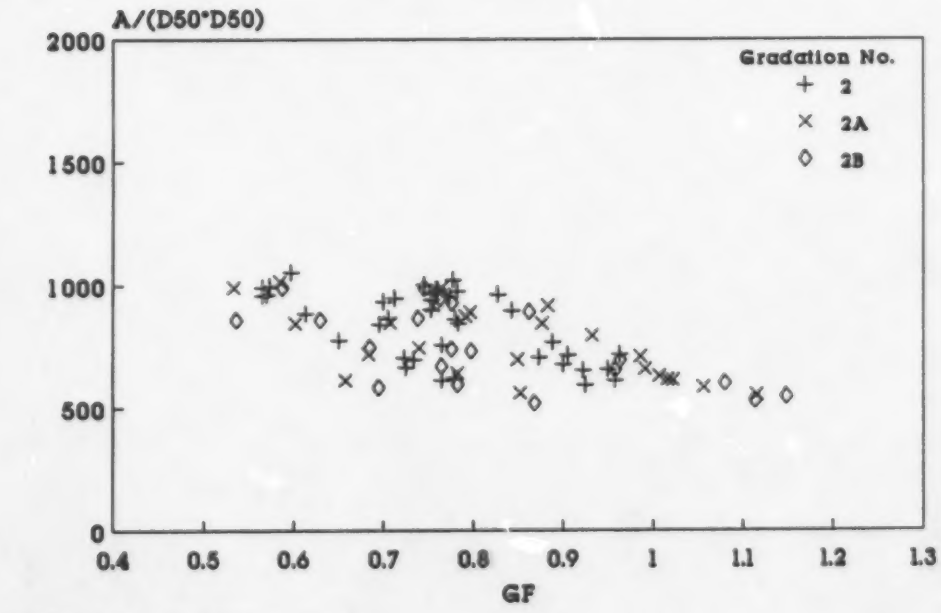

FIGURE 3.44 A/(D50*D50) vs GF

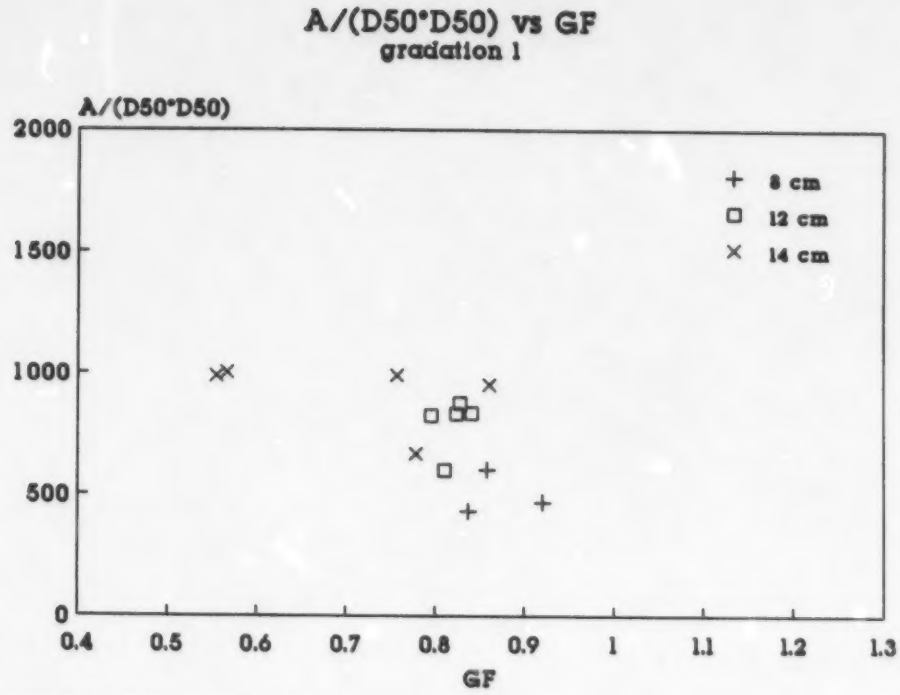

FIGURE 3.45 A/(D50*D50) vs GF

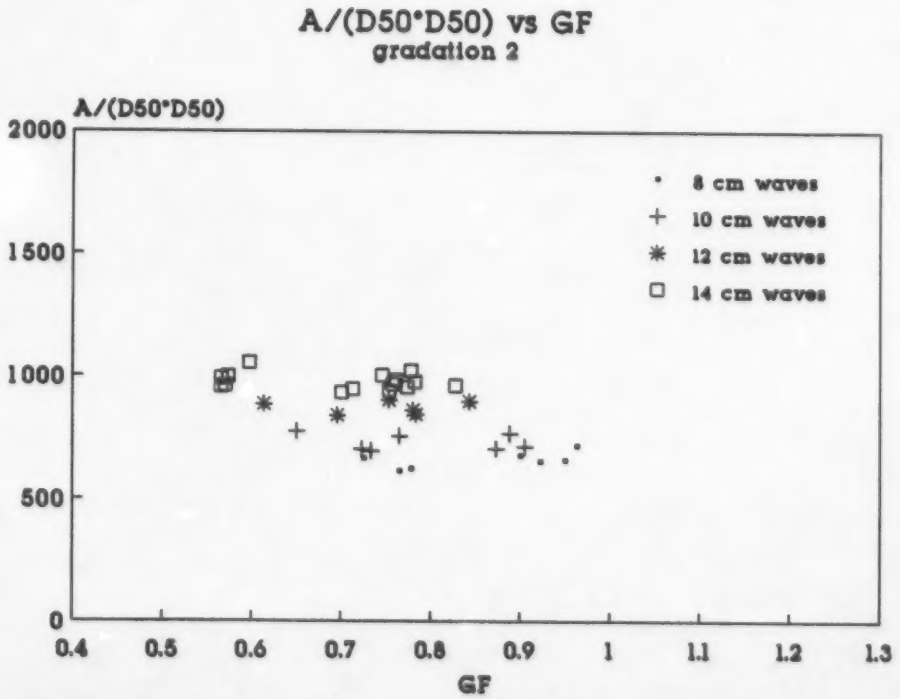

FIGURE 3.46 A/(D50*D50) vs GF

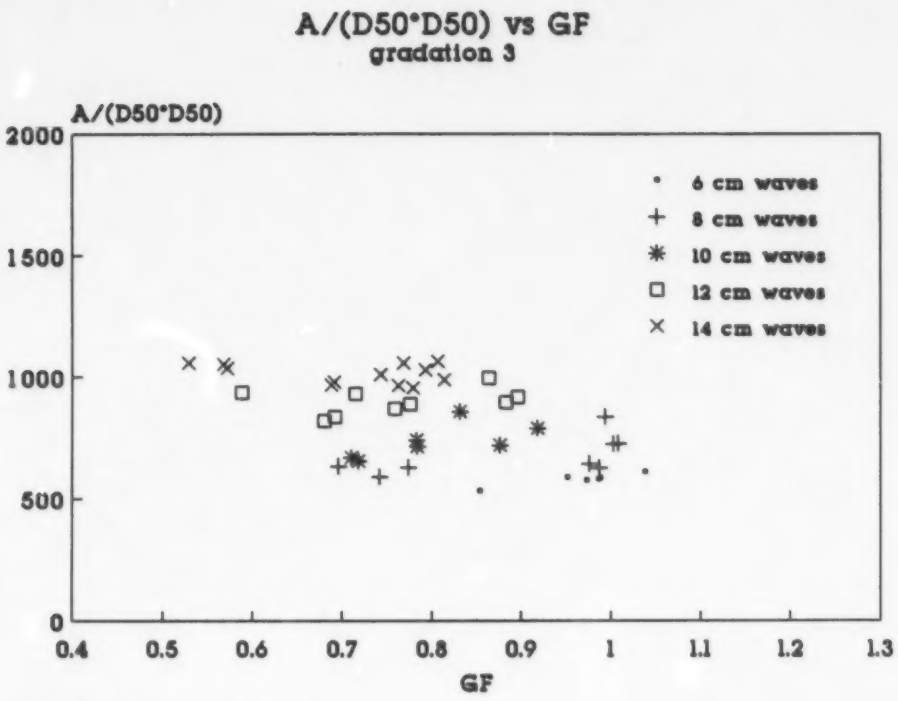

FIGURE 3.47 A/(D50*D50) vs GF

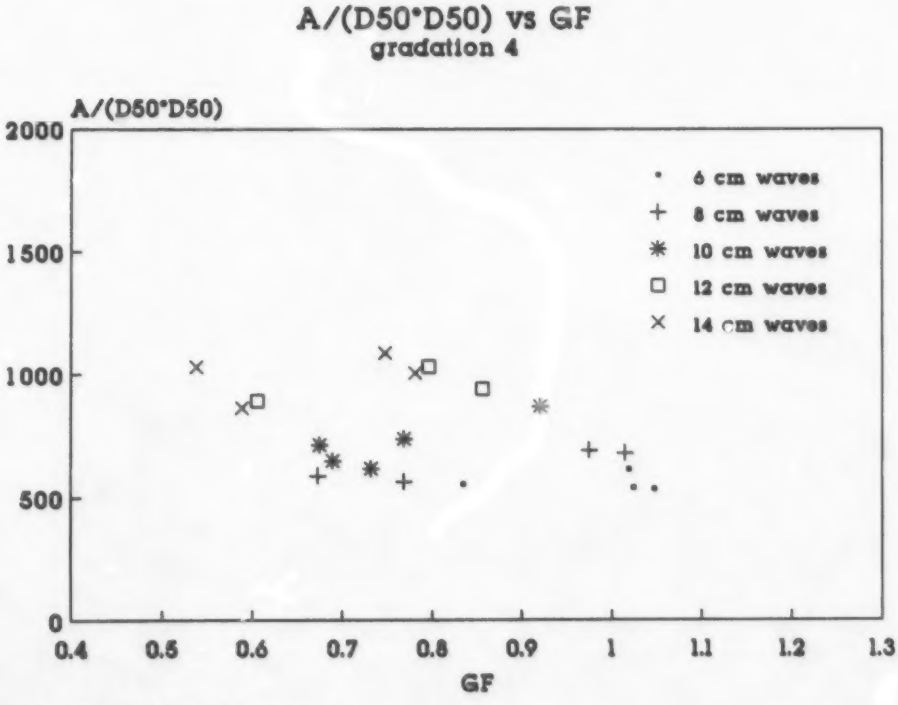

FIGURE 3.48 A/(D50*D50) vs GF

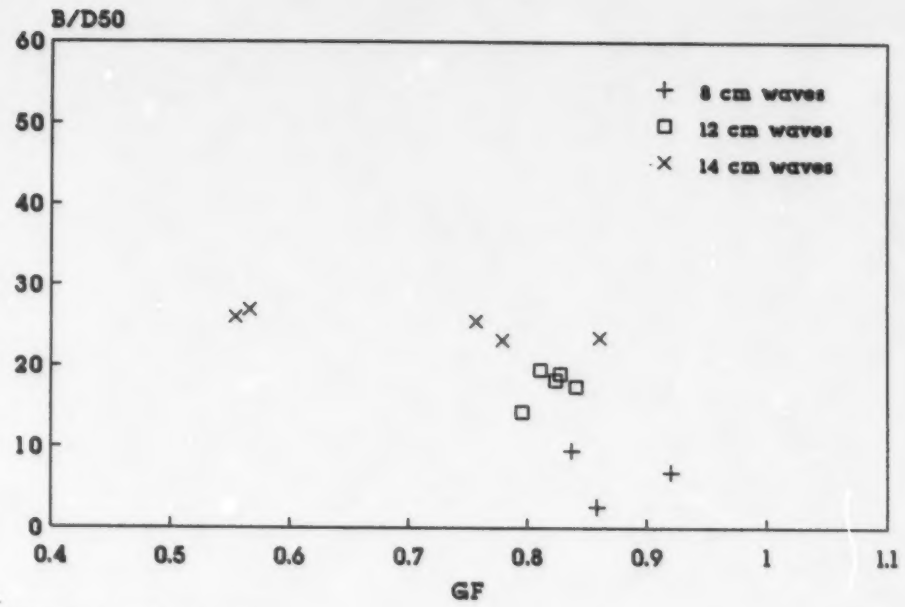

FIGURE 3.49 B/D50 vs GF

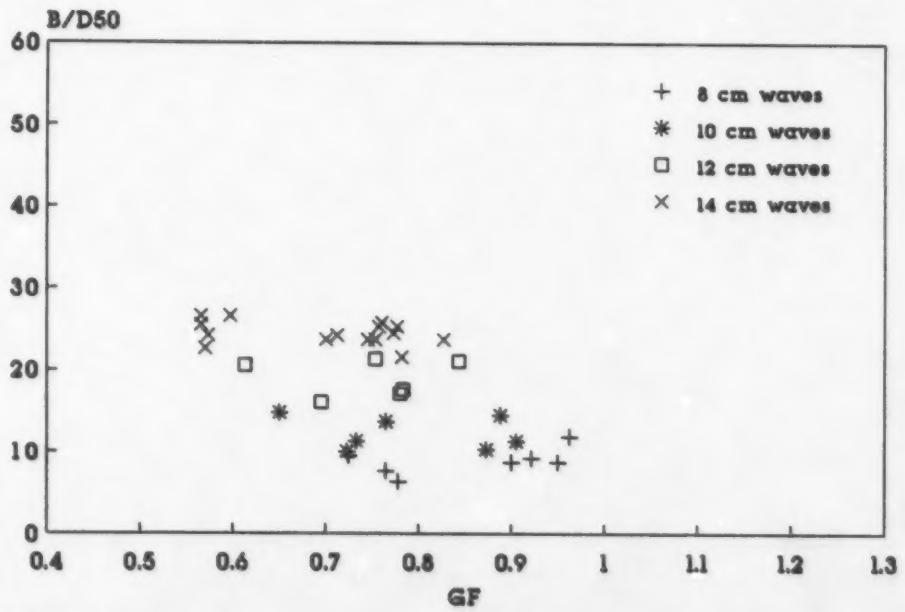

FIGURE 3.50 B/D50 vs GF

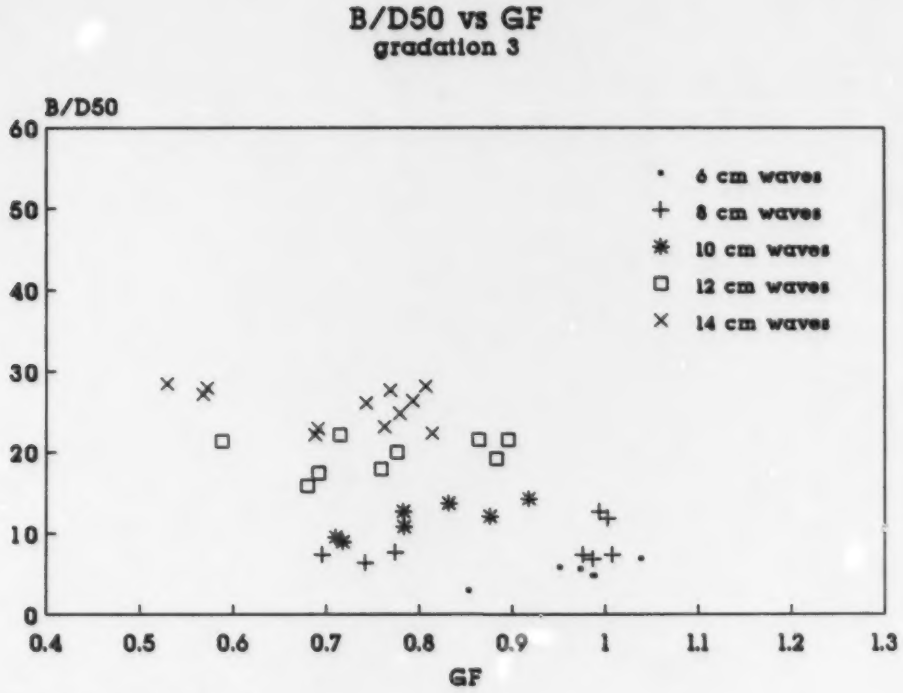

FIGURE 3.51 B/D50 vs GF

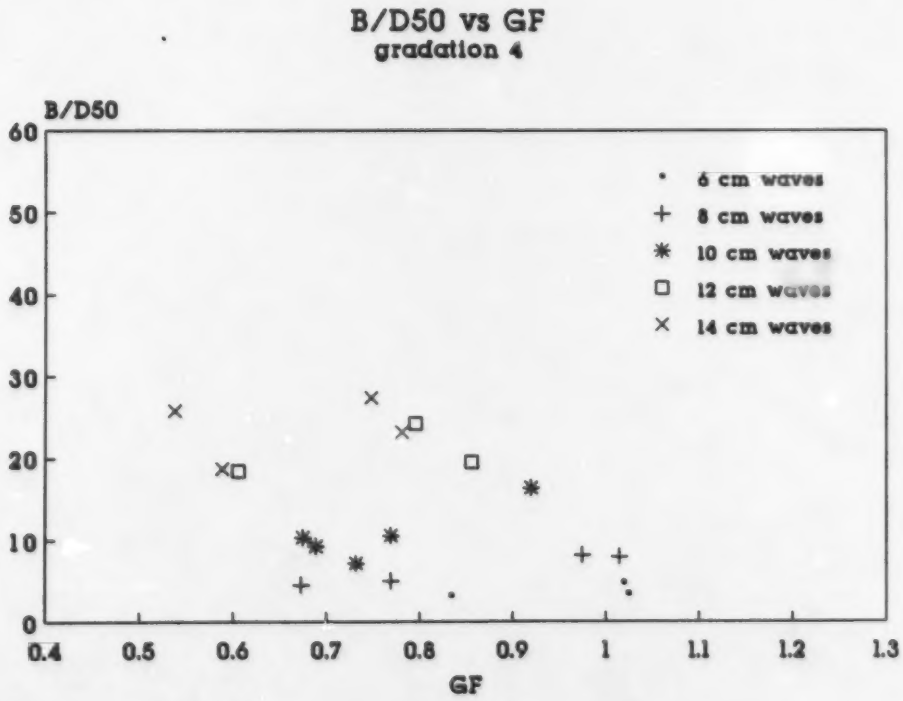

FIGURE 3.52 B/D50 vs GF

breakwaters researchers have realized that the stability of individual armour units is not longer the governing criteria. Instead, research has been concentrated on determining the volume of armour material (i.e. bulk movement) required for the waves to reshape the structure into a stable profile while still maintaining an adequate coverage of armour units to protect the core. As a result micro-changes in the wave climate (such as changes in GF) do not have a significant effect on the stability of dynamically stable breakwaters.

3.4.2.5 Effect of wave steepness H_s/L_o

Toe width (L)

Figure 3.53 shows the relationship of L/D_{50} with H_s/L_o for all data sorted according to wave height. No obvious dependence of the dimensionless toe width on the wave steepness is observed. If the wave height is constant, any change in steepness implies a change in period. Therefore, this indirectly shows that there is no dependence on wave period. Replotting the same data in figure 3.54 according to gradation shows no distinct trends in the relationship between dimensionless toe width and wave steepness.

Volume of armour (A)

Based on the observation made in the previous paragraph it seems likely that the volume of armour stones required for reshaping will not be dependent on the wave steepness.

All gradations of stones were sorted according to wave height and plotted against wave steepness as shown in figure 3.55. It can be seen that except for the 8 cm waves, which show more scatter, all the data for the same value of wave height lie on near horizontal straight lines, indicating that the volume of stones required for reshaping is independent of wave steepness. Since the data are presented for constant wave height, this also implies that A/D_{50}^2 is also independent of wave period.

The bulk of the data were then sorted according to gradation and replotted in figures 3.56 to 3.59 for gradations 1, 2, 3 and 4. Again, no significant dependence is observed. There appears to be slightly more reshaping with increasing wave steepness for wave heights of 8 cm and 10 cm, interacting on a breakwater built with armour stones gradation 3. Such a trend is not obvious for gradation 2. As the data is limited for 8 cm and 10 cm waves,this dependence cannot be considered conclusive.

Width of berm eroded (B)

Figure 3.60 shows the dimensionless width of berm eroded plotted against wave steepness for all data sorted according to wave height respectively. Within the scatter of the data, no obvious dependence of the dimensionless width of berm eroded with wave steepness is evident.

Figures 3.61 to 3.64 show the width of berm eroded plotted as a function of wave steepness for each individual gradation. No obvious dependence is observed. There is considerable scatter.

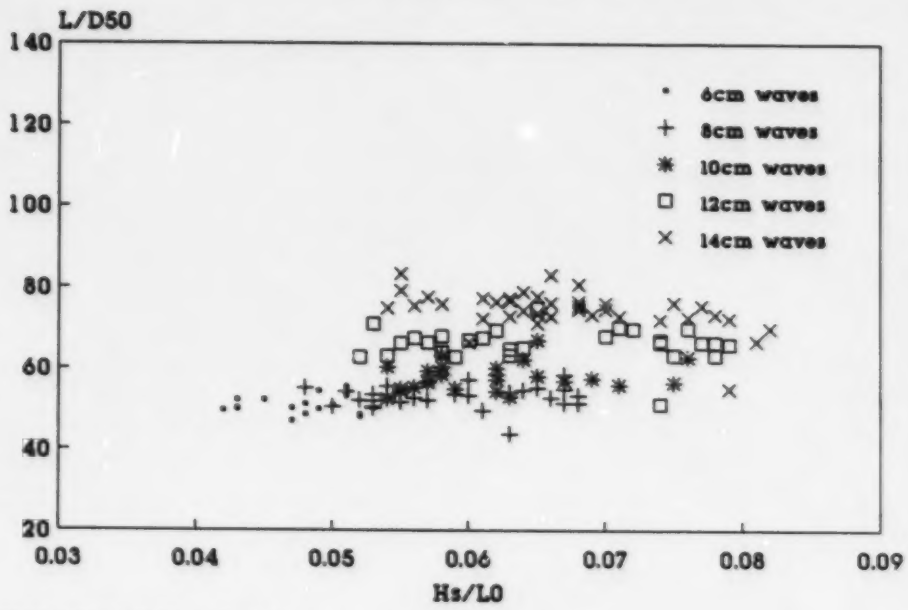

FIGURE 3.53 L/D50 vs Hs/L0

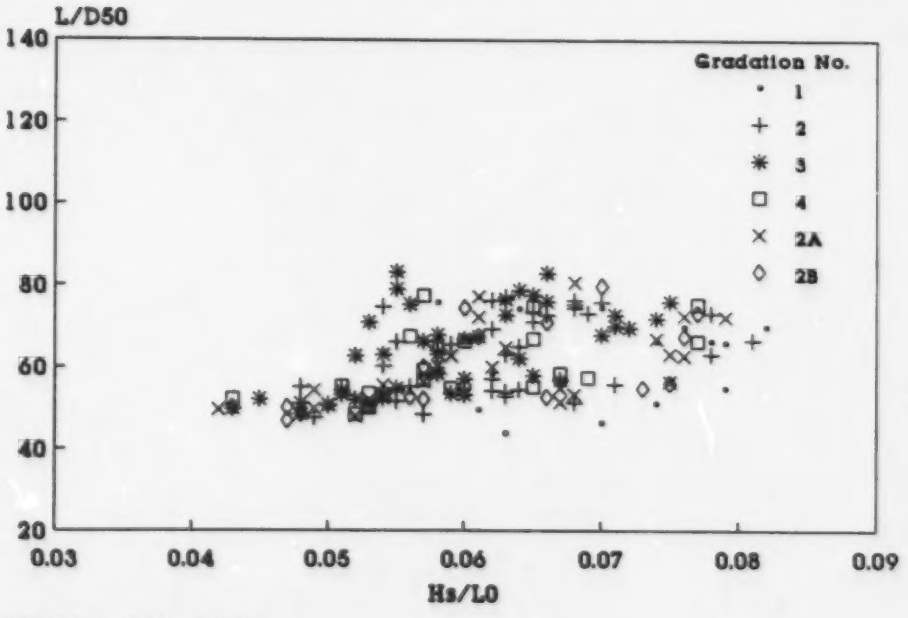

FIGURE 3.54 L/D50 vs Hs/L0

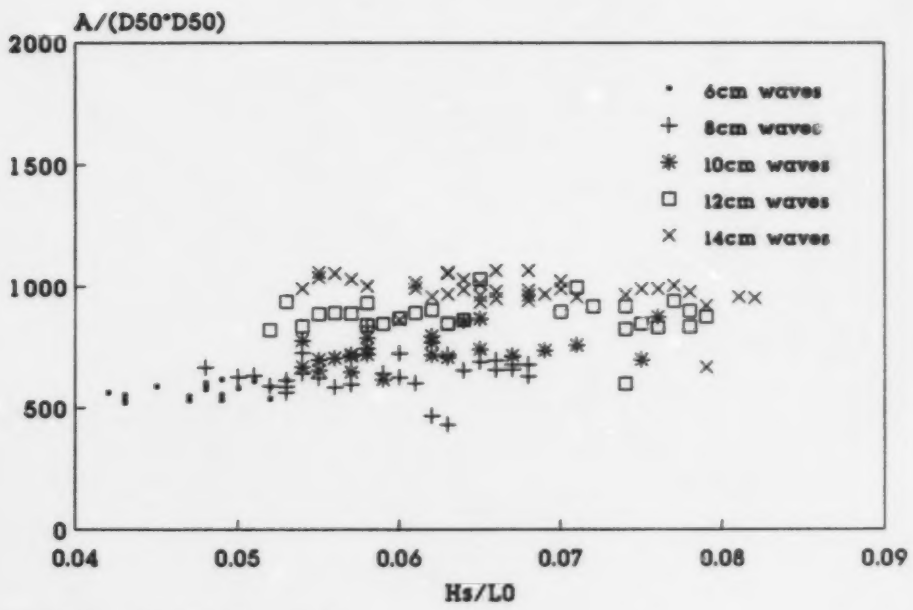

FIGURE 3.55 A/(D50*D50) vs Hs/L0

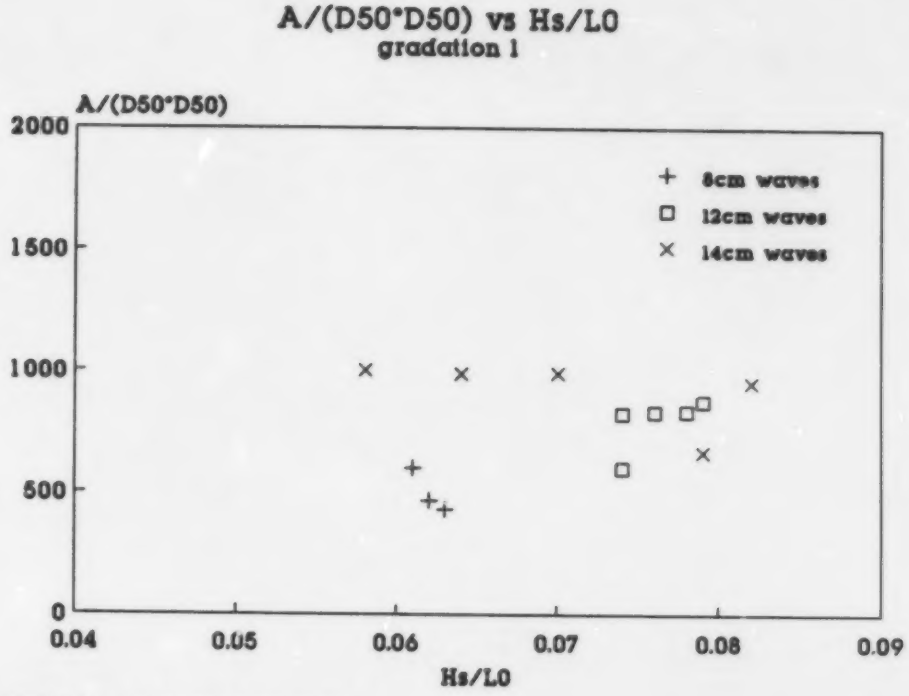

FIGURE 3.56 A/(D50*D50) vs Hs/L0

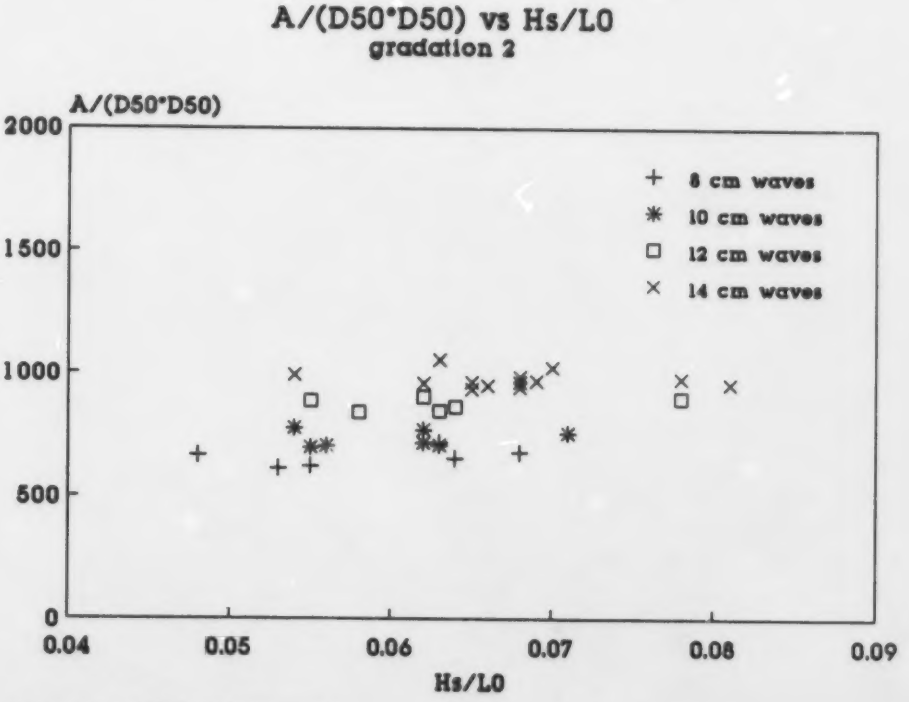

FIGURE 3.57 A/(D50*D50) vs Hs/L0

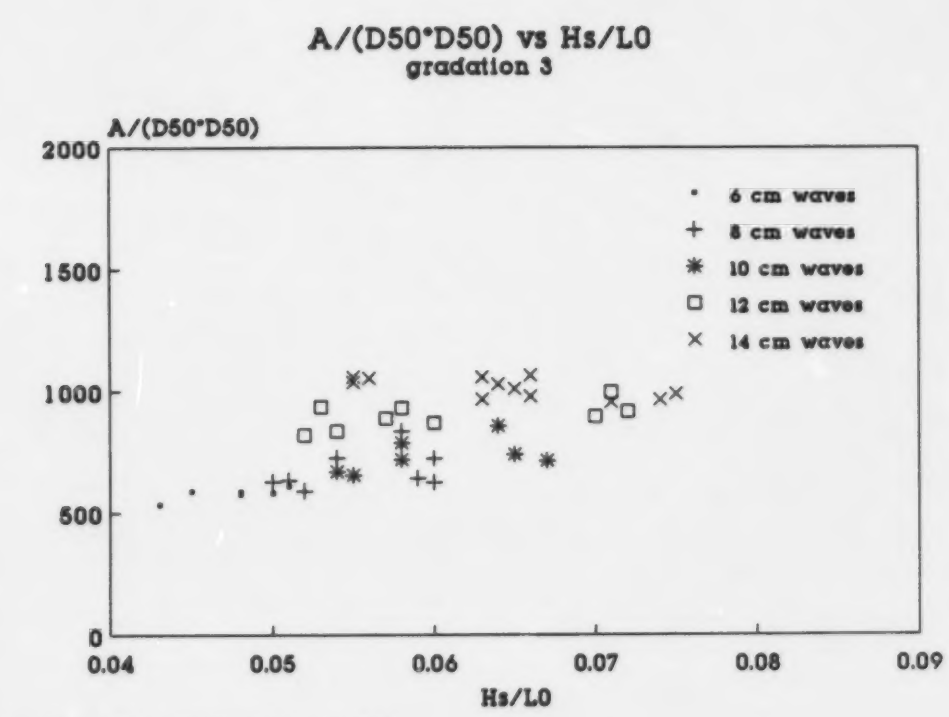

FIGURE 3.58 A/(D50*D50) vs Hs/L0

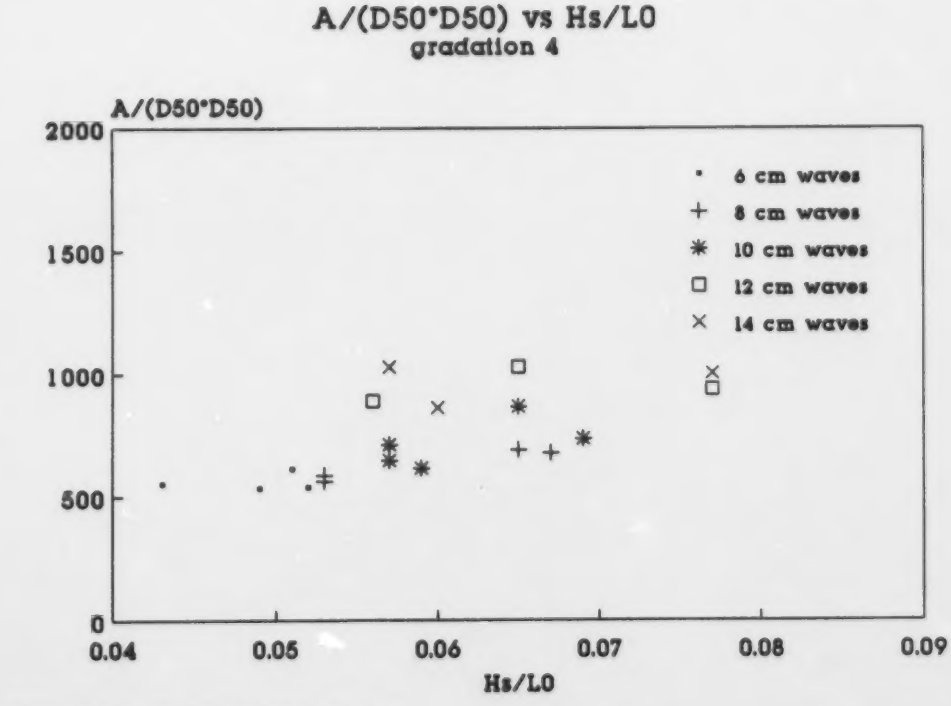

FIGURE 3.59 A/(D50*D50) vs Hs/L0

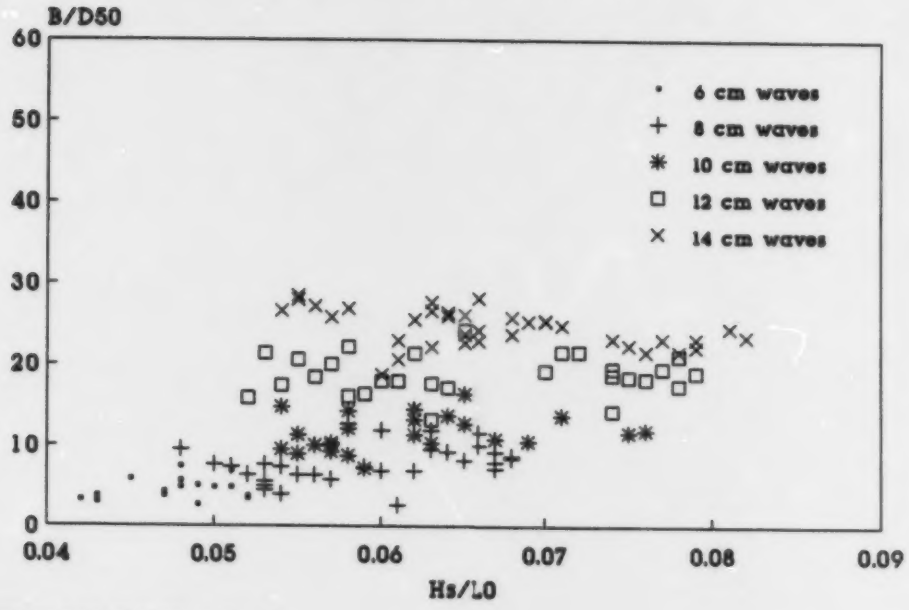

FIGURE 3.60 B/D50 vs Hs/L0

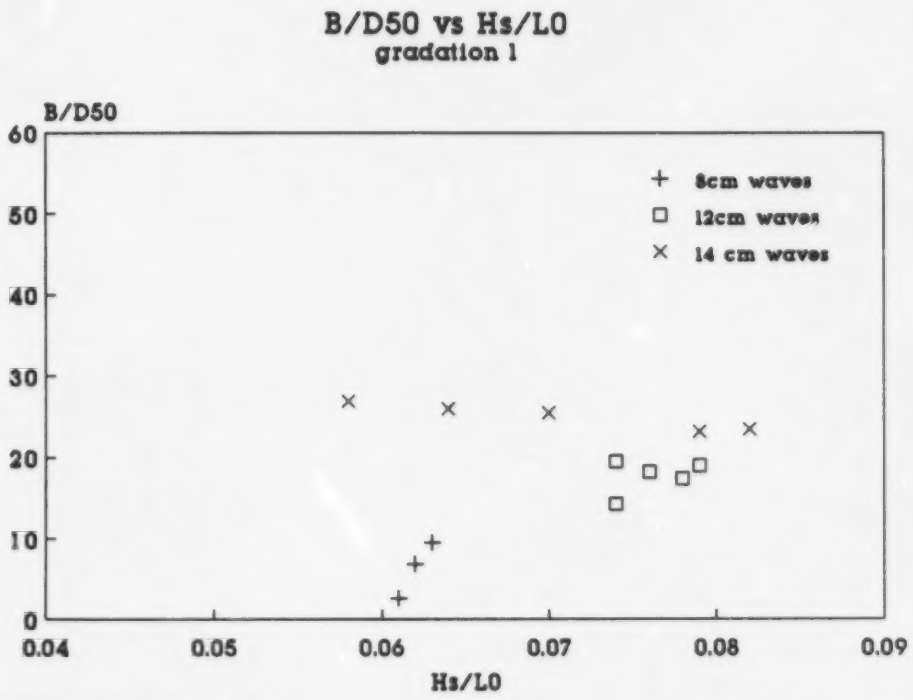

FIGURE 3.61 B/D50 vs Hs/L0

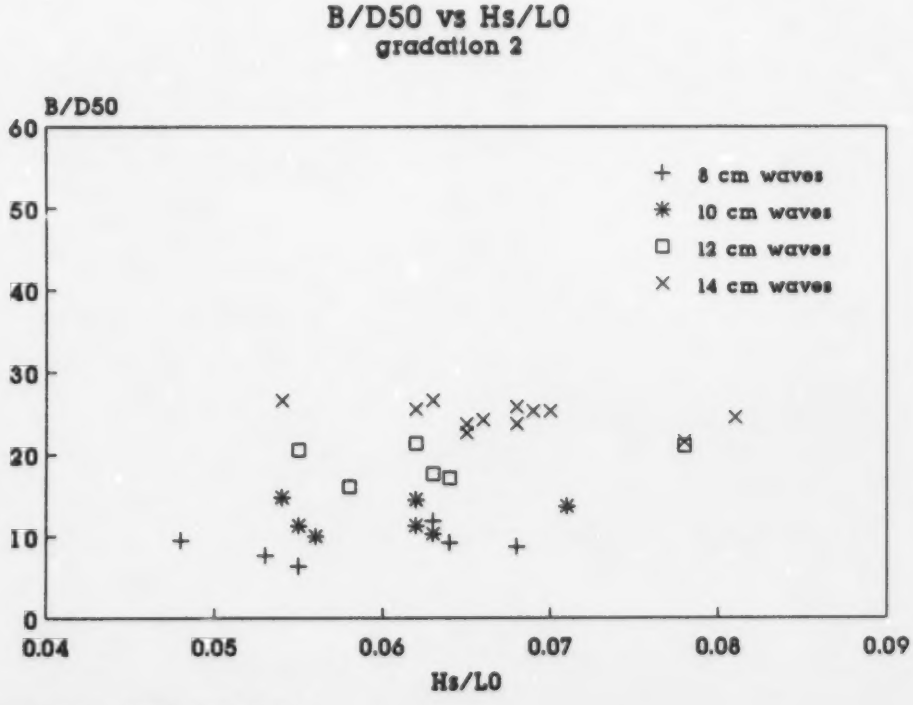

FIGURE 3.62 B/D50 vs Hs/L0

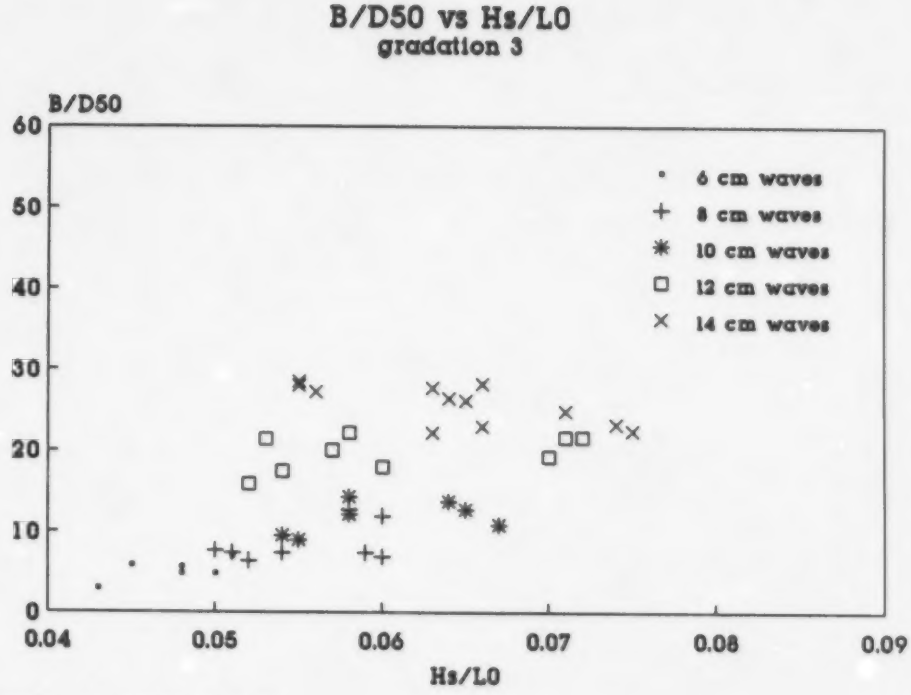

FIGURE 3.63 B/D50 vs Hs/L0

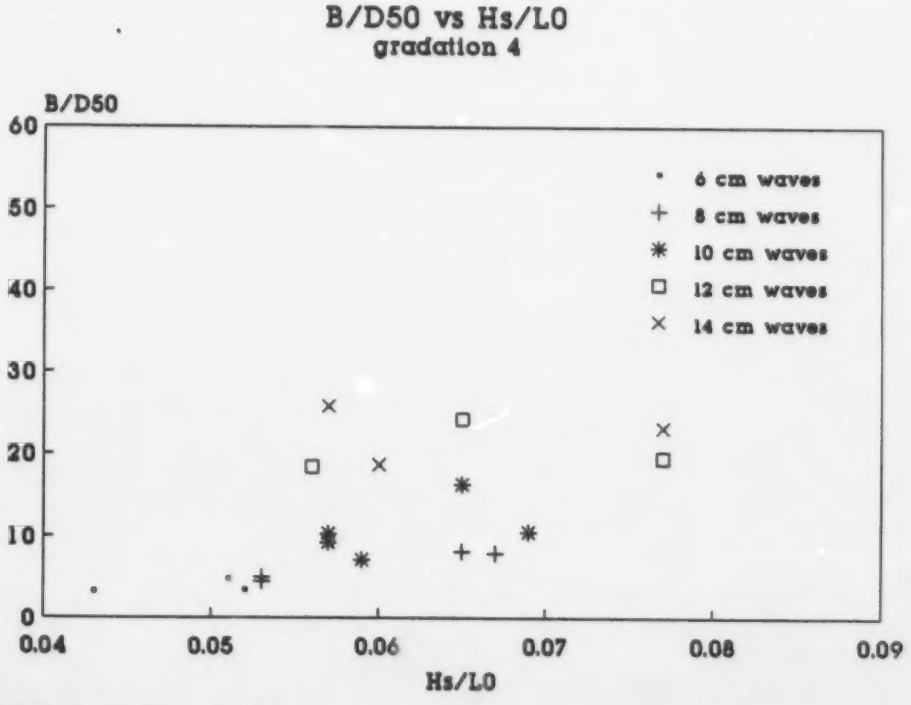

FIGURE 3.64 B/D50 vs Hs/L0

3.4.2.6 Effect of spectral peak period T_p

The spectral peak period is the wave period of a sea state at which the spectral energy is a maximum.

Toe width (L)

Values of L/D_{50} plotted against spectral peak period, T_p, are shown in figure 3.65. Individual data are characterized by wave heights, but not by armour stone gradations. It appears that L/D_{50} does not vary significantly with T_p, for a given value of wave height.

Replotting part of the data after separating into different gradations likewise shows no strong relationship between L/D_{50} and T_p. Figures 3.66 to 3.69 show plots of L/D_{50} versus T_p for gradations 1, 2, 3 and 4 respectively.

Volume of stones (A)

The volume of stones required for reshaping was found to be independent of the spectral peak period, as shown in figures 3.70 to 3.74. Figure 3.70 shows the data for all gradations of armour stones, figures 3.71 to 3.74 show the data for armour stones of gradations 1, 2, 3 and 4 respectively.

In figure 3.70, the data for a wave height of 8 cm shows considerable scatter compared with the 12 cm and 14 cm waves. The reason for such scatter is that with smaller waves incident on the structure, the breakwater acts like more like a statically stable breakwater and , thus, erosion is dependent on the initial construction, packing, etc. However, after significant reshaping by the larger waves, the influence of packing and construction method is minimized. The end result is that larger wave heights produce a more homogeneous mass and the resulting parameters describing the structure shows much less variation.

Width of berm eroded (B)

Figure 3.75 shows the dimensionless width of berm eroded plotted against spectral peak period for all waves. No distinct relationship between B/D_{50} and T_p was found. Figures 3.76 to 3.79 show the width of berm eroded against the spectral peak period for armour stones of gradations 1, 2, 3 and 4 respectively, sorted according to wave height. The results appear quite scattered and in general do not give a distinct trend for most values of wave height.

3.4.2.7 Effect of average wave period T_{av}

The same trends as noted in Section 3.4.2.6 (effect of peak spectral period) were observed for L/D_{50}, A/D_{50}^2 and B/D_{50} as a function of average wave period. The average wave period is calculated using zero crossing methods.

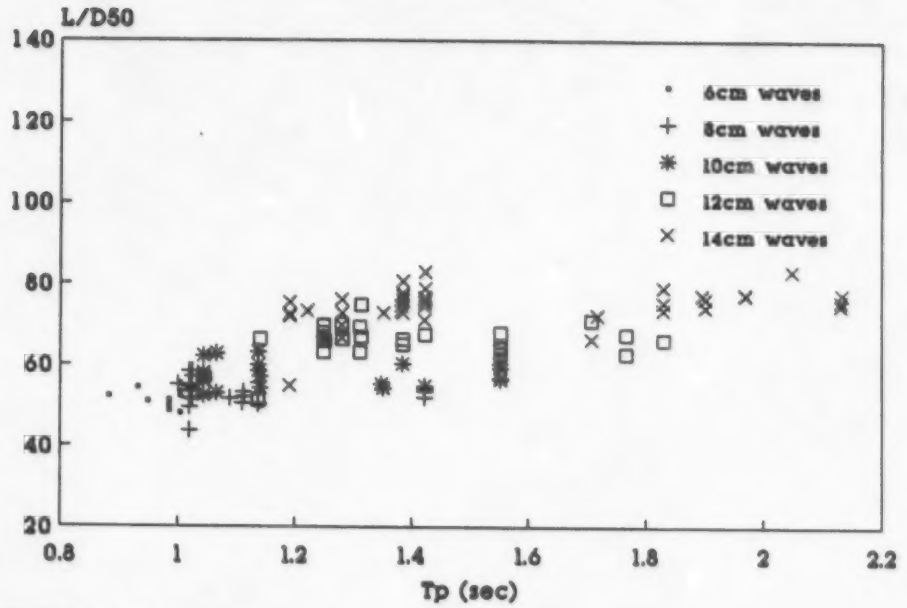

FIGURE 3.65 L/D50 vs Tp

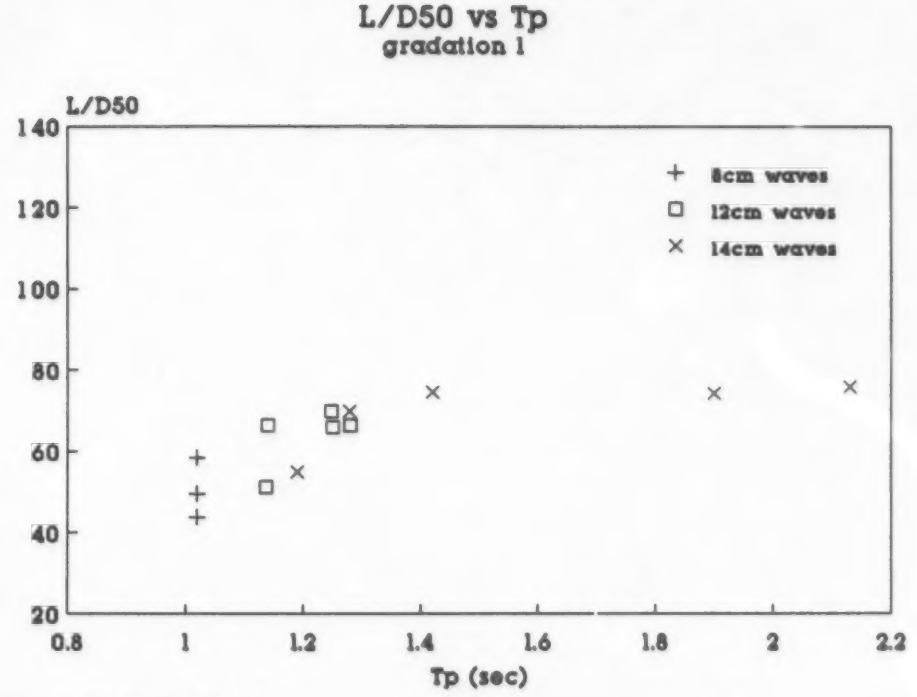

FIGURE 3.66 L/D50 vs Tp

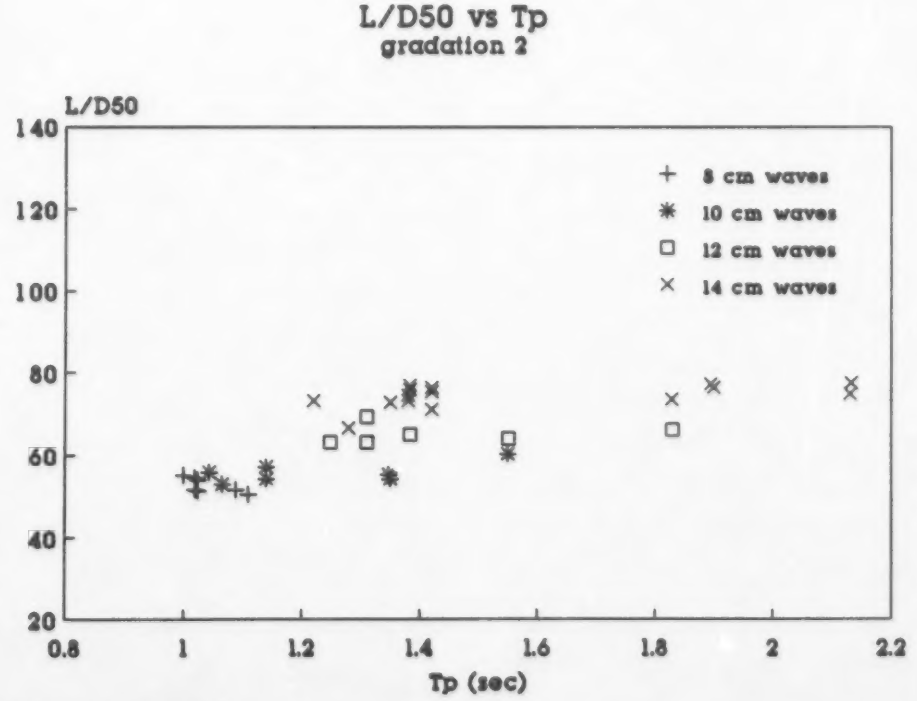

FIGURE 3.67 L/D50 vs Tp

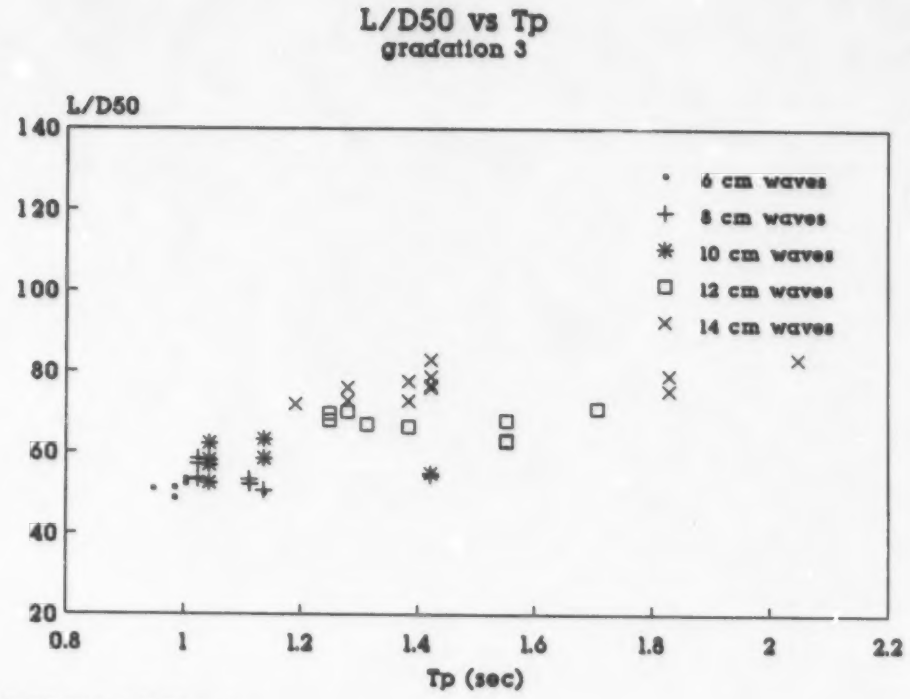

FIGURE 3.68 L/D50 vs Tp

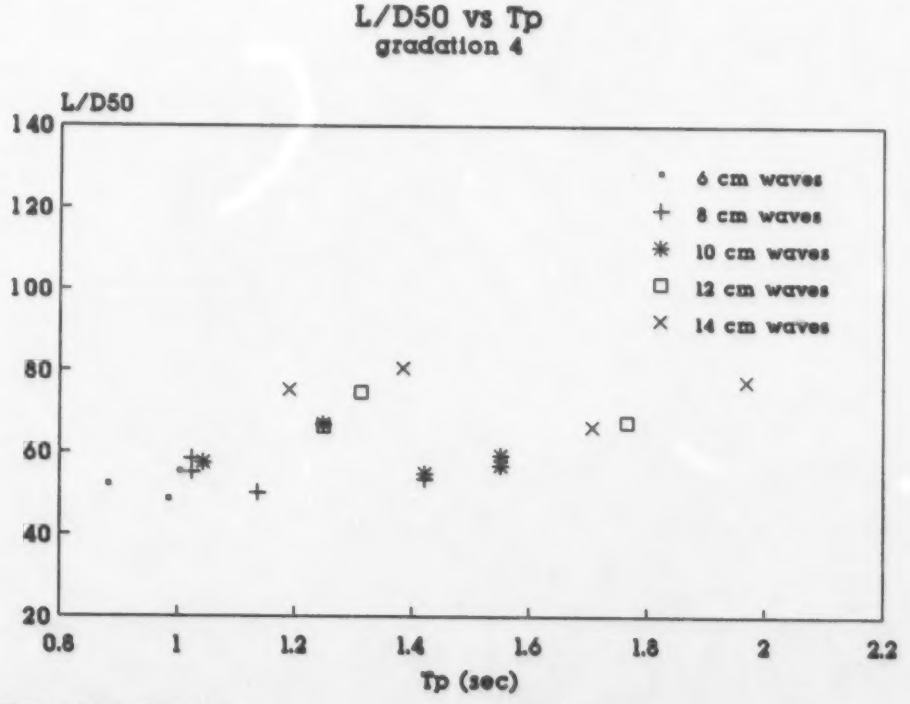

FIGURE 3.69 L/D50 vs Tp

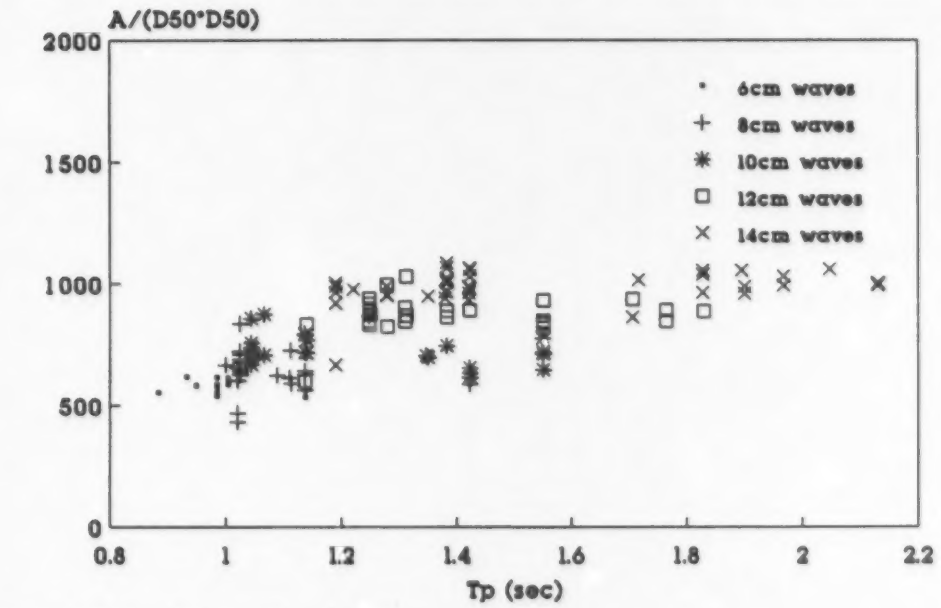

FIGURE 3.70 A/(D50*D50) vs Tp

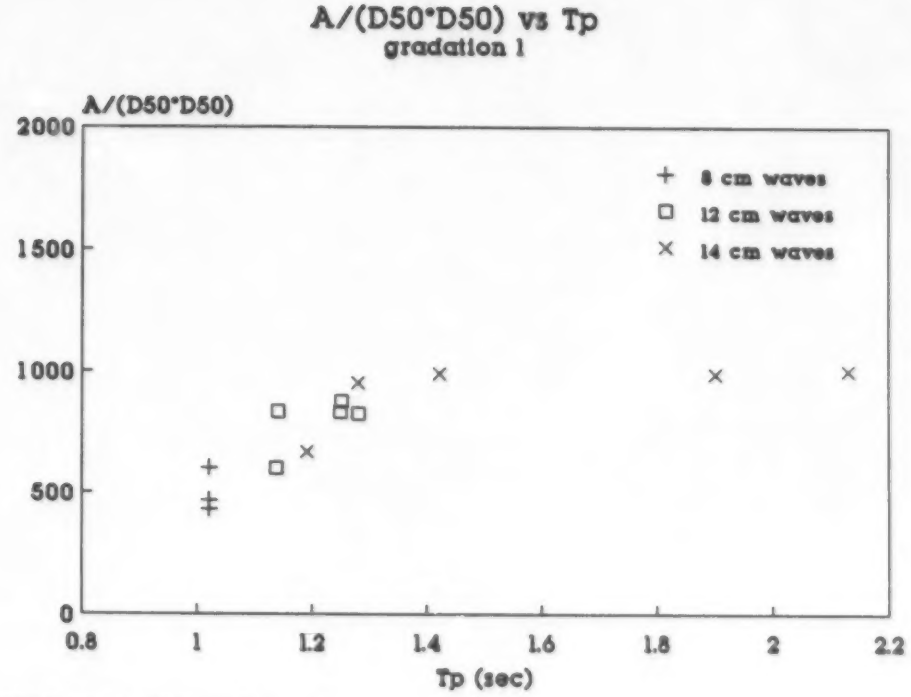

FIGURE 3.71 A/(D50*D50) vs Tp

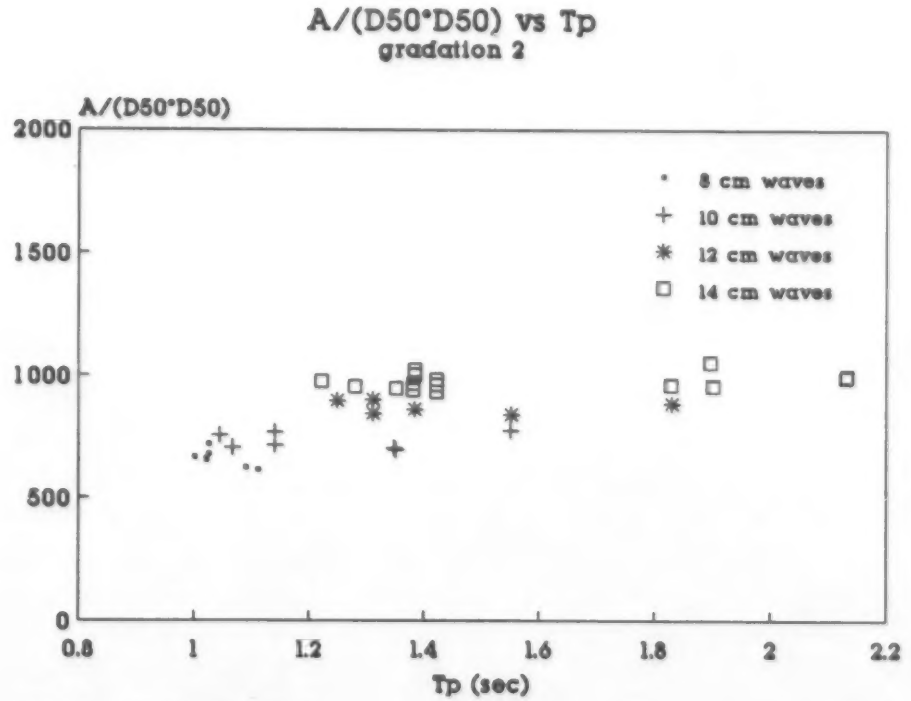

FIGURE 3.72 A/(D50*D50) vs Tp

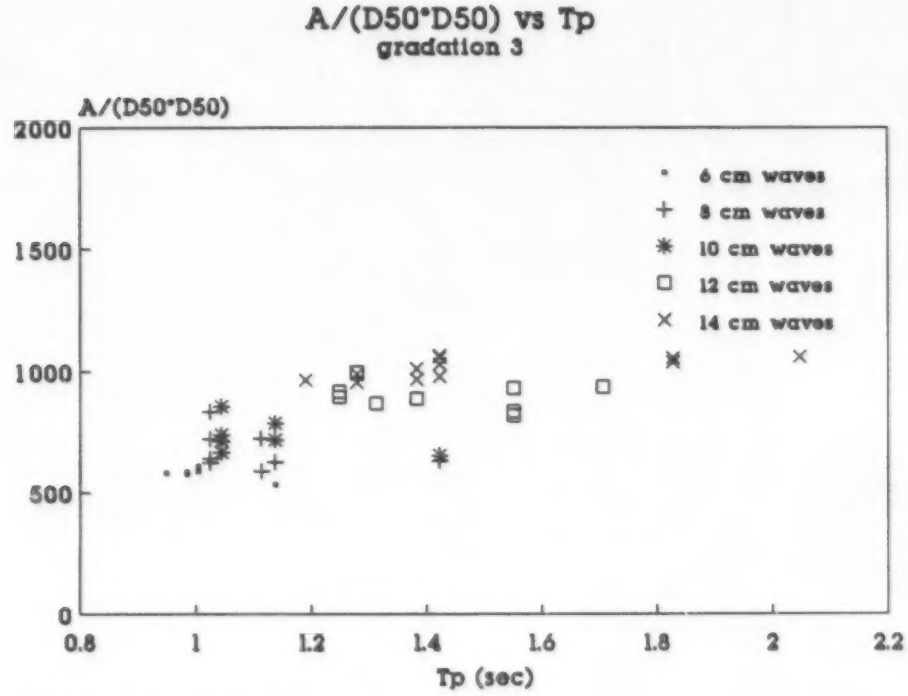

FIGURE 3.73 A/(D50*D50) vs Tp

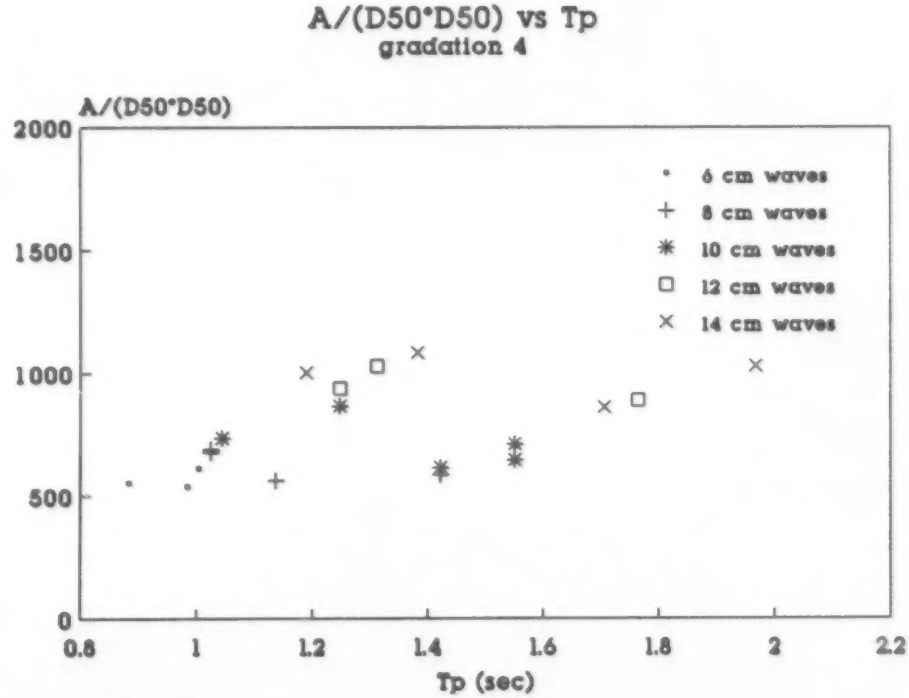

FIGURE 3.74 A/(D50*D50) vs Tp

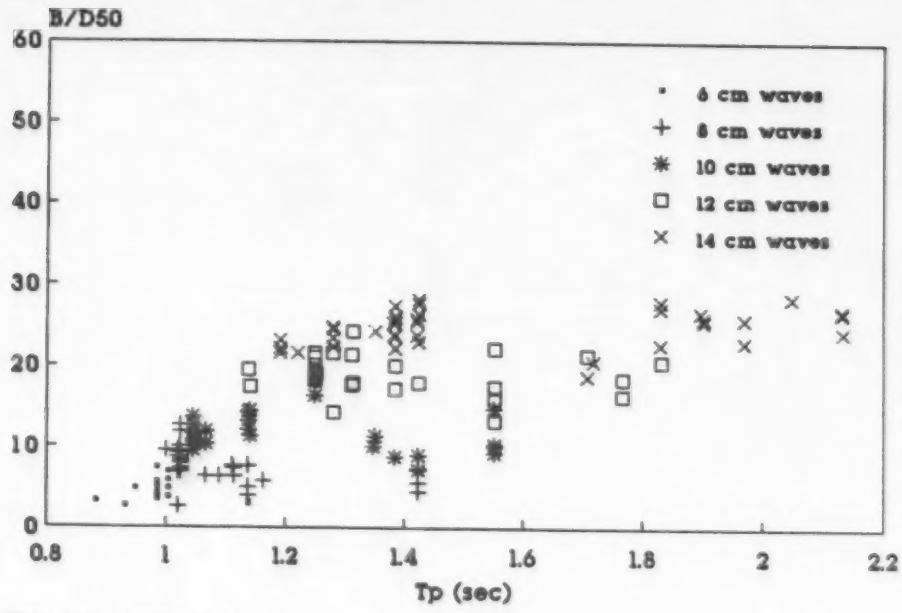

FIGURE 3.75 B/D50 vs Tp

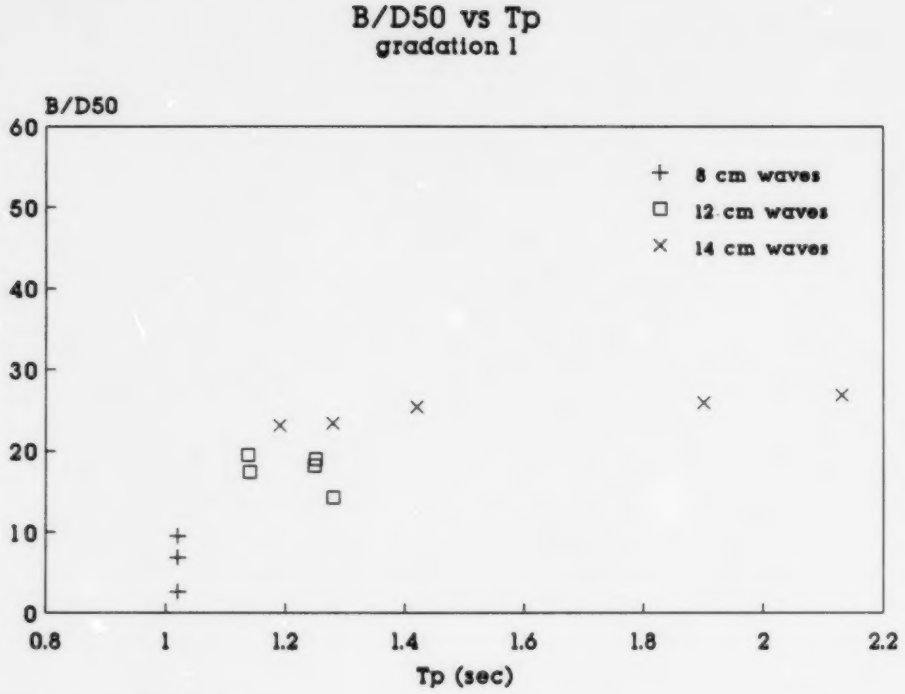

FIGURE 3.76 B/D50 vs Tp

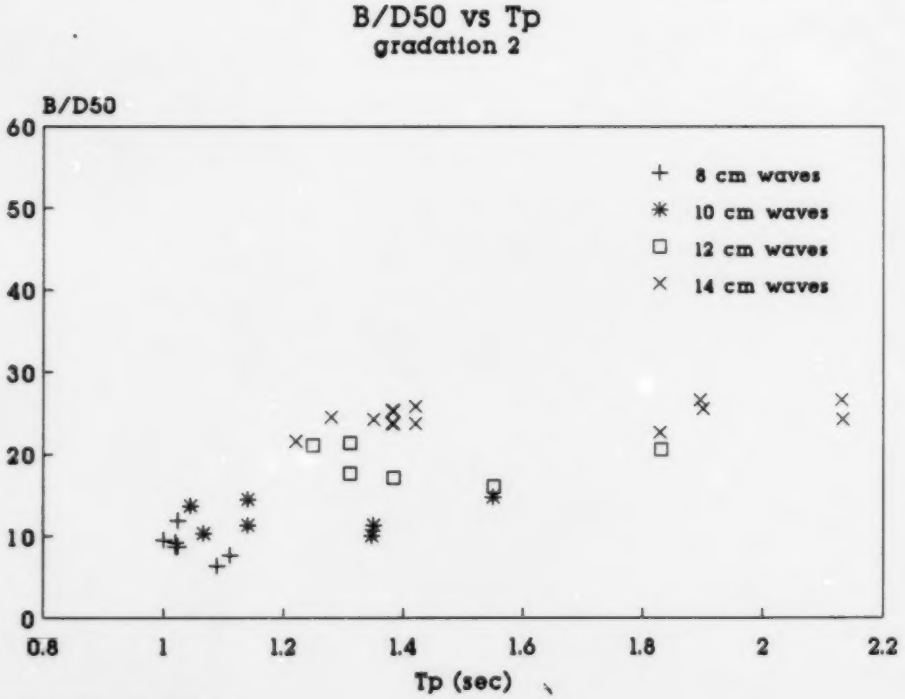

FIGURE 3.77 B/D50 vs Tp

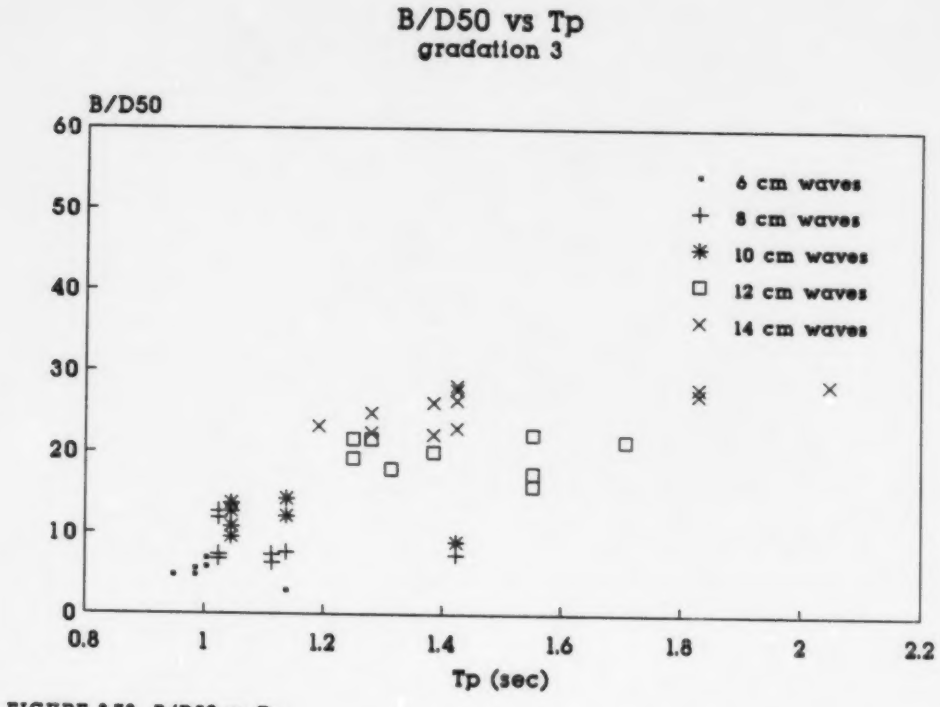

FIGURE 3.78 B/D50 vs Tp

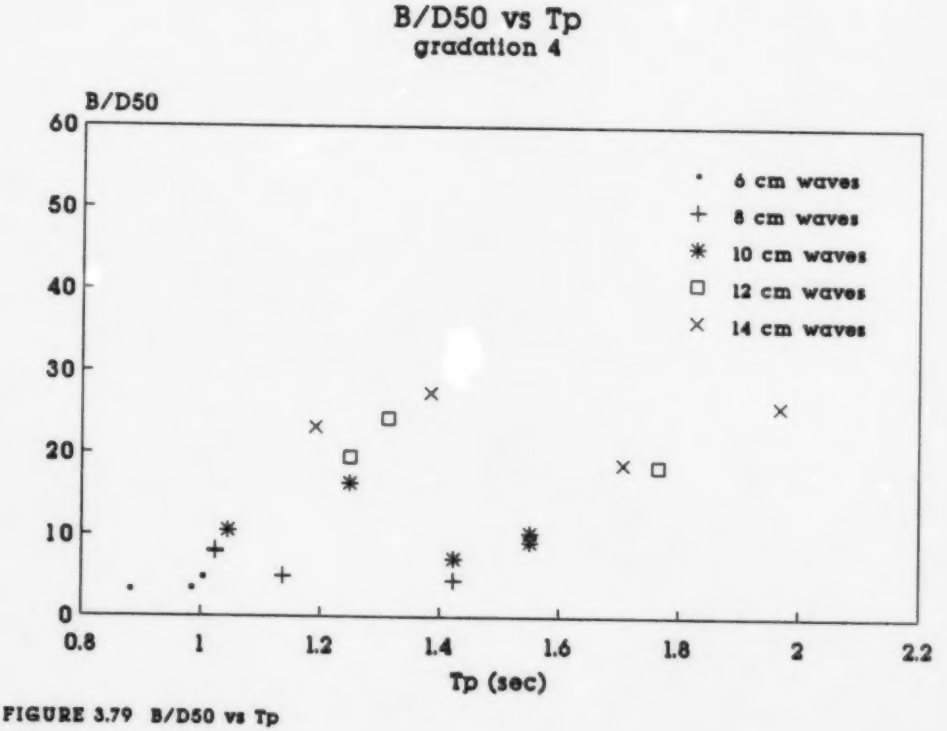

FIGURE 3.79 B/D50 vs Tp

3.4.2.8 Effect of duration of storm

Several sets of data were collected for different storm durations (i.e. segments of storm that lasted longer or shorter than 3000 waves). These tests were carried out for gradations 2 and 3 and consisted of tests 12, 13, 14, 15, 16, 17, 27, 28, 29, and 30 (see tables 4.7 to 4.12). Evaluating the influence of storm duration on the stability of reshaping breakwaters in particularly important since there is often uncertainty over the expected duration of the design storm. In analyzing these data,the respective values of A, L and B were divided by the corresponding values formed after the attack of 3000 waves and were called relative area, relative toe width and relative width of berm eroded respectively. The number of waves was also divided by 3000 to give the relative number of waves, N_R, (number of waves/3000). The above relative parameters were independent of wave height, wave period, wave groupiness, gradation and shape. As such, all the data could be considered and plotted on one graph. The only drawback of this plot is that since different tests are involved, there is considerable scatter, especially for small values of $H_s/((S_r-1)D_{50})$, where the variability due to initial construction can be considerable. However, as there is no way such effects can be eliminated, this method must be adopted.

The wave data and breakwater profiles were measured every five hundred waves. It was found that the first 5 to 10 big waves of each segment (the effect of the larger waves obviously being worse), in fact, caused most of the erosion. As a result, it is considered that for future tests, subjecting the structure to 500 to 1000 waves will give a reasonably good idea of the total reshaping and thus, tests need not be carried out for a duration of 3000 waves. Consequently, the duration of tests can be shortened considerably and hence the equipment need not be tied up for too long.

The results of the duration tests are discussed below:

Toe width (L)

The relative toe width $(L/D_{50})_R$, was plotted against the relative number of waves, N_R,in figure 3.80. The first 500 waves caused most of the reshaping (about 90% of that of 3000 waves). After 3000 waves, the process of reshaping was found to slow down considerably, but actually never stopped. After the attack of 36000 waves, additional reshaping of about 10% more than the total toe width formed after 3000 waves attack was observed.

Volume of stones (A)

Fig. 3.81 shows the relationship between A/D_{50}^2 and N_r for all data. As with L/D_{50}, the first 500 waves causes most of the change in A/D_{50}^2, with $(A/D_{50}^2)_{500}$ equal to approximately 90-95% of $(A/D_{50}^2)_{3000}$. A/D_{50}^2 was found to increase by approximately 3% between $N_R = 1$ and $N_R = 12$.

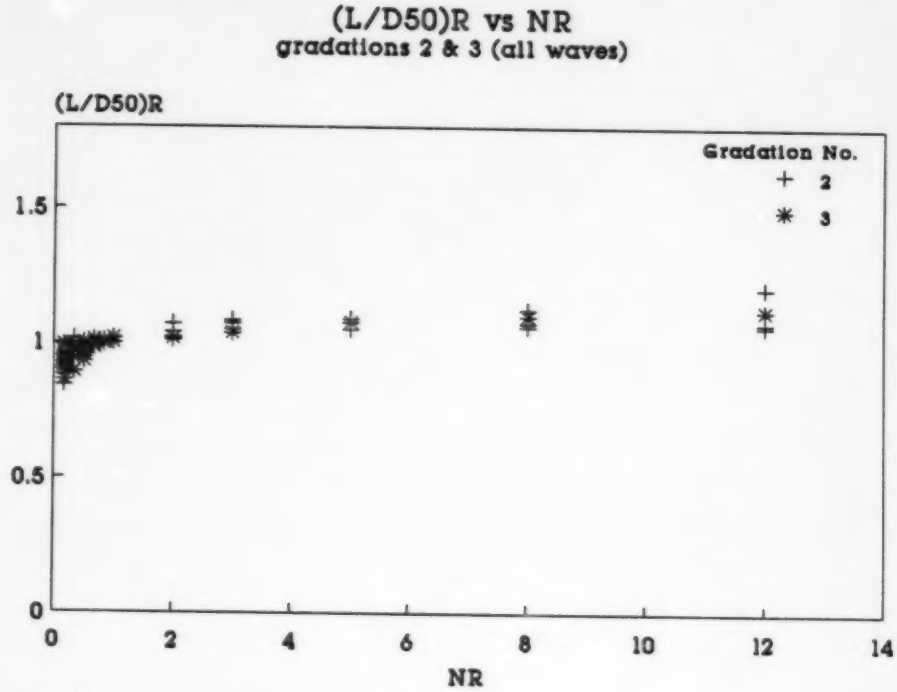

FIGURE 3.80 (L/D50)R vs NR

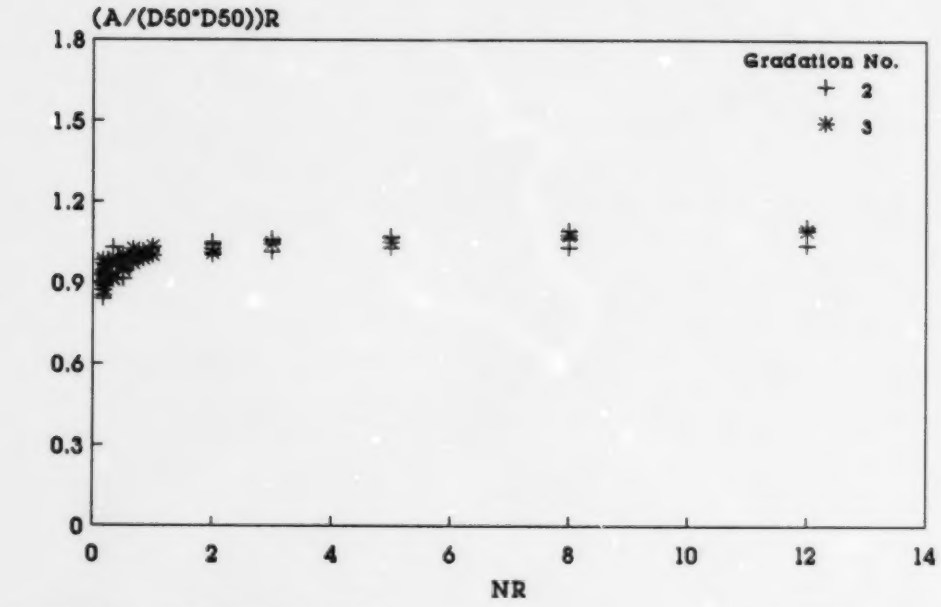

FIGURE 3.81 (A/(D50*D50))R vs NR

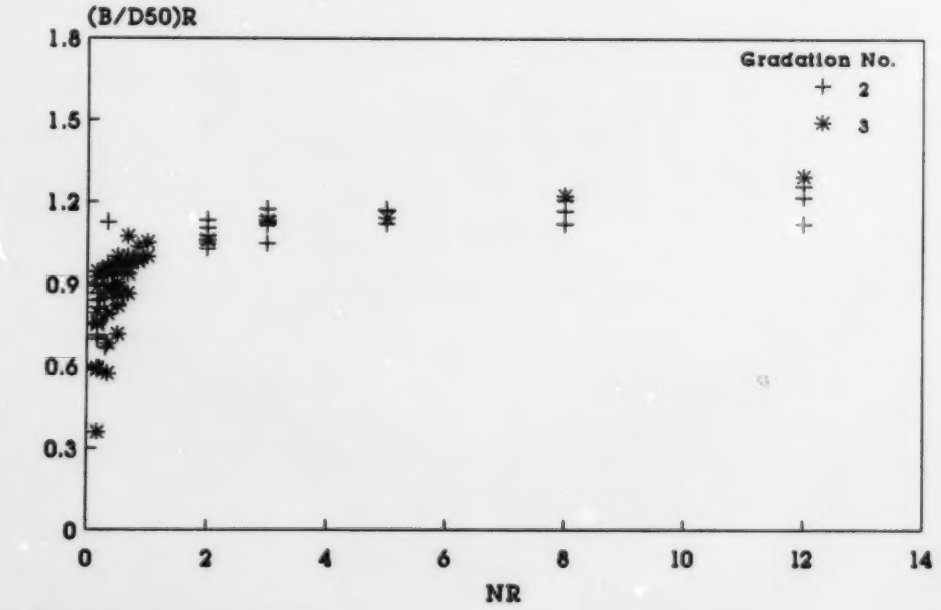

FIGURE 3.82 (B/D50)R vs NR

Width of Berm (B)

Figure 3.82 shows the relative berm width eroded, $(B/D_{50})_R$, against relative number of waves. In general the same trend as described above was observed. The results showed comparatively more scatter than previous results indicating that this parameter is sensitive to unknown errors. A close inspection of those particular points indicated that they are for small wave heights (6 cm and 8 cm) and could be influenced by initial construction. Furthermore, the width of berm eroded is approximately 10 cm and considering that D_{50} is 1.9 cm, the error in reading half of the size of the median stone would account for 10% of the berm eroded.

3.5 CONCLUSIONS

The dependent parameters exhibited a wide variety of dependence on the various independent or design parameters. These relationships are summarized below:

Toe width

The toe width was found to be dependent on wave height, uniformity of armour stones and duration of storm.

Volume of stones

The volume of stones required for reshaping was found to depend on wave height, uniformity of armour stones and duration.

Width of berm eroded

The width of berm eroded was found to depend on wave height, uniformity of stones, shape of stones and duration. The results for this parameter were found to exhibit more scatter.

4. THREE-DIMENSIONAL TESTS

4.1 TEST PROGRAMME

4.1.1 Facilities

Tests were undertaken in a 22 by 26 metre wave basin using irregular long crested waves. Figure 4.1 shows the layout of the basin and the approximate location of the test structures. The three dimensional tests were undertaken using the same time series of water surface variations as were used in the two dimensional tests.

For the initial series of three dimensional tests, a false floor fronted by a 1:15 slope was installed and the test section was placed on top of the false floor. This was utilized in order to allow a direct comparison of the results of the three and two dimensional tests (in which the model was located at the top of a 1:15 slope). The wave-wave interaction in the two sets of test should be consistent.

Once the two three dimensional comparative tests had been undertaken, all subsequent testing in the three dimensional basin was carried out with the model placed on the floor of the basin (horizontal). A comparison between results obtained in three dimensions with the model built on either the horizontal floor or with the 1:15 slope fronting the test structure was made.

Profiles of the test breakwaters were measured at several locations along the structure following each segment of the design storm. These locations are documented in section 4.1.4. The profiler used to measure the three dimensional profiles was a trailing arm profiler which provided a continuous reading of the elevation of the breakwater with horizontal distance.

4.1.2 Materials

Tests undertaken in the three dimensional modelling programme utilized a core material identical to that undertaken in the two dimensional model tests. The armour gradations used were the same as gradations 2, 3 and 4 of the two dimensional tests (see tables 3.1 and 3.2), with the exception of Tests 1 to 14. In this test series the armour (Gradation 5) was comprised of stones having a D_{50} of 1.4 cm (compared with 1.9 cm) and with a D_{85}/D_{15} ratio of approximately 1.9. This compares with gradation 2 from the two dimensional tests ($D_{85}/D_{15} = 1.9$). Since the data analysis is undertaken utilizing dimensional methods the change in D_{50} should not preclude direct comparison between results of the two and three dimensional tests.

4.1.3 Wave Climate

The notation of a design storm consisting of several segments of specific wave height-period combinations, which altogether simulate the growth and decay of waves during a hypothetical design storm was utilized in both the two dimensional and three dimensional tests. The two dimensional design storms were discussed in section 3.2.4. The absolute maximum significant wave height in the two dimensional tests was limited by the generation capabilities of the flume wave generator (limit of approximately 14 cm significant wave height). At typical model scales

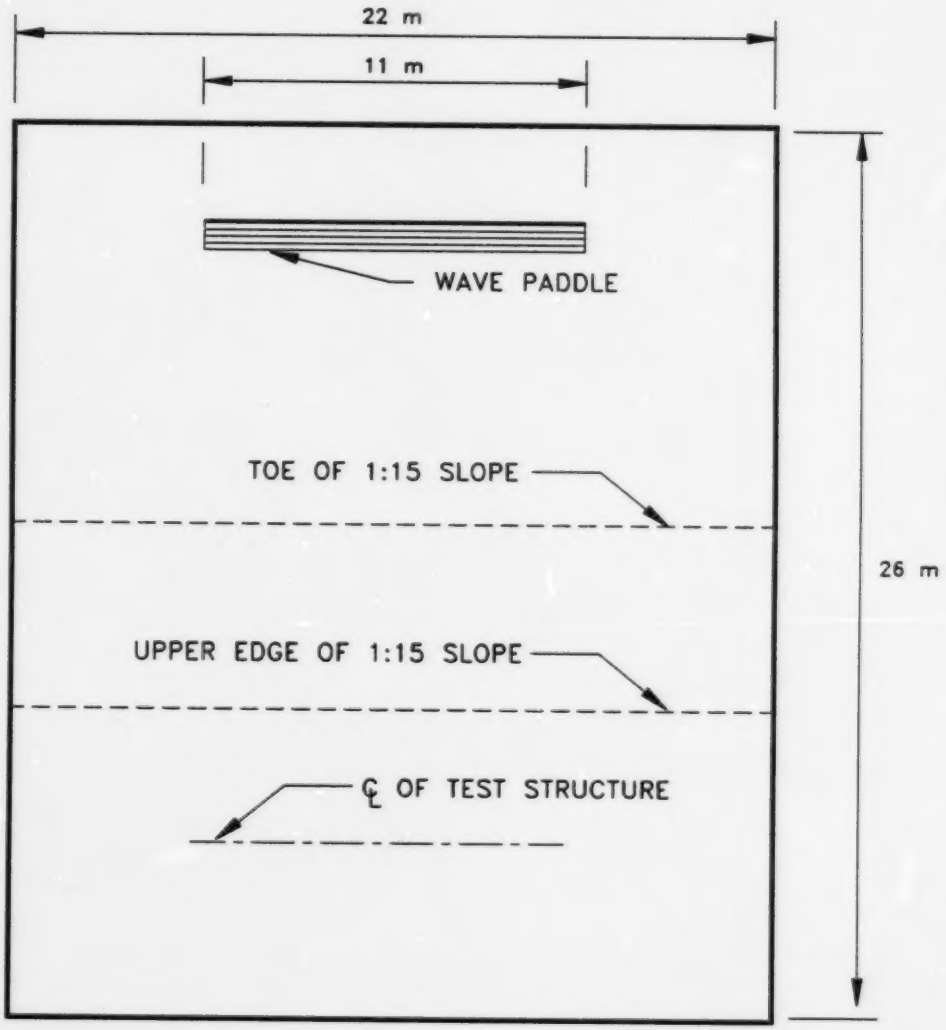

FIGURE 4.1 BASIN LAYOUT

of 1:30 to 1:40, this wave height is sufficient to reproduce the wave climate for most Canadian coastal locations. However, the three dimensional wave generation capabilities allow for the generation of waves having significant wave heights of up to 24 cm depending on the wave period. Consequently, several new design storms were synthesized which utilized the available increase in wave height. This would allow for a later comparison of "size effects" in the model. (these are discussed later). A total of four design storms were utilized in the three dimensional tests and are detailed in Tables 4.1 to 4.4. Design storm 1 is an exact duplication of design storm 4 from the two dimensional tests, thus a direct comparison can be made between two and three dimensional tests.

Table 4.1 Wave Climate # 1-3D

Segment	H_s (m)	T_p (s)	Duration (min)
1	.06	1.2	60
2	.08	1.4	70
3	.1	1.6	80
4	.12	1.8	90
5	.14	2.0	100
6	.12	1.8	90
7	.10	1.6	80
8	.08	1.4	70

Table 4.2 Wave Climate 2 - 3D

Segment	H_s (m)	T_p (s)	Duration (min)
1	.08	1.2	60
2	.10	1.4	70
3	.12	1.6	80
4	.14	1.8	90
5	.16	2.0	100
6	.14	1.8	90
7	.12	1.6	80
8	.10	1.4	70

Table 4.3 Wave Climate 3 - 3D

Segment	H_s (m)	T_p (s)	Duration (min)
1	.10	1.2	60
2	.12	1.4	70
3	.14	1.6	80
4	.16	1.8	90
5	.18	2.0	100
6	.16	1.8	90
7	.14	1.6	80
8	.12	1.4	70

Table 4.4 Wave Climate 4 - 3D

Segment	H_s (m)	T_p (s)	Duration (min)
1	.12	1.2	60
2	.14	1.4	70
3	.16	1.6	80
4	.18	1.8	90
5	.20	2.0	100
6	.18	1.8	90
7	.16	1.6	80
8	.14	1.4	70

4.1.4 Test Programme

Four separate series of tests were completed during the three dimensional phase of the testing programme.

Series 1

The first series of tests (SERIES 1) were undertaken to evaluate the influence of flume width on the reshaping of dynamically stable breakwaters. Although there have been no significant studies undertaken to evaluate three dimensional stability of reshaping breakwaters, Hall et al. (1983), Hall (1987) and Burcarth and Frigaard (1987) have shown that significant three dimensional effects can exist. There effects may be classified as purely three dimensional effects (due to attenuation of energy within the cross section) or effects resulting from the variation of the angle of wave attack, thus affecting the erosion prone areas (particularly the head of the breakwater). The later effects are typically what is thought of as being dominant; however, Hall et al. (1983) have shown that the difference between test results from narrow flumes and wider three dimensional test sections (for incident waves parallel to the trunk of the structure) can be substantial. Test Series 1 is designed to evaluate these effects, in particular to evaluate if flume width influences the reshaping of these breakwaters.

Test Series 1 was run in the three dimensional basin where three separate "flumes" having widths of 1.2, 2.4 and 4.0 metres were constructed parallel to each other. Figure 4.2 shows the layout of the flumes within the basin. The 1:15 slope fronting the test sections was in place during this test series. Identical test structures were built in each of the "flumes" and were then

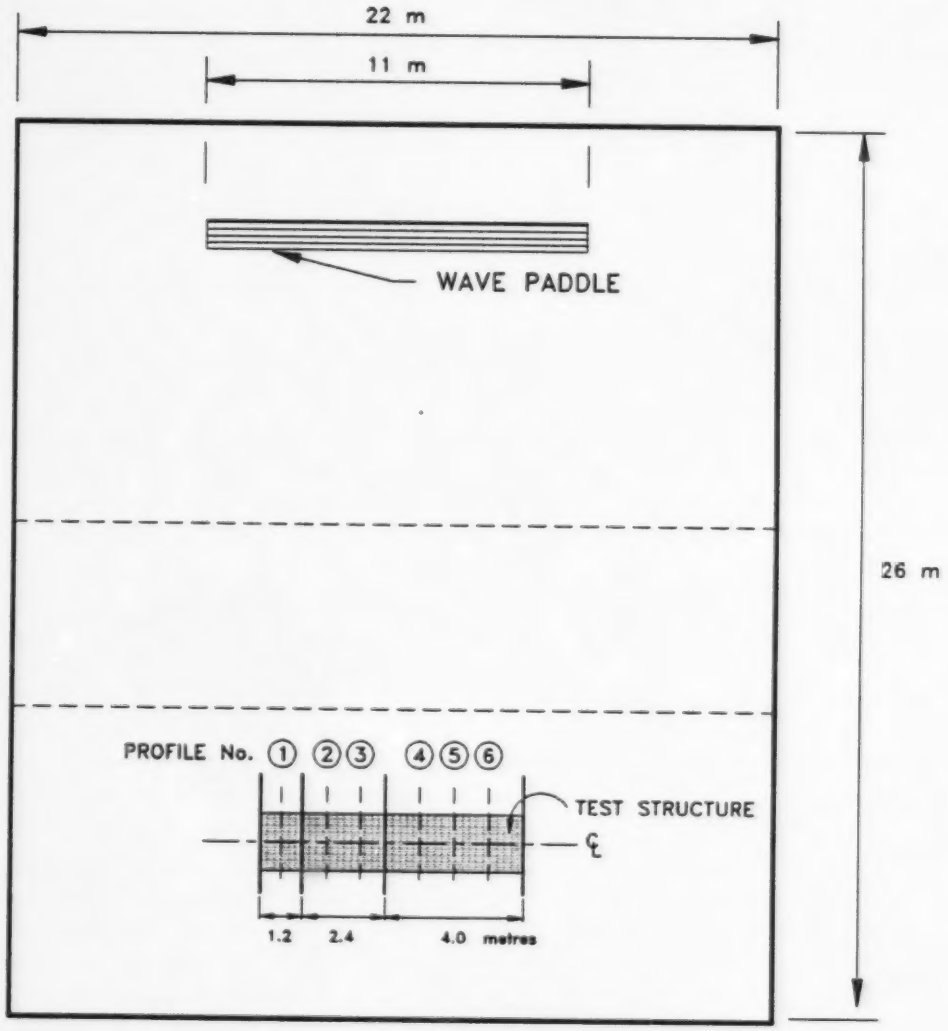

FIGURE 4.2 SERIES 1 LAYOUT

simultaneously subjected to the same wave conditions. Profiles (at locations shown in Figure 4.2) were measured following each segment of the design storm. A total of 12 tests were undertaken in Series 1 and are described in Table 4.5. The armour layer in all tests in this series was constructed using gradation 5.

Table 4.5

Test Number	Wave Climate	Initial Berm Width (m)
1	1-3D	.40
2	1-3D	.45
3	2-3D	.50
4	2-3D	.50
5	2-3D	.60
6	3-3D	.60
7	3-3D	.70
8	4-3D	.70
9	4-3D	.60
10	2-3D *GF=0.2	.45
11	2-3D *GF=0.75	.45
12	2-3D *GF=1.2	.45

As in the two dimensional tests, a test was terminated if the erosion extended into the 1:3 upper slope of the breakwater.

Series 2

The second series of tests were undertaken to evaluate the reshaping of a fully three dimensional breakwater. Gradation 5 was used as the armour material and thus the results can be directly compared with tests undertaken in Series 1. The layout of the test structure in the wave basin is shown in Figure 4.3. Profiles were measured at seven locations shown in Figure 4.3. The 1:15 slope fronting the breakwater was in place during this test series. A total of four tests were undertaken and are listed below in Table 4.6.

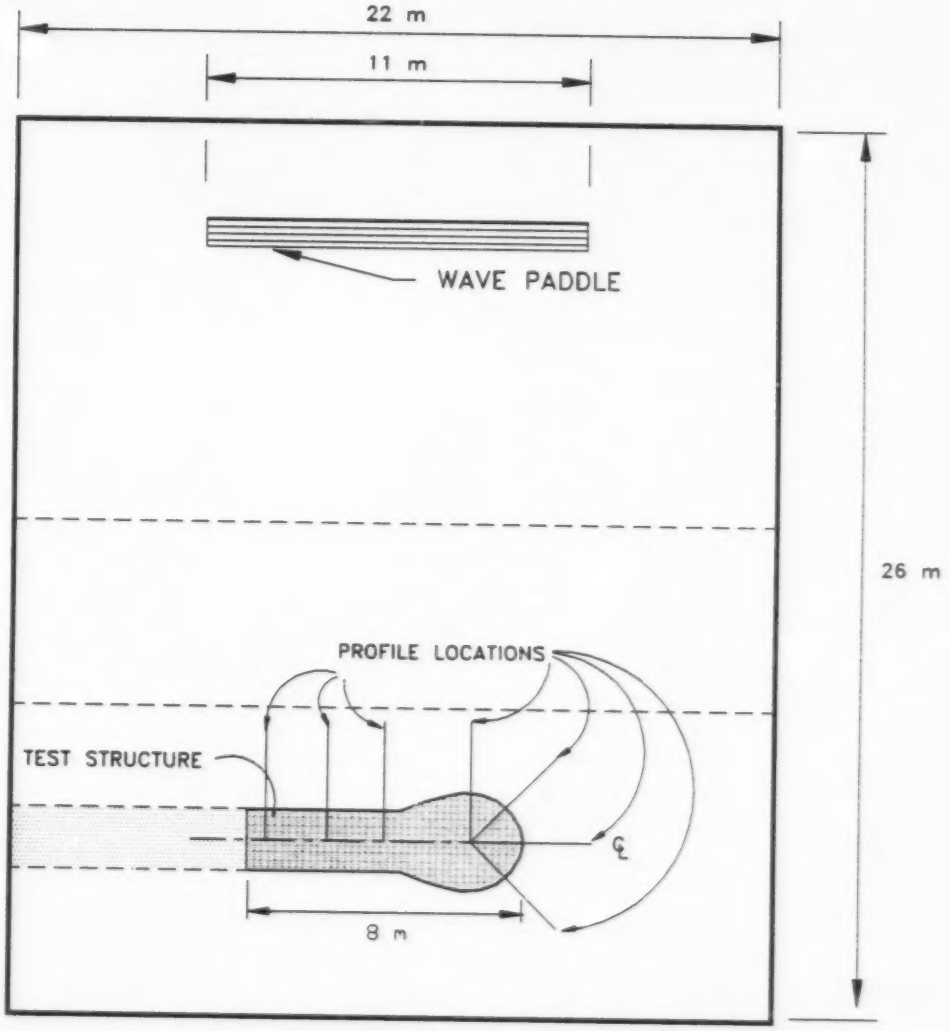

FIGURE 4.3 SERIES 2 LAYOUT

Table 4.6

Test Number	Wave Climate	Initial Berm Width (m)
13	4-3D	.60 head/trunk
14	4-3D	.75 trunk/1.0 head
15	4-3D	.75 trunk/1.0 head
16	3-3D	.75 trunk/1.0 head

Series 3 (To be completed)

Series 3 consisted of repeating some of the tests in Series 2, but with the 1:15 slope fronting the breakwater and the "false-floor" removed; thus the structure was constructed in a constant depth with a horizontal bottom between the wave paddle and the model. Comparison of the results obtained in test series 3 and 2 would enable a determination of the importance of wave transformation on the 1:15 slope utilized in all of the two dimensional testing. The layout of the test structure in the basin and the location of the profile lines are similar to those shown in Figure 4.3 (for series 2). The tests undertaken in series 3 are summarized below.

Table 4.7

Test Number	Wave Climate	Initial Berm Width (m)
17		
18		
19		
20		

Series 4 (To be completed)

This series was undertaken to evaluate the influence of the angle of wave attack on the stability of the dynamic breakwaters. All testing prior to this series was completed with waves normally incident on the structure (which produces the most significant reshaping along the trunk of the structure). However, waves attacking the structure with some angle of incidence to the trunk will create a lateral component of movement which is particularly noticeable at the head of the structure. The tests in series 4 were selected to facilitate comparison of the results with previous 3-dimensional and 2-dimensional tests. The test conditions were selected so that the range of parameters varied in the two dimensional tests would be covered (although each individual test is not repeated). Figure 4.4 shows the layout of the wave basin for this test series. Table 4.8 summarizes the tests in Series 4.

Table 4.8 Test Series 4 (tentative)

Test #	Wave Climate	Gradation	Angle of Incidence	Initial Berm Width
21	1-3D	5	15	a
22	1-3D	5	15	b
23	1-3D	5	30	a
24	1-3D	5	30	b
25	1-3D	5	45	a
26	1-3D	5	45	b
27	1-3D	2	15	
28	1-3D	2	30	
29	1-3D	2	45	
30	4-3D	2	15	
31	4-3D	2	30	
32	4-3D	2	45	
33	4-3D	4	0	
34	4-3D	4	15	
35	4-3D	4	30	
36	4-3D	4	45	

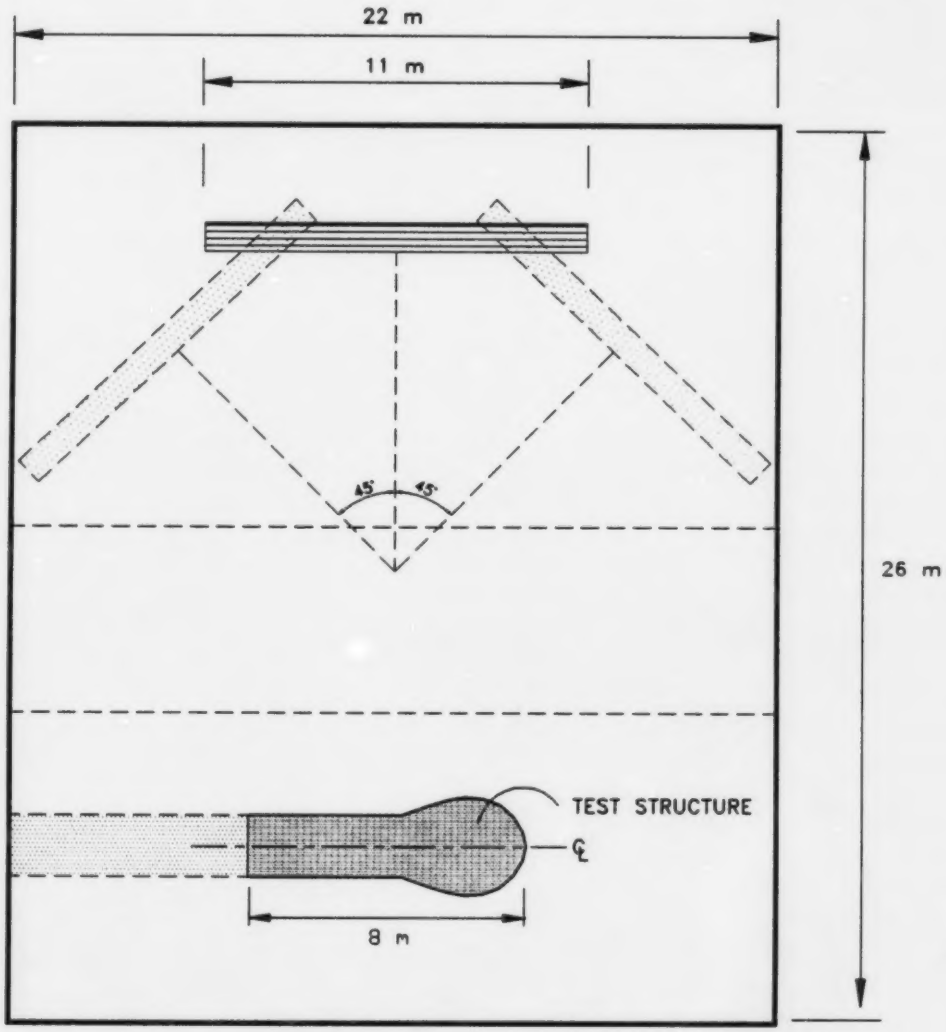

FIGURE 4.4 SERIES 4 LAYOUT SHOWING PADDLE LOCATIONS

4.2 TEST RESULTS

4.2.1 Series 1

Series 1 tests were undertaken to evaluate the influence of flume width on the overall performance of the reshaping breakwaters. Details of the tests are provided in Section 4.1.

Figures 4.5 to 4.17 illustrate the recession of the berm following each segment of the design storm for each individual tests. Separate data points are plotted on the figure for each of the flume widths. The vertical axes, "average B" provides an indication of the amount of recession, measured from the seaward edge of the berm. All tests results are presented regardless of whether the design section "failed" or not (failure being determined as berm erosion reaching the upper 3:1 slope). In the subsequent analysis evaluating the regression models, all data will not be used; only those tests meeting the stability requirements outlined earlier in this report were used. However, comparison of the recession of the berm during the growth segments of the storm as a function of flume width can be completed for any test.

In general Figs. 4.5 to 4.17 show comparable recession rates in each flume over the course of the design storm. The net recession in each flume at the end of the test is typically within a range of 5-10%. Considering that on average 45 to 50 cm of erosion is experienced and given that D_{50} = 1.4 cm then ± one stone would give a resolution of approximately 6%. Thus the range of 5-10% indicates no significant difference in the performance of each section.

In order to more carefully evaluate the influence of flume width on stable breakwaters only tests in which the berm meet the required stability criteria are considered in the following analysis.

Figures 4.18 to 4.26 provide an illustration of the relationship between flume width and B/H_{peak}, where B is the starting berm width (equal to the amount of recession) and H_{peak} is the significant wave height at the peak of the design storm (see section 4.1).

Figures 4.18 to 4.21 show that, in general, B/H_{peak} increases with increasing flume width (thus indicating more reshaping) for all wave climates. Values of B/H_{peak} are maximum for the 4 m flume. The interrelation between reshaping and wave climate is shown on Figure 4.22 (all wave climates). Wave climate 1-3D, 3-3D, and 4-3D all produced similar results, whereas slightly more reshaping occurred for wave climate 2-3D.

Figures 4.23 to 4.26 show the influence of groupiness factor on relative shaping (B/H_{peak}). Figure 4.23 indicates that for low values of groupiness, no significant difference in reshaping exists (as a function of flume width). As the groupiness factor is increased (Fig. 4.24, groupiness factor = 0.75 and figure 4.25, groupiness factor = 1.2) then the flume width becomes more important. The most significant difference in reshaping between the 4 m and the 1.2 and 2.4 m flumes occurs at the highest value of groupiness. Figure 4.26 shows all values of groupiness factor plotted on one figure. Values of B/H_{peak} for flume widths of 1.2 and 2.4 m are relatively constant, whereas B/H_{peak} shows an increase with increasing groupiness for the 4 m flume results.

Table 4.9 shows the predictive ability of the equations developed from the two dimensional test

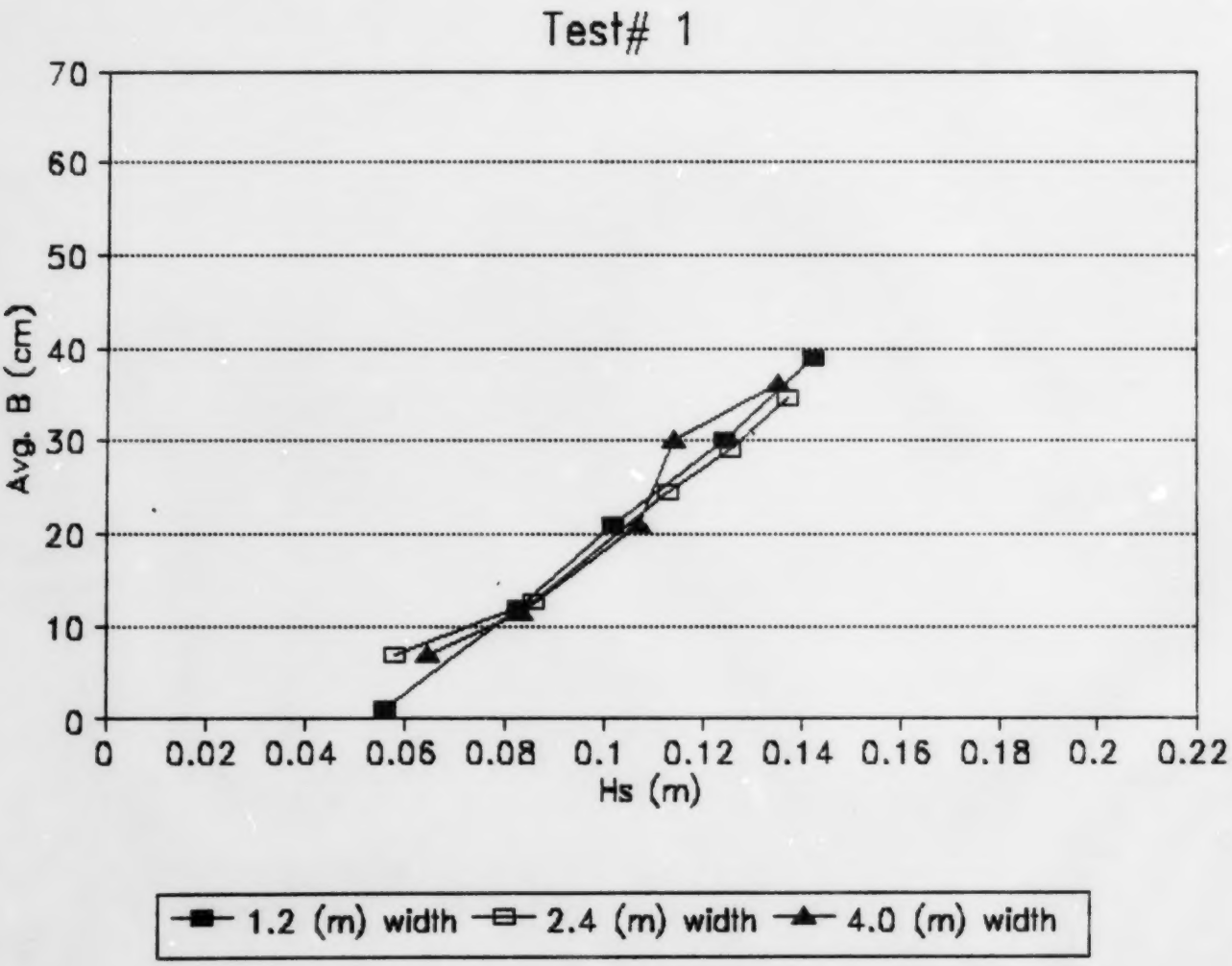

FIGURE 4.5

FIGURE 4.5

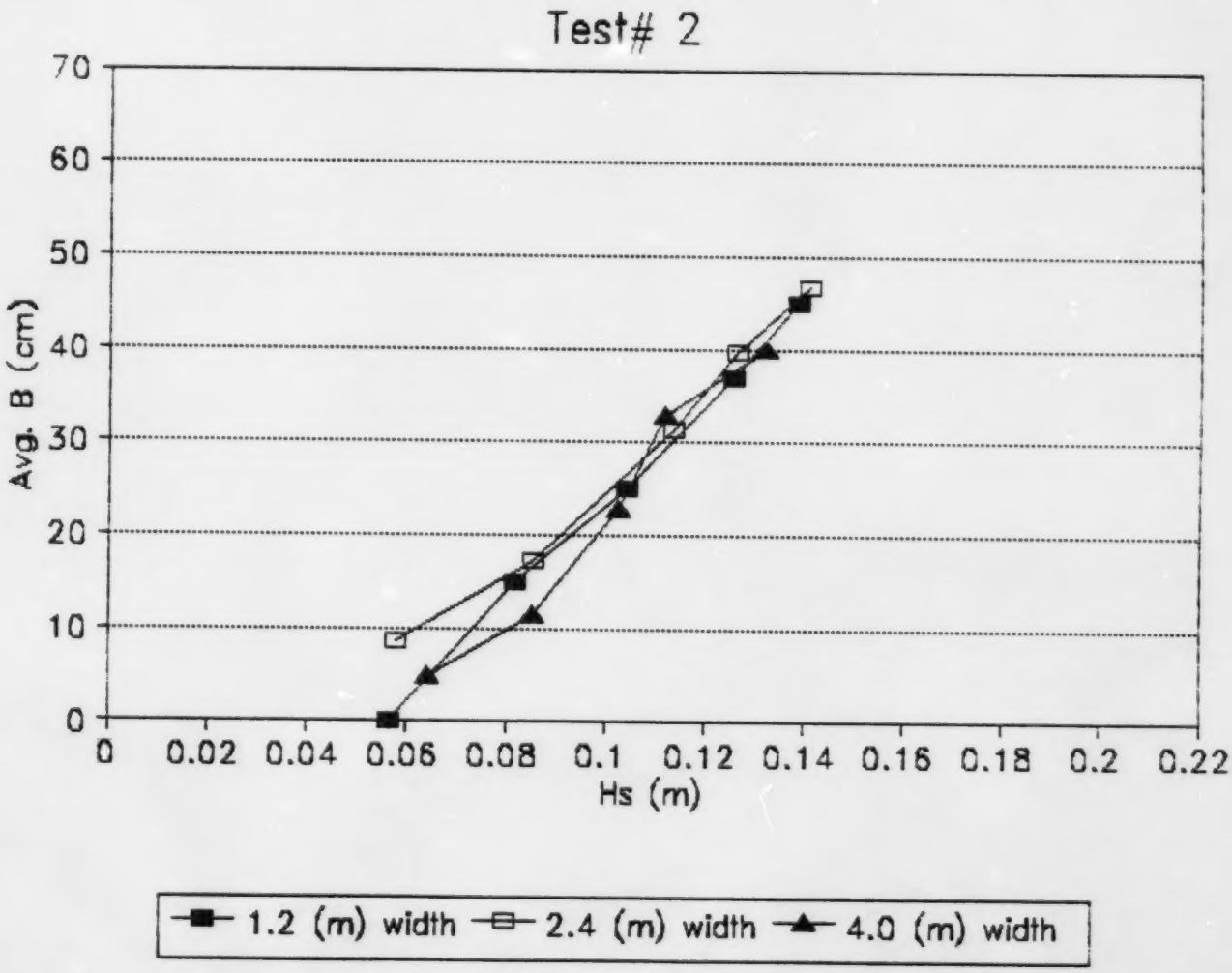
Test# 2
70
60
50
40
30
20
10
0
Avg. B (cm)
0
0.02
0.04
0.06
0.08
0.1
0.12
0.14
0.16
0.18
0.2
0.22
Hs (m)
1.2 (m) width
2.4 (m) width
4.0 (m) width

FIGURE 4.6

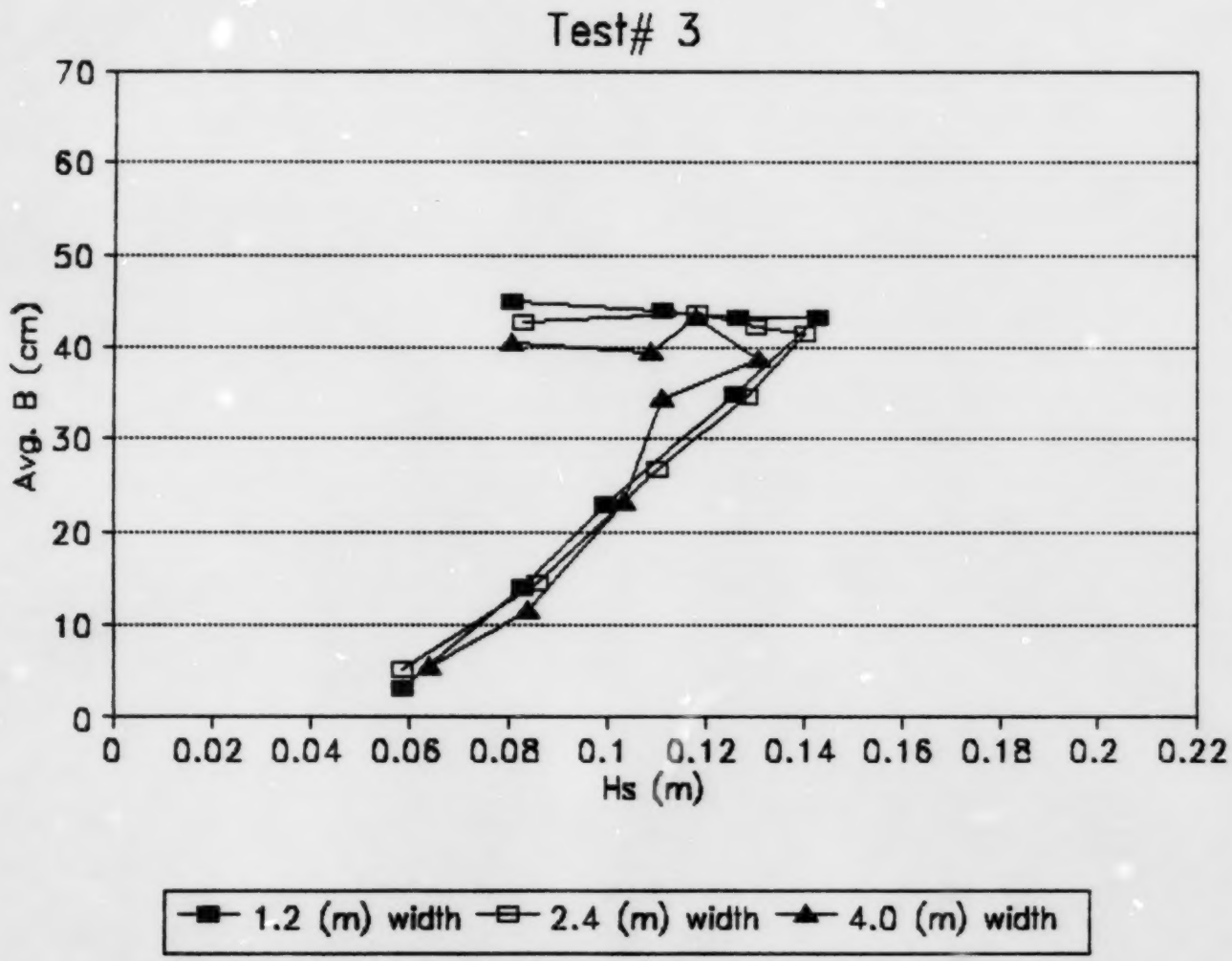
Test# 3
70
60
50
40
30
20
10
0
Avg. B (cm)
0
0.02
0.04
0.06
0.08
0.1
0.12
0.14
0.16
0.18
0.2
0.22
Hs (m)
1.2 (m) width
2.4 (m) width
4.0 (m) width

FIGURE 4.7

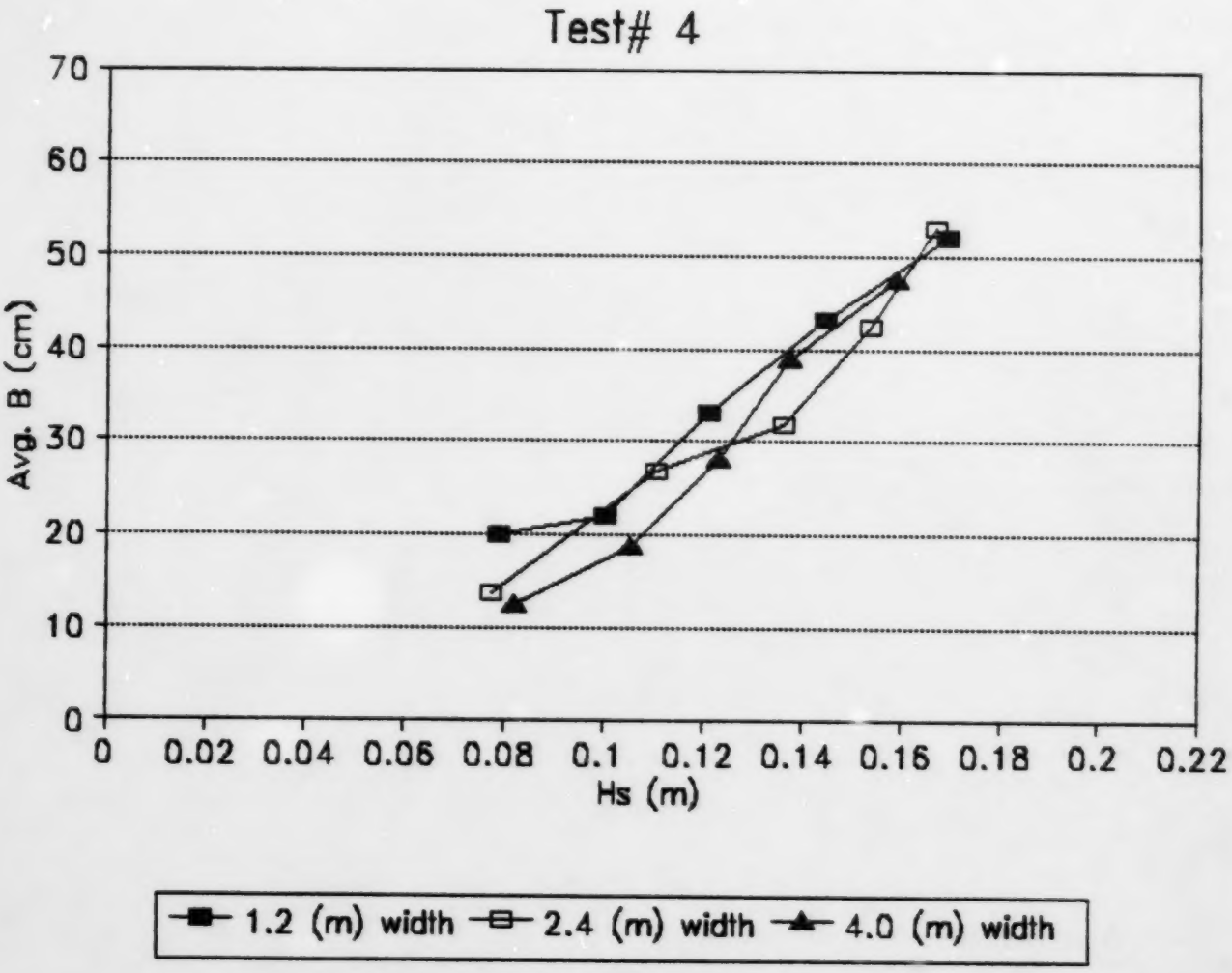
Test# 4
70
60
50
40
30
20
10
0
Avg. B (cm)
0
0.02
0.04
0.06
0.08
0.1
0.12
0.14
0.16
0.18
0.2
0.22
Hs (m)
1.2 (m) width
2.4 (m) width
4.0 (m) width

FIGURE 4.8

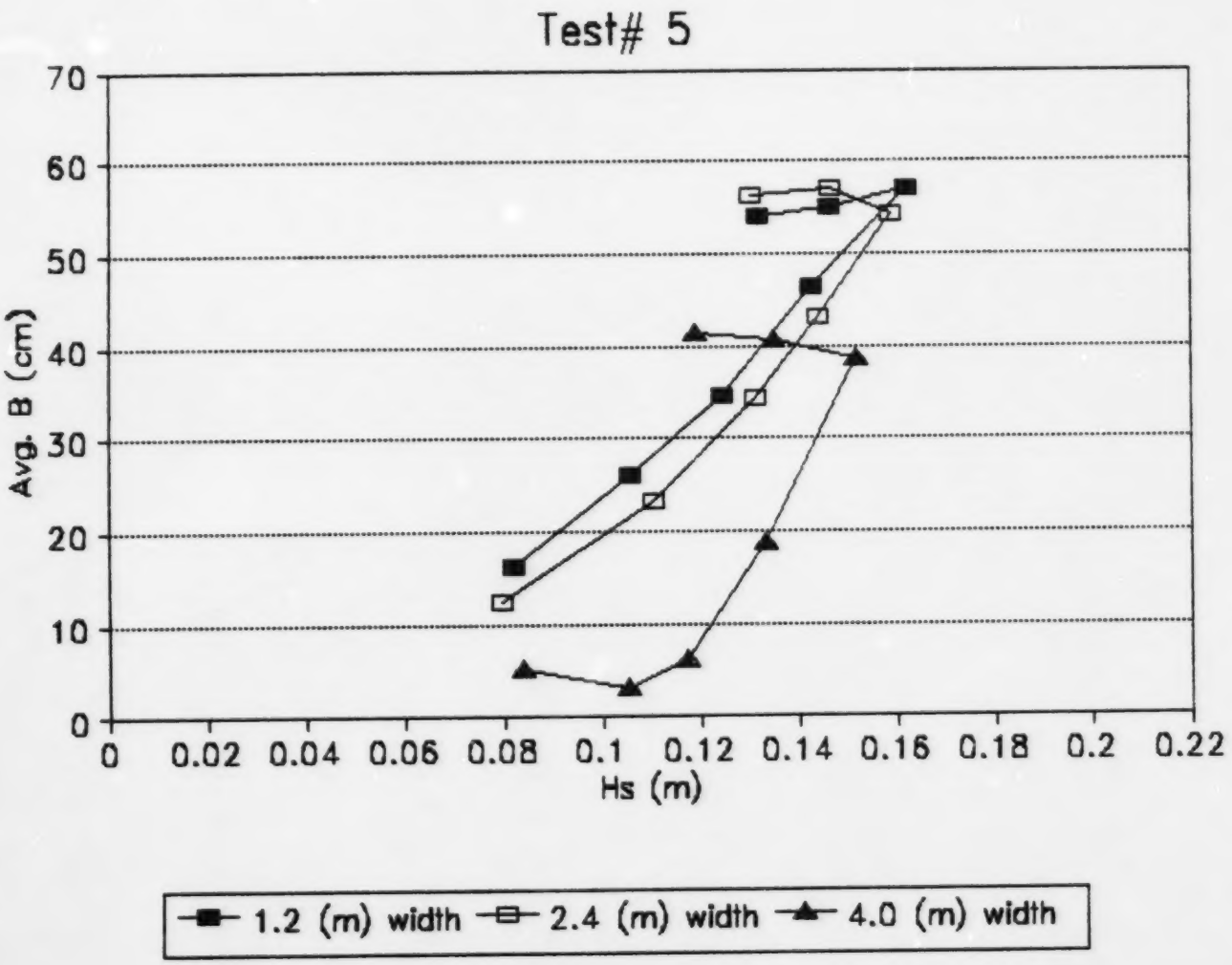
Test# 5
Avg. B (cm)
70
60
50
40
30
20
10
0
0
0.02
0.04
0.06
0.08
0.1
0.12
0.14
0.16
0.18
0.2
0.22
Hs (m)
1.2 (m) width
2.4 (m) width
4.0 (m) width

FIGURE 4.9

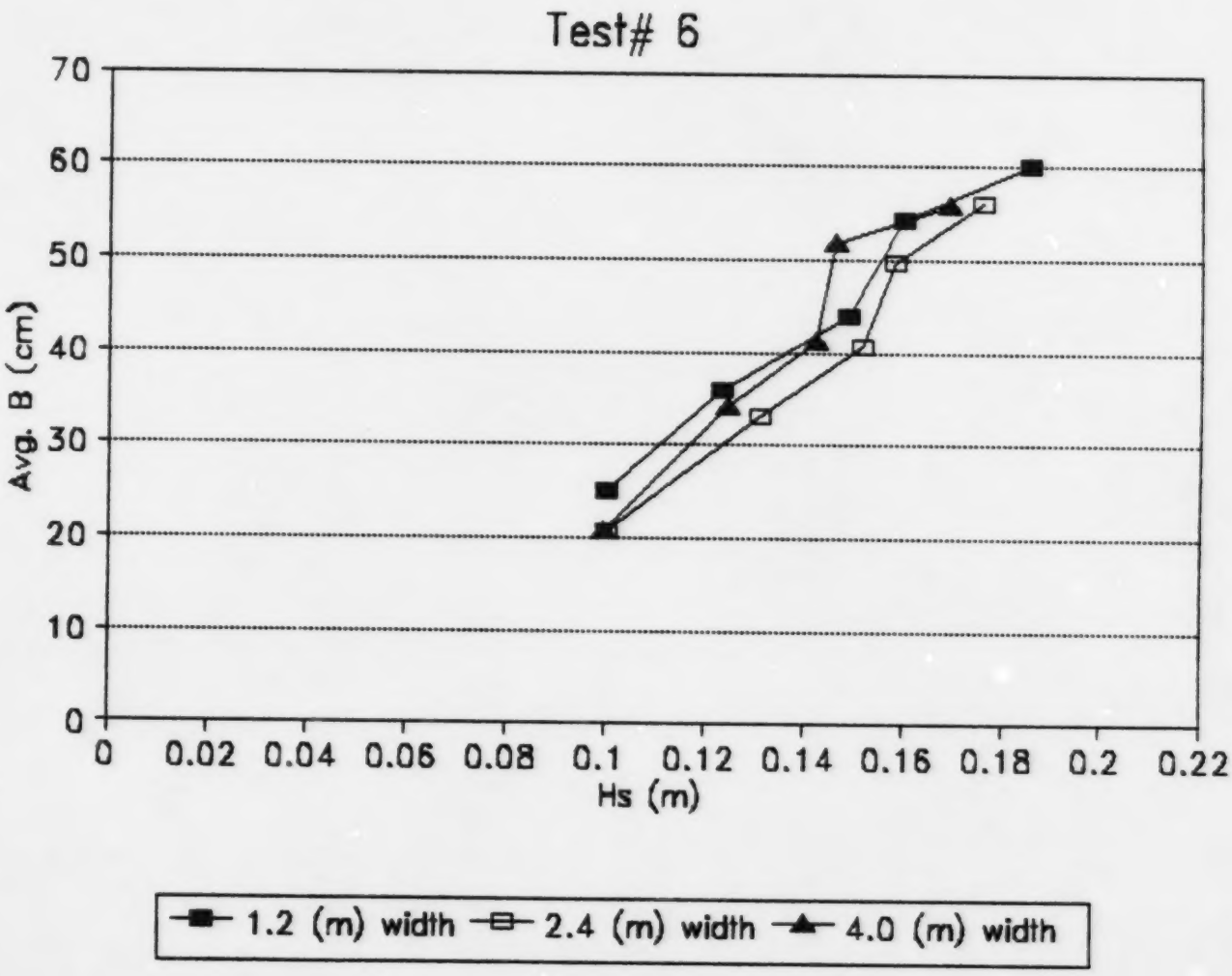
Test# 6
70
60
50
40
30
20
10
0
Avg. B (cm)
0
0.02
0.04
0.06
0.08
0.1
0.12
0.14
0.16
0.18
0.2
0.22
Hs (m)
1.2 (m) width
2.4 (m) width
4.0 (m) width

FIGURE 4.10

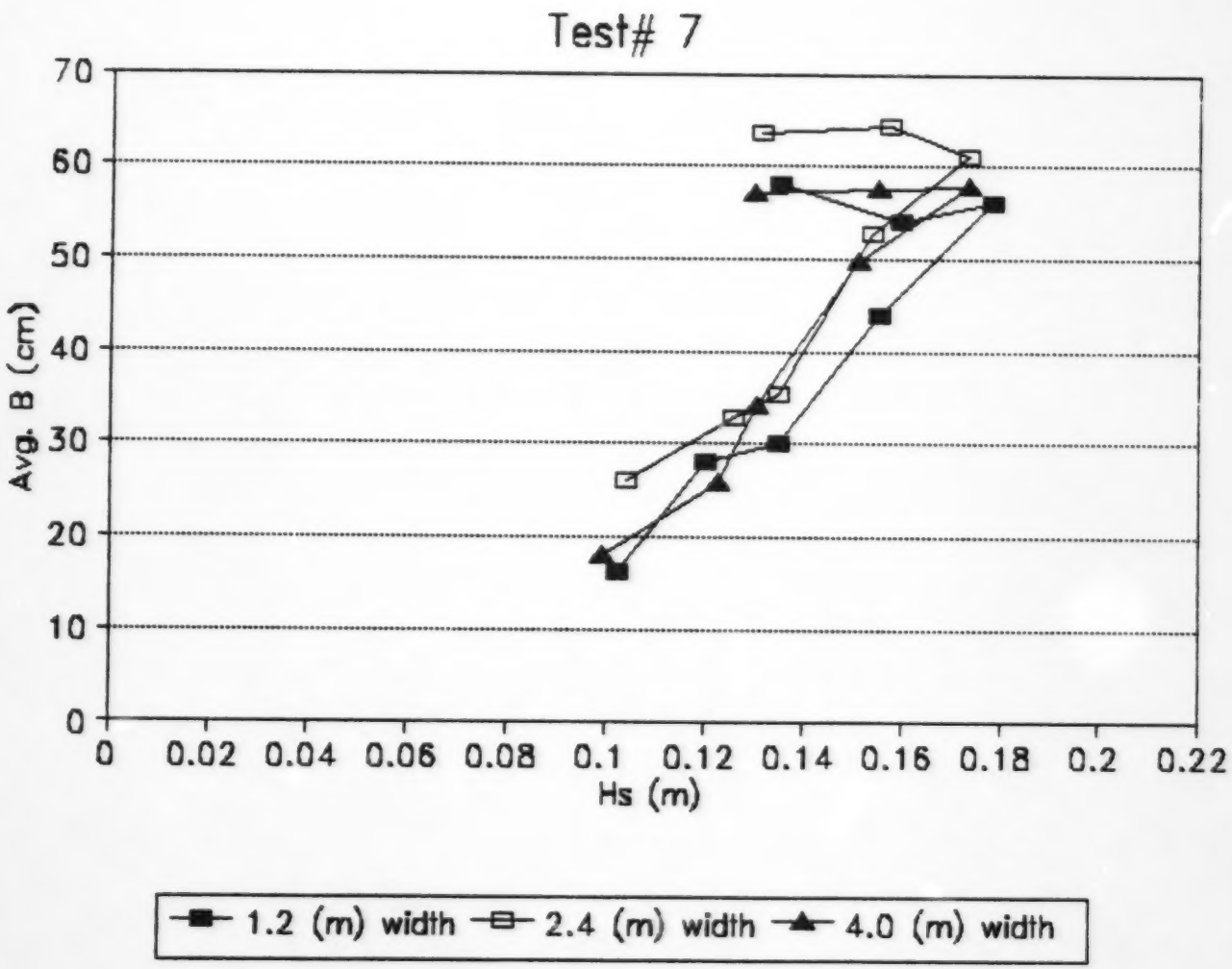
Test# 7
Avg. B (cm)
70
60
50
40
30
20
10
0
0
0.02
0.04
0.06
0.08
0.1
0.12
0.14
0.16
0.18
0.2
0.22
Hs (m)
1.2 (m) width
2.4 (m) width
4.0 (m) width

FIGURE 4.11

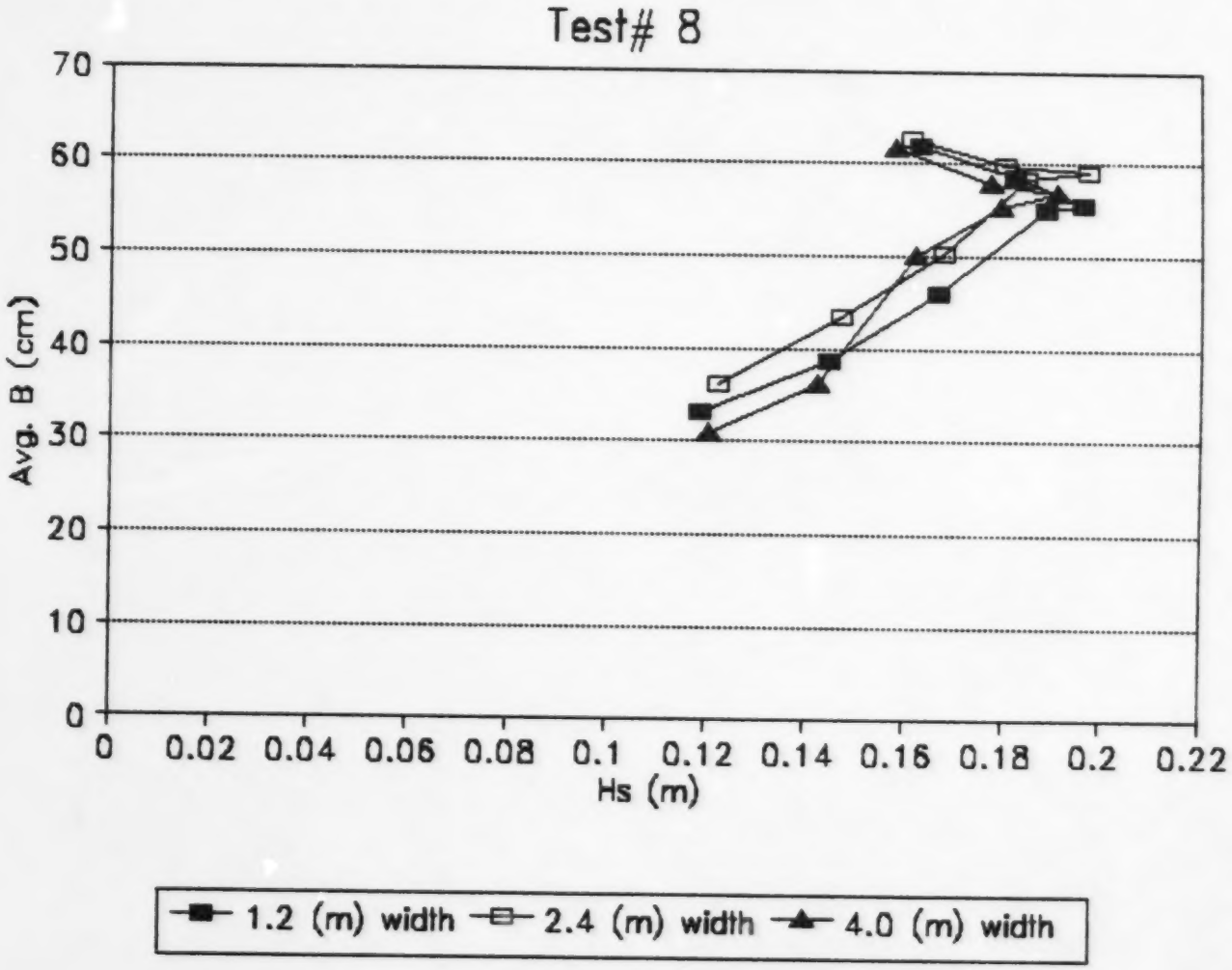
Test# 8
70
60
50
40
30
20
10
0
Avg. B (cm)
0
0.02
0.04
0.06
0.08
0.1
0.12
0.14
0.16
0.18
0.2
0.22
Hs (m)
1.2 (m) width
2.4 (m) width
4.0 (m) width

FIGURE 4.12

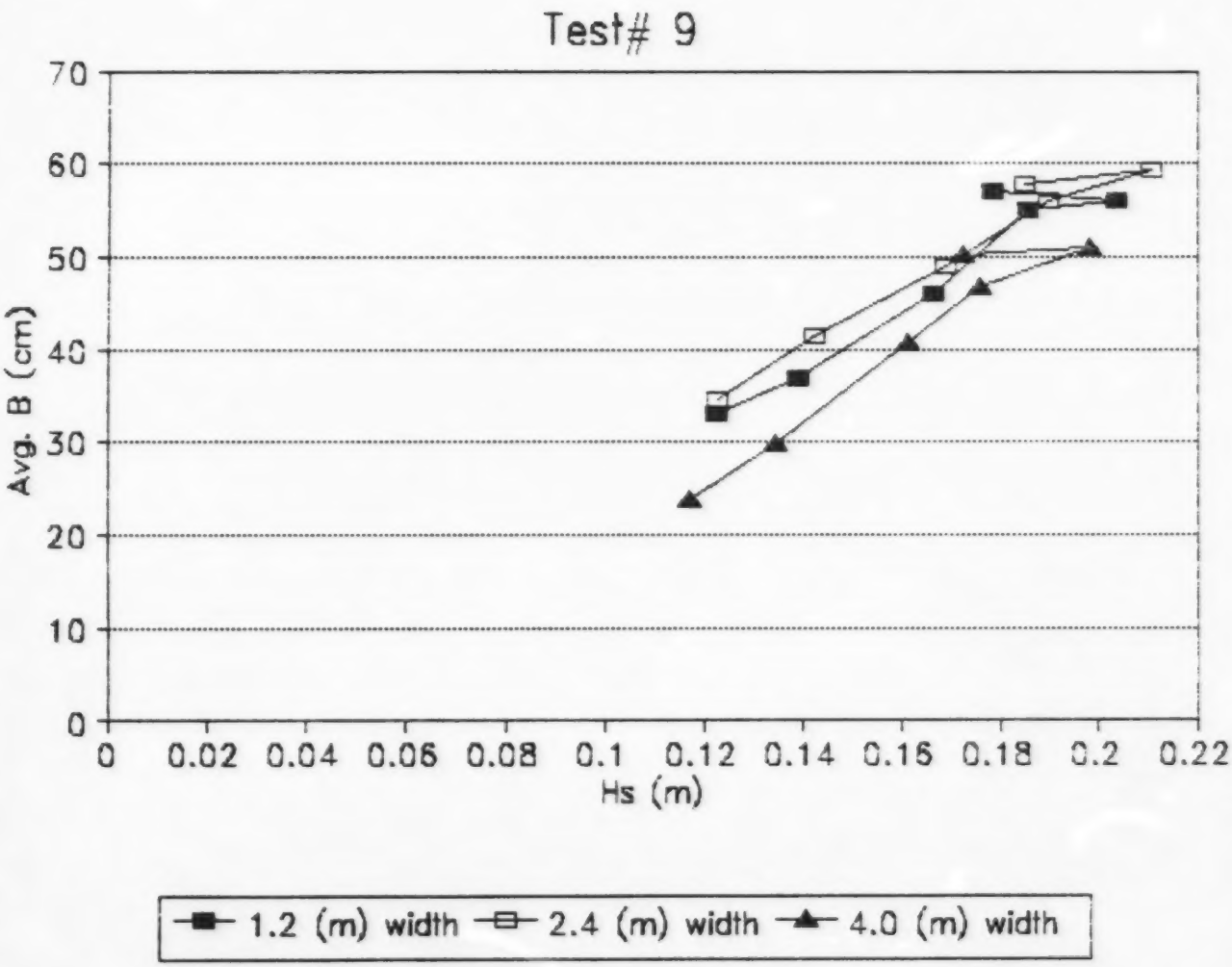
Test# 9
70
60
50
40
30
20
10
0
Avg. B (cm)
0
0.02
0.04
0.06
0.08
0.1
0.12
0.14
0.16
0.18
0.2
0.22
Hs (m)
1.2 (m) width
2.4 (m) width
4.0 (m) width

FIGURE 4.13

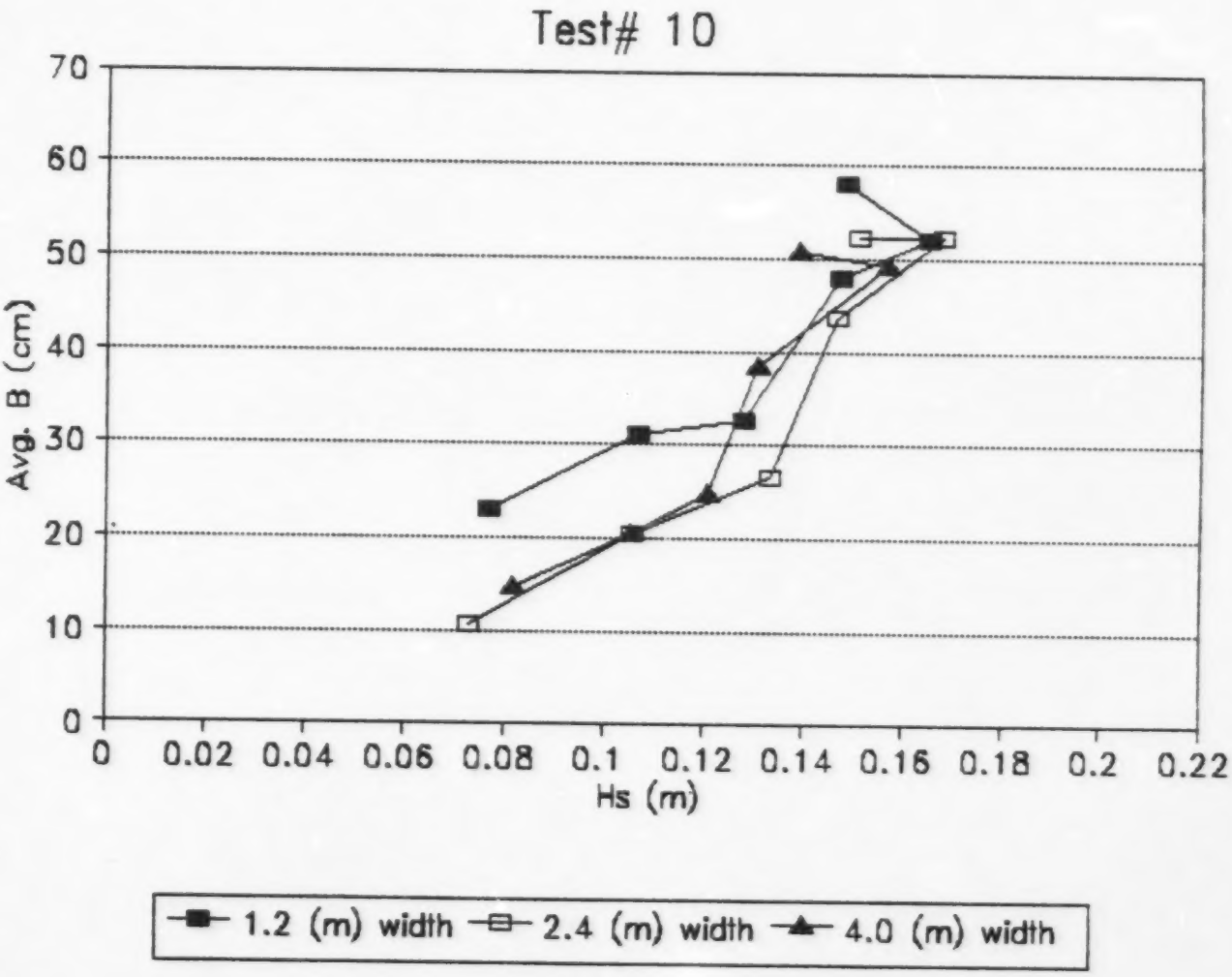
Test# 10
70
60
50
40
30
20
10
0
Avg. B (cm)
0
0.02
0.04
0.06
0.08
0.1
0.12
0.14
0.16
0.18
0.2
0.22
Hs (m)
1.2 (m) width
2.4 (m) width
4.0 (m) width

FIGURE 4.14

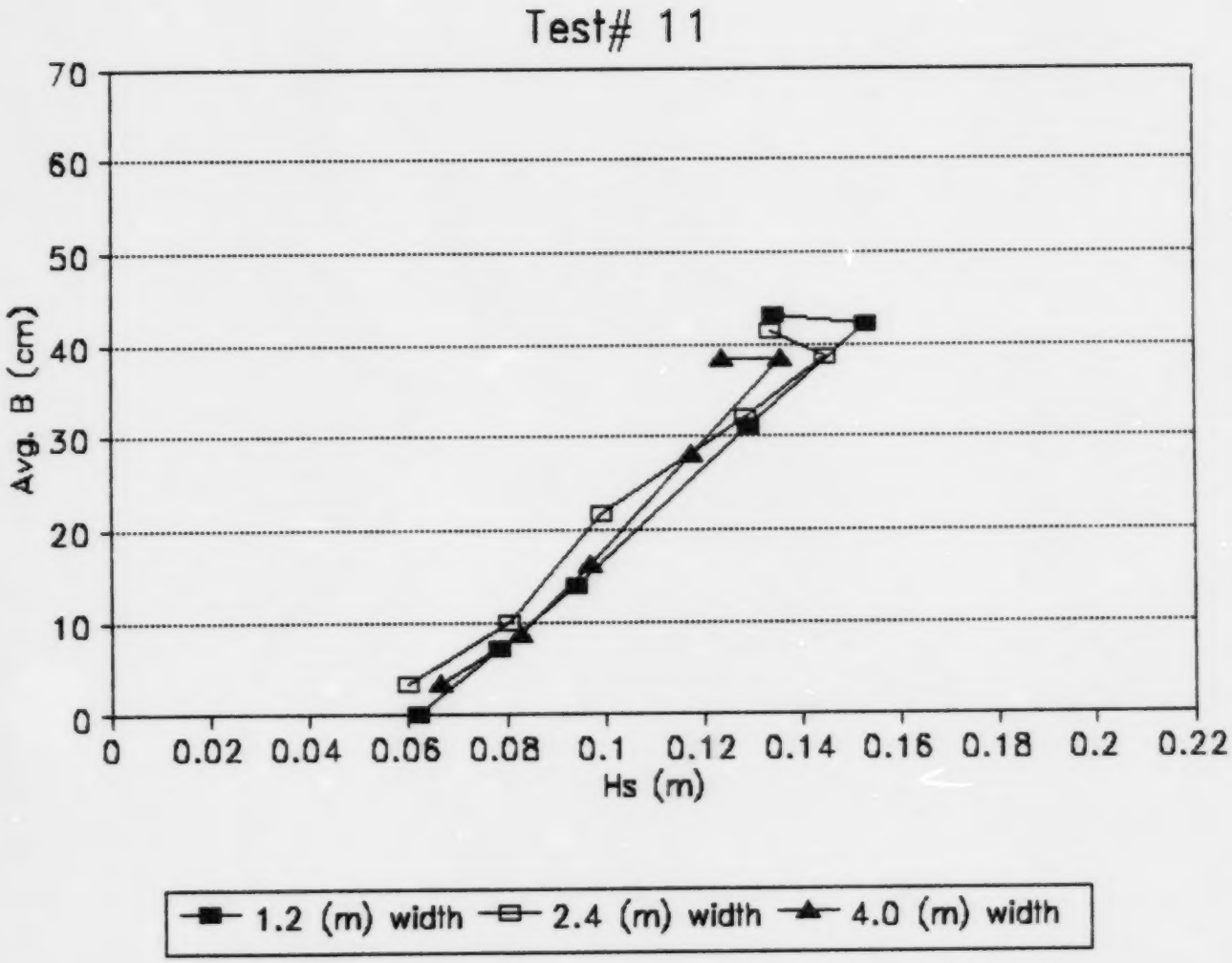
Test# 11
70
60
50
40
30
20
10
0
Avg. B (cm)
0
0.02
0.04
0.06
0.08
0.1
0.12
0.14
0.16
0.18
0.2
0.22
Hs (m)
1.2 (m) width
2.4 (m) width
4.0 (m) width

FIGURE 4.15

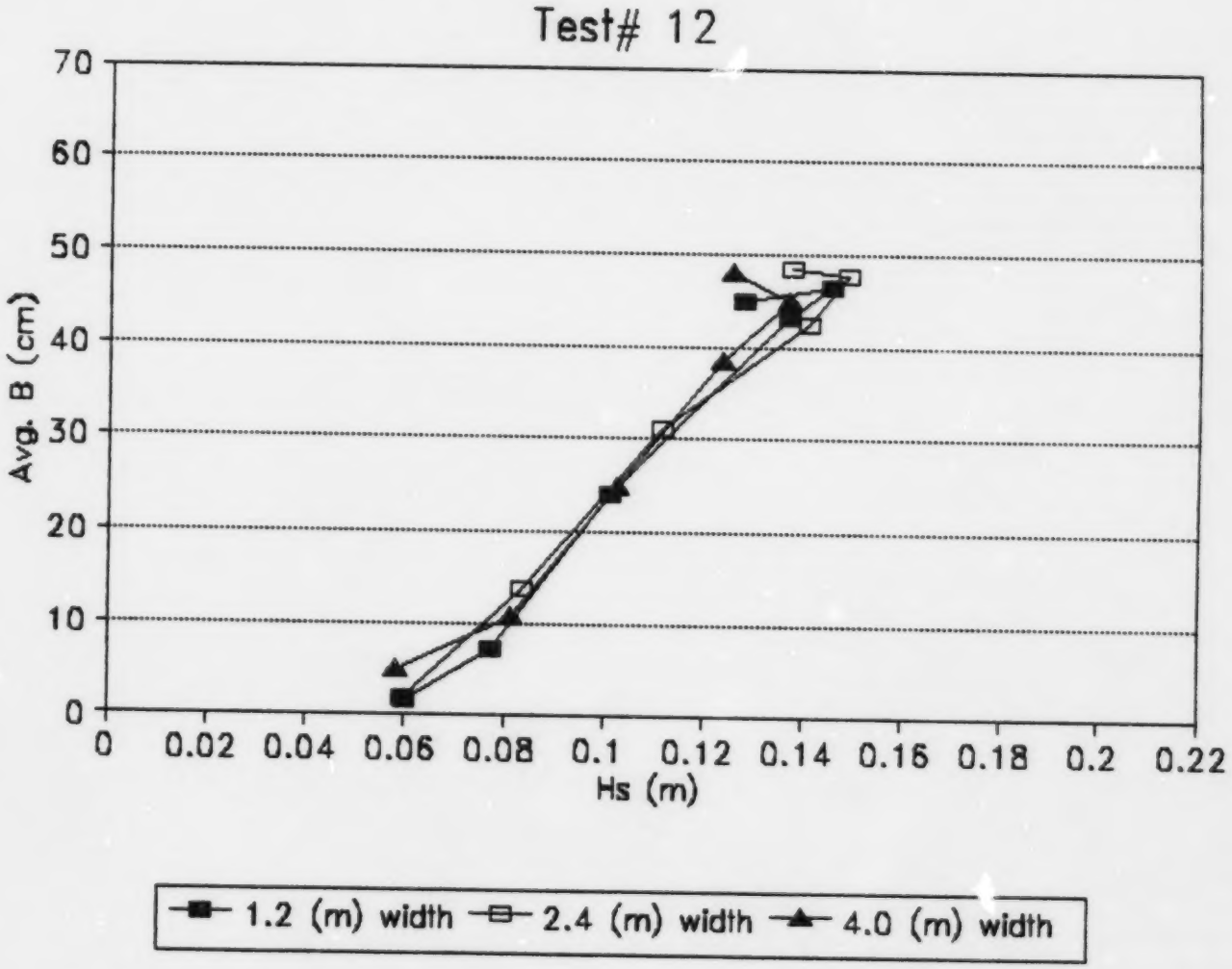
Test# 12
70
60
50
40
30
20
10
0
Avg. B (cm)
0
0.02
0.04
0.06
0.08
0.1
0.12
0.14
0.16
0.18
0.2
0.22
Hs (m)
1.2 (m) width
2.4 (m) width
4.0 (m) width

FIGURE 4.16

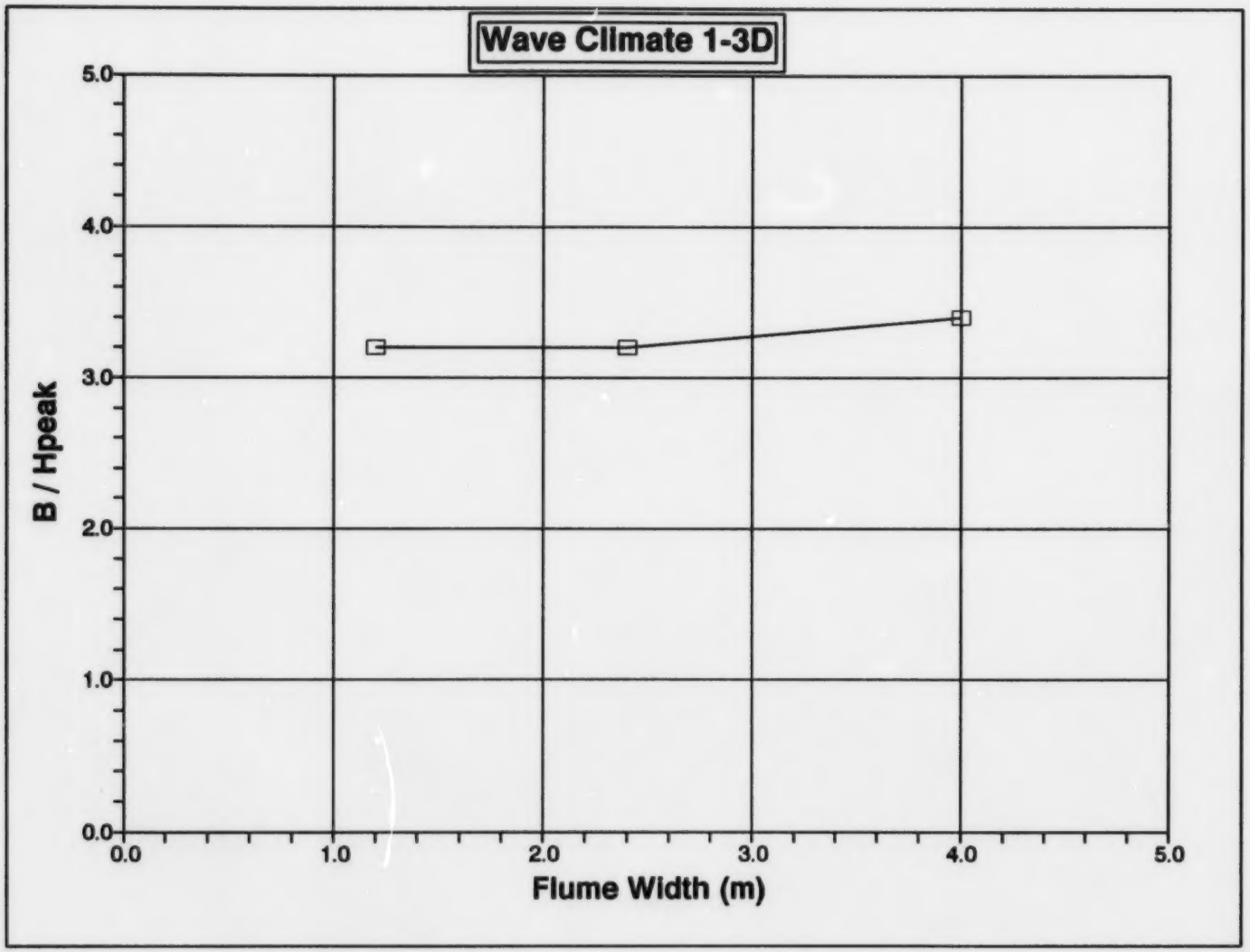
Wave Climate 1-3D
B / Hpeak
5.0
4.0
3.0
2.0
1.0
0.0
0.0
1.0
2.0
3.0
4.0
5.0
Flume Width (m)

FIGURE 4.18

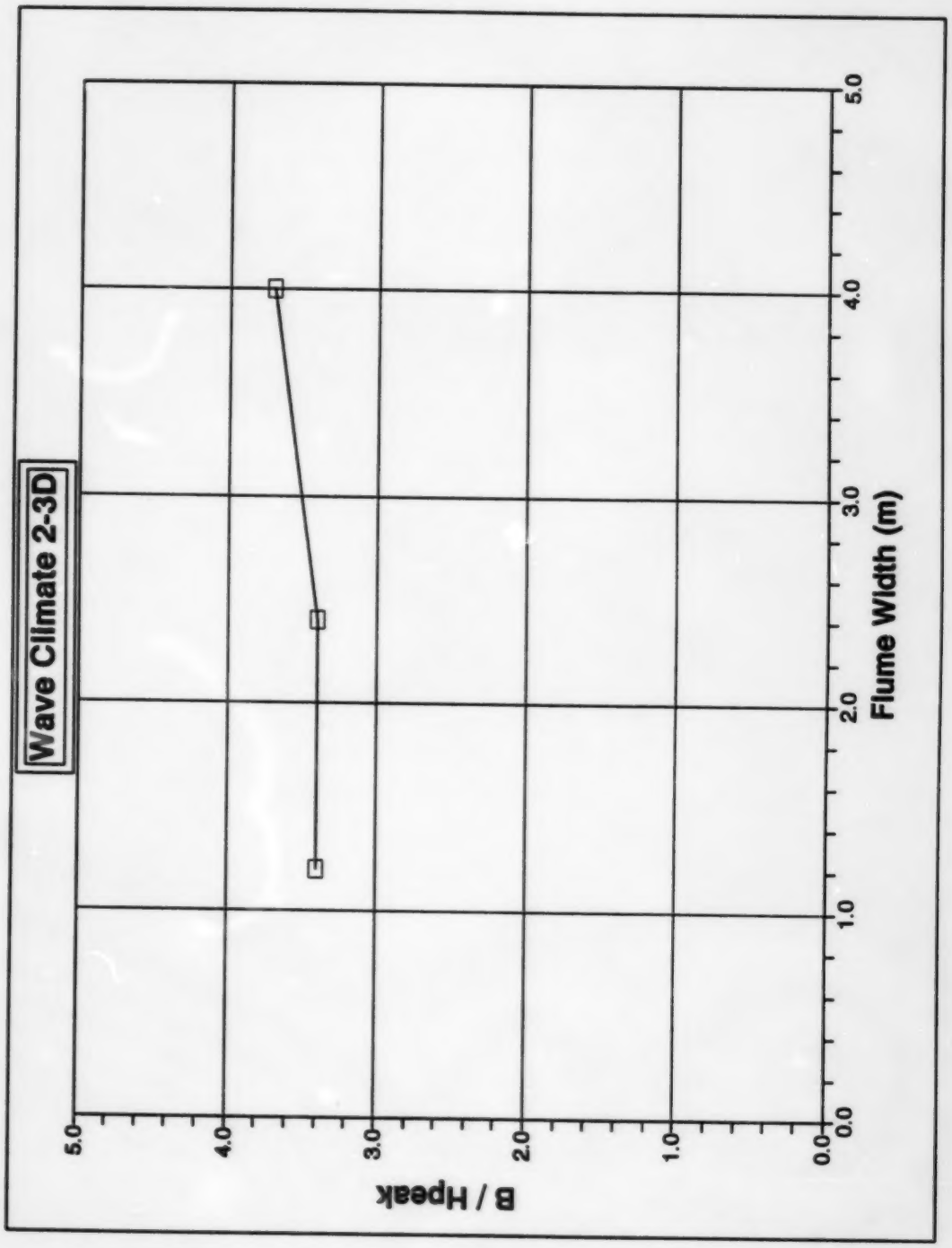

FIGURE 4.19

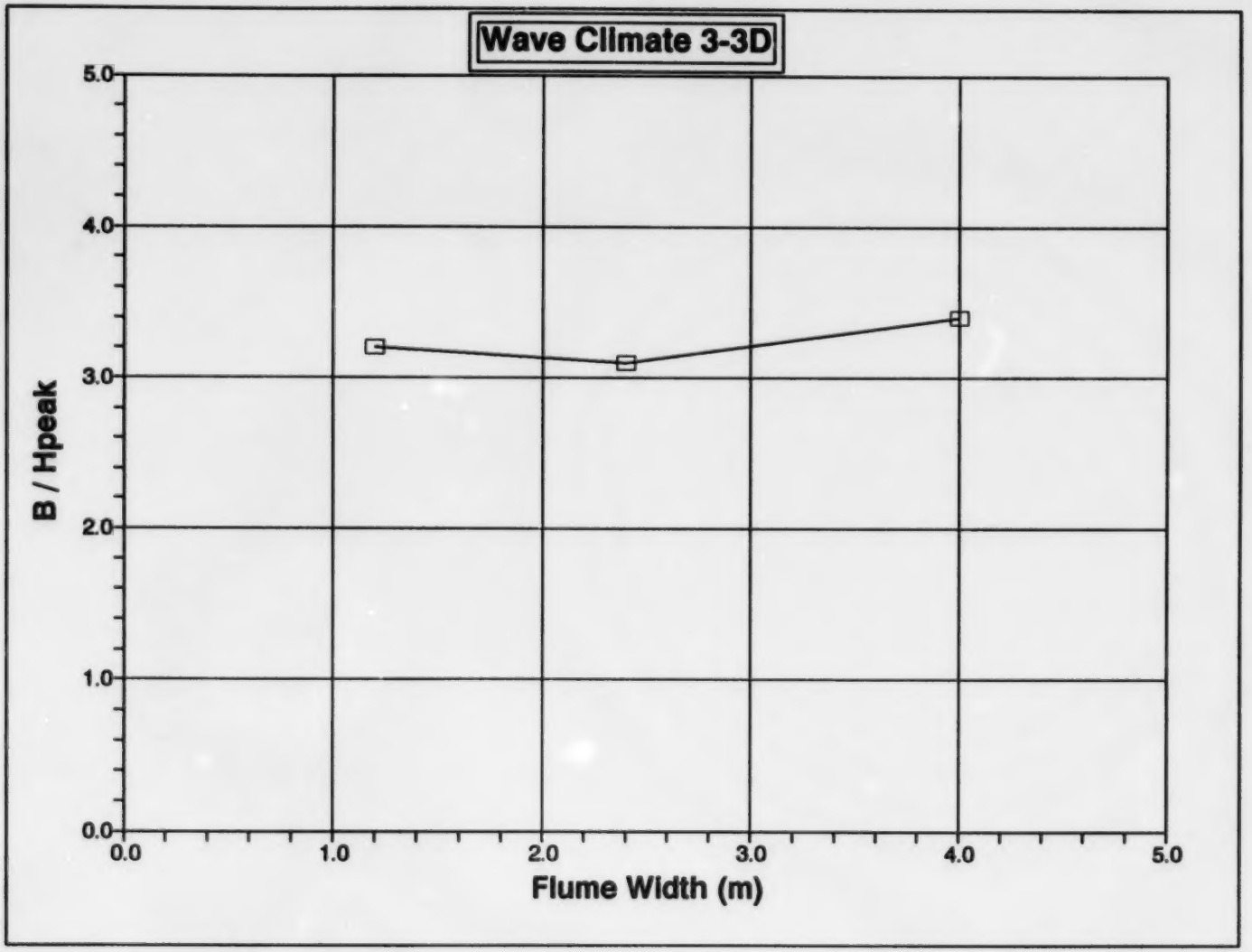
Wave Climate 3-3D
B / Hpeak
5.0
4.0
3.0
2.0
1.0
0.0
0.0
1.0
2.0
3.0
4.0
5.0
Flume Width (m)

FIGURE 4.20

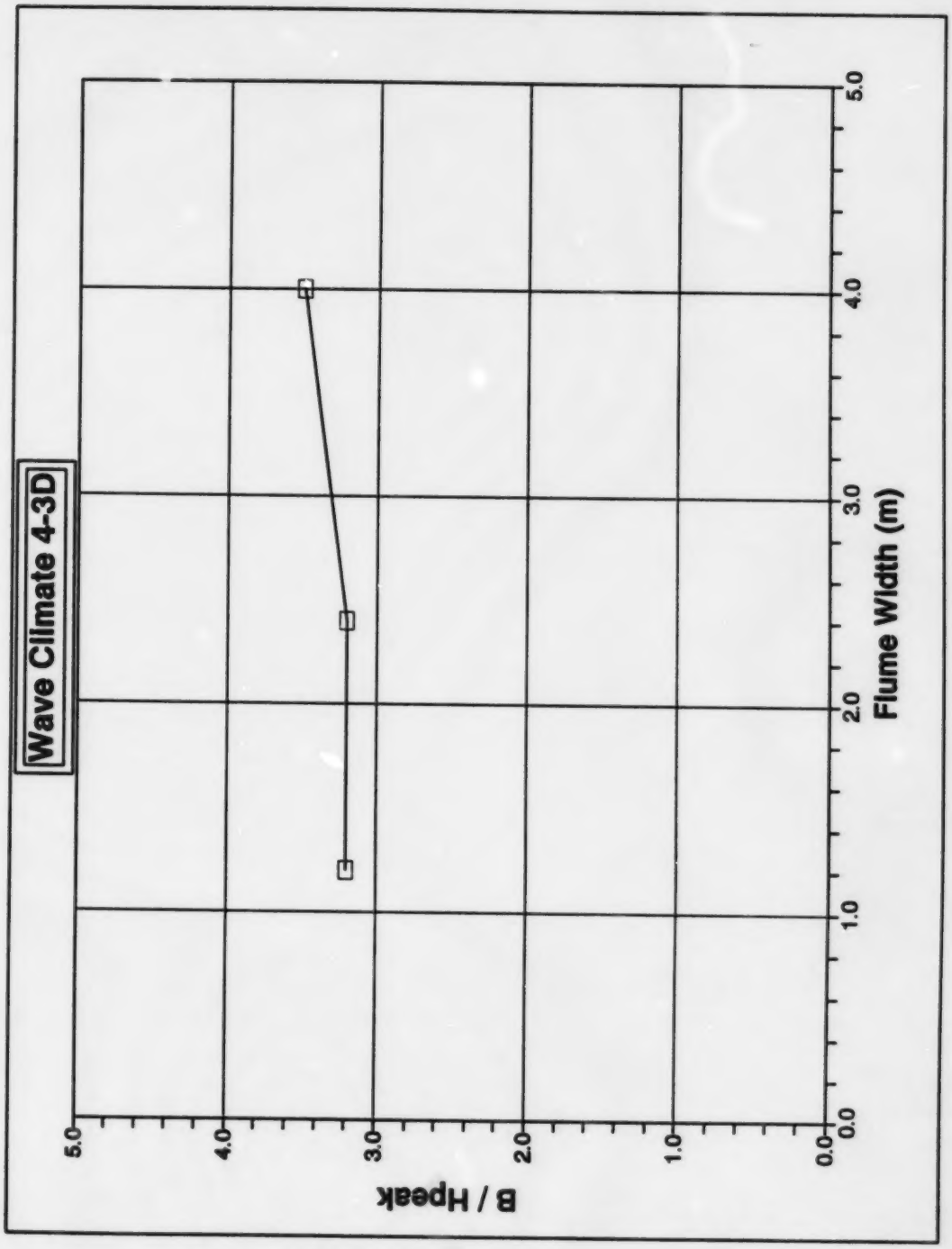
Wave Climate 4-3D
B / Hpeak
Flume Width (m)
0.0
1.0
2.0
3.0
4.0
5.0
0.0
1.0
2.0
3.0
4.0
5.0

FIGURE 4.21

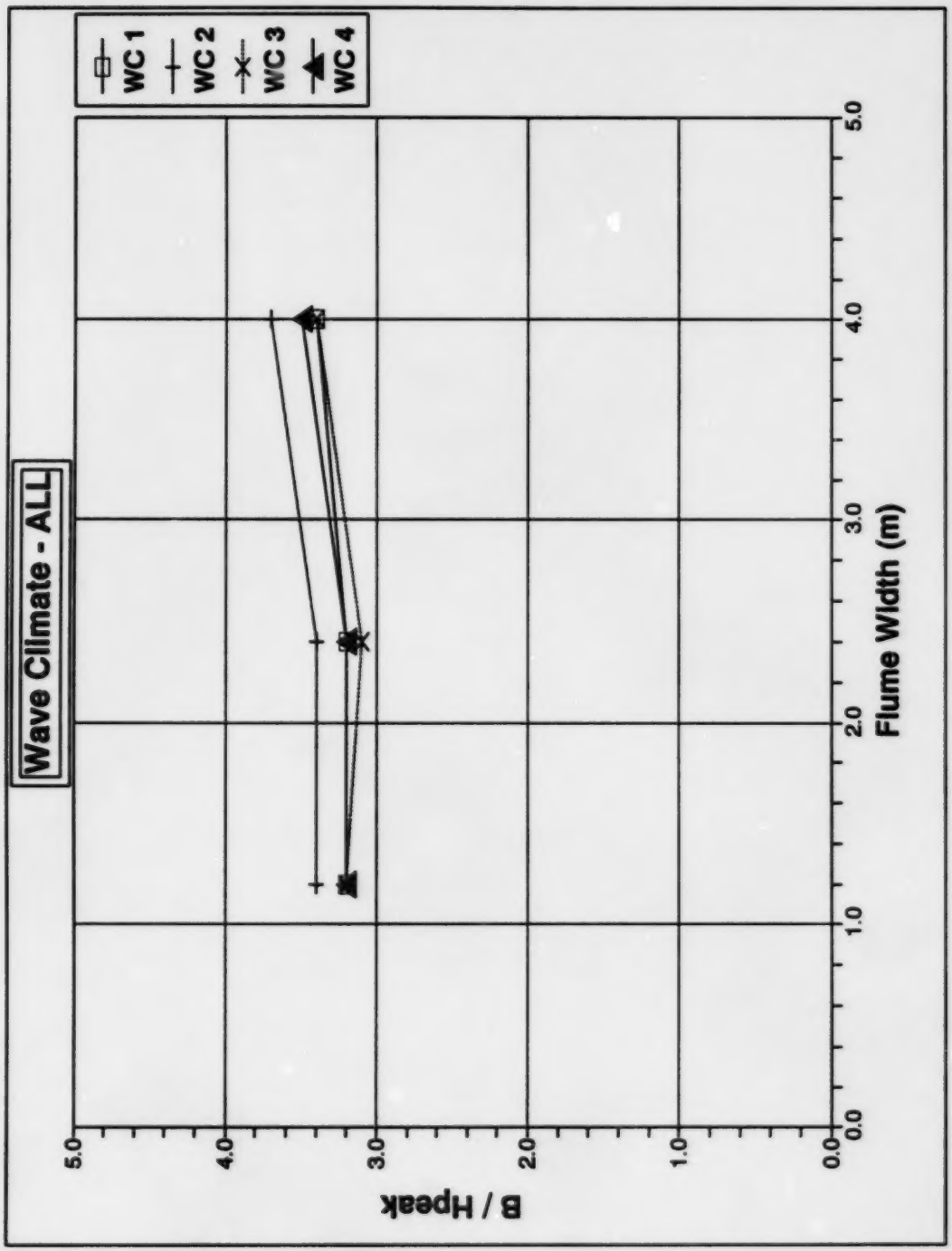
Wave Climate - ALL
WC 1
WC 2
WC 3
WC 4
B / Hpeak
Flume Width (m)
0.0
1.0
2.0
3.0
4.0
5.0

FIGURE 4.22

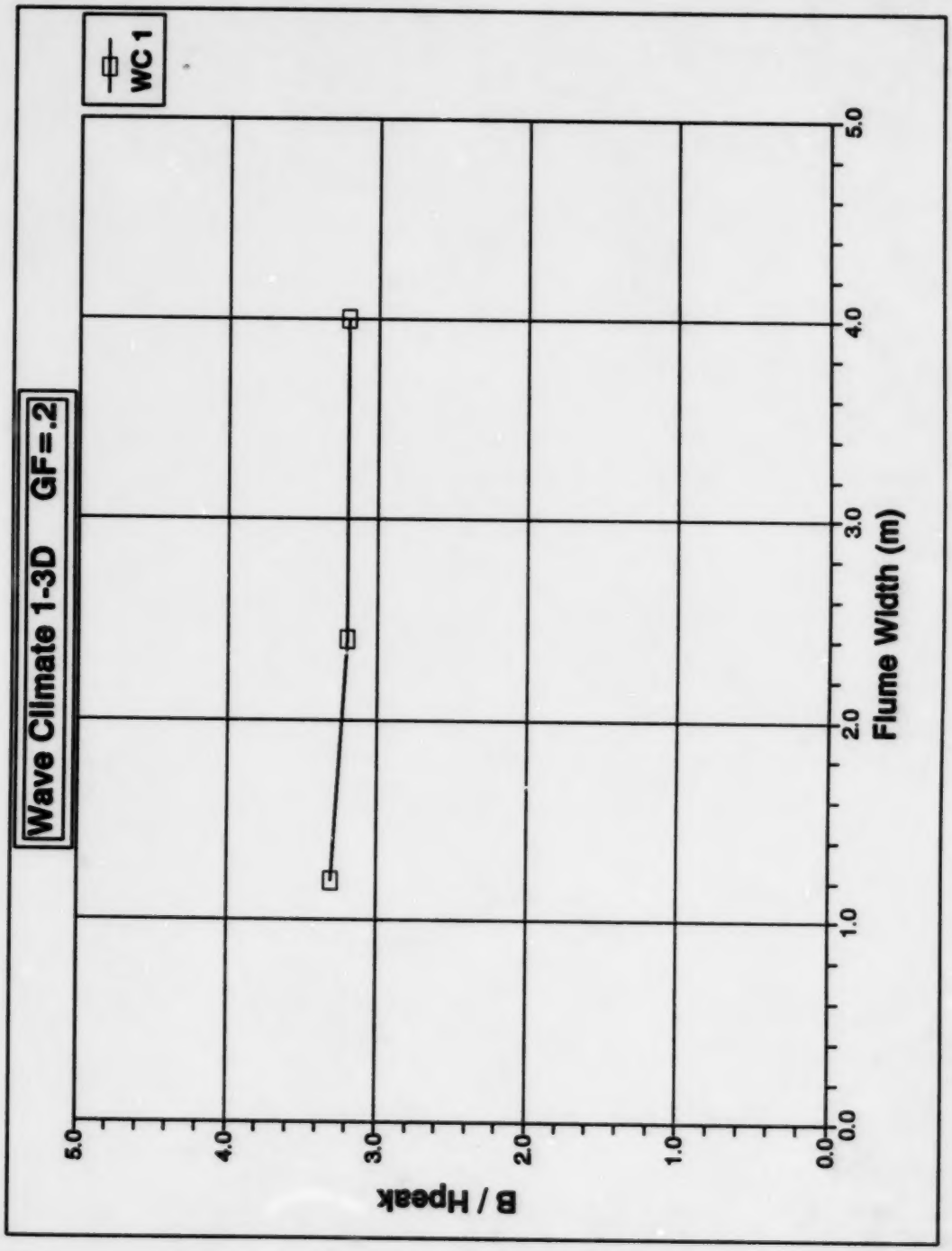

FIGURE 4.23

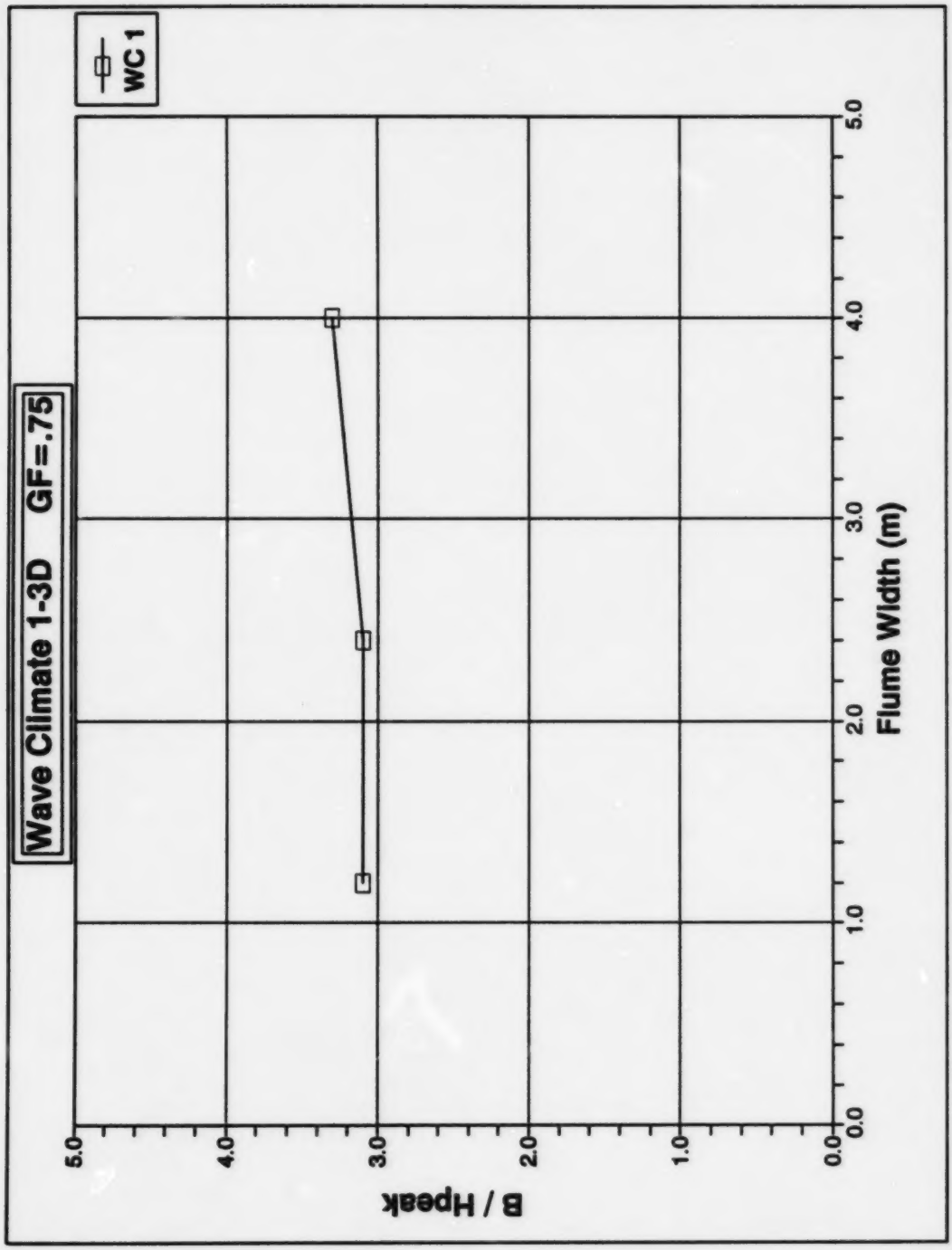
Wave Climate 1-3D GF=.75
WC 1
B / Hpeak
Flume Width (m)
0.0
1.0
2.0
3.0
4.0
5.0

FIGURE 4.24

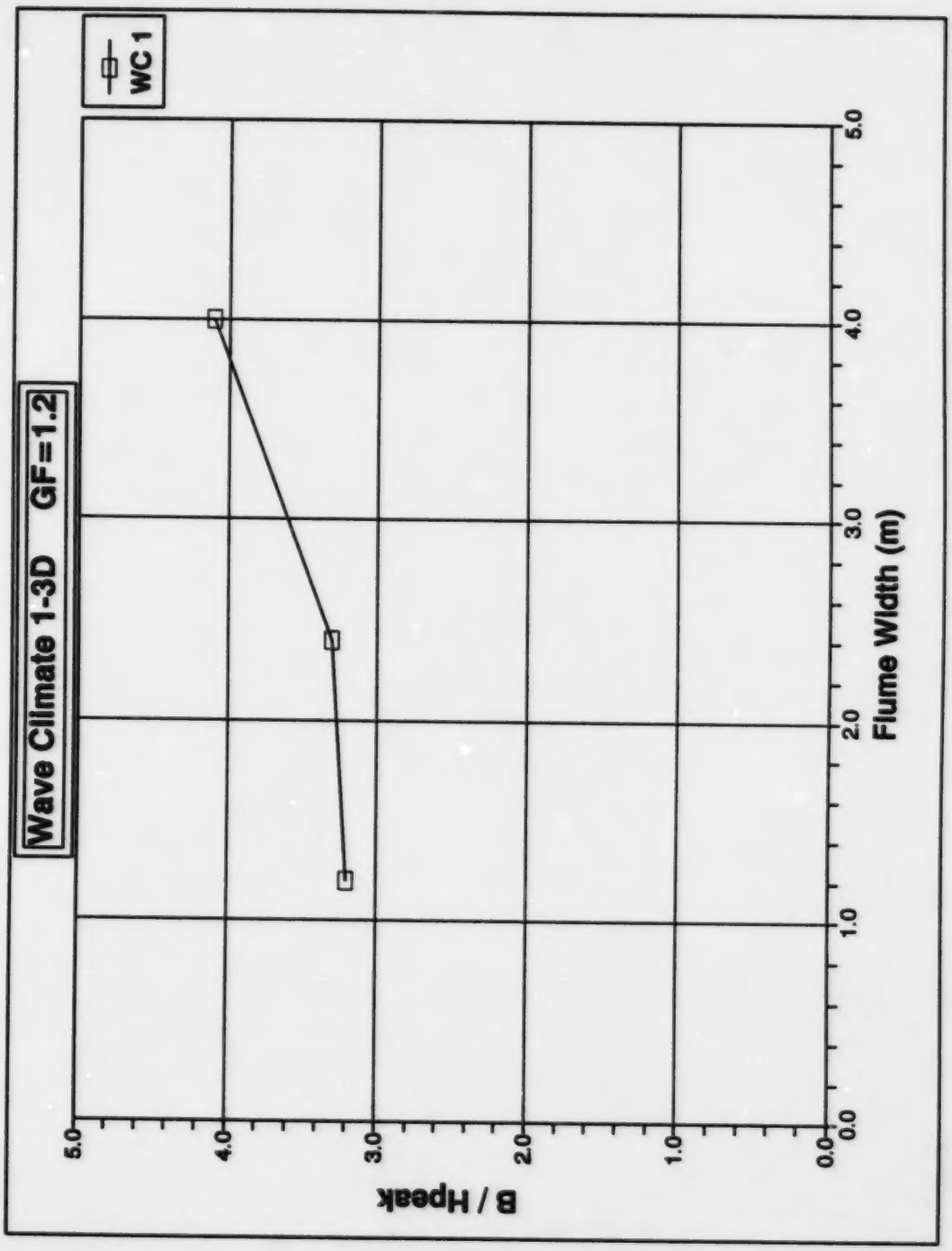
Wave Climate 1-3D GF=1.2
WC 1
B / Hpeak
Flume Width (m)
0.0
1.0
2.0
3.0
4.0
5.0

FIGURE 4.25

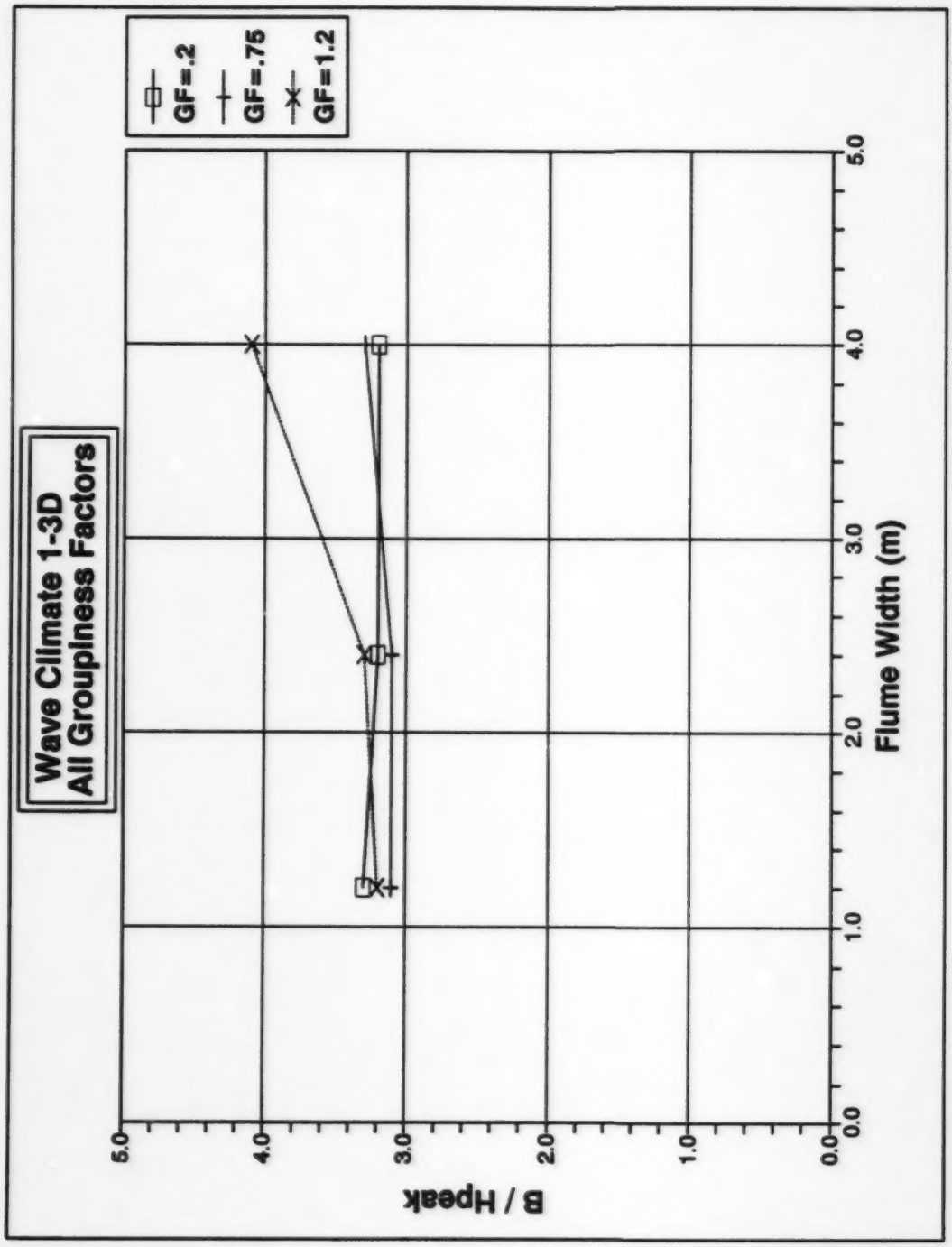
Wave Climate 1-3D
All Groupiness Factors
GF=.2
GF=.75
GF=1.2
B / Hpeak
Flume Width (m)
0.0
1.0
2.0
3.0
4.0
5.0

FIGURE 4.26

results compared with data acquired in tests 1-12 of the three-dimensional tests. Only structures considered stable were utilized in the analysis. The data are sorted according to the wave climate tested. Values of B and A acquired in the tests have been normalized so that the results can be compared directly.

Table 4.9

Comparison of Measured and Predicted Berm Width and Volume of Stones

Wave Climate	Flume Width	$B_{measured}$ (cm)	$B_{predicted}$ (cm)	$A_{measured}$ (cm^2)	$A_{predicted}$ (cm^2)
1-3D	1	44.7	58	3000	2900
	2.4	45.4	58	3100	2900
	4.0	47.4	58	3200	2900
2-3D	1	53.7	83	3400	3500
	2.4	54.3	83	3400	3500
	4.0	60.3	83	3700	3500
3-3D	1	57.4	120	3600	4100
	2.4	56.3	120	3500	4100
	4.0	60.3	120	3700	4100
4-3D	1	65	157	3900	4800
	2.4	64	157	3900	4800
	4.0	70.5	157	4100	4800
1-3D GF = .2	1	46	58	3100	2900
	2.4	45.5	58	3100	2900
	4.0	46.3	58	3000	2900
1-3D GF = .75	1	43.4	58	3000	2900
	2.4	43.5	58	3000	2900
	4.0	46.3	58	3100	2900
1-3D GF = 1.2	1	44.4	58	3000	2900
	2.4	46.6	58	3100	2900
	4.0	56.8	58	3500	2900

Notes: B predicted using equation [6.3]
A predicted using equation [6.2]

5.0 DATA ANALYSIS

5.1 TWO DIMENSIONAL TESTS

The inter-relationship between various parameters that affect the reshaping process were shown in section 3. The presentation of data in the plots provides a basis for the design of dynamically stable breakwaters. It is considered that the plots will give the designer a visual impression of the scatter in the results, so that the designer may decide what confidence can be placed on the relationships. Obviously for data exhibiting a large degree of scatter, more caution should be attached to the use of the data points and a conservative value should perhaps be chosen.

Presentation of a design formula may often cause the designer to lose sight of the physical significance, origin and the circumstances under which the data were obtained. The designer will often be tempted to apply the equation to any circumstances without noting the limitations and may get erroneous results. It is for this purpose that limitations of the equations derived using multi-regresson analysis will be laid out.

5.1.1 Regression Analysis

A regression Analysis was carried out using the software SYSTAT, by Wilkinson (1989).

Linear regression was attempted in as many cases as possible. For those equations that were not linear but intrinsically linear, transformation into a linear equation and subsequent linear regression was attempted.

In carrying out the regression analyses, use was made of the dimensionless parameters and the relationship between them, discussed in Section 3. For example, the relationship between L/D_{50} and $H_s/((S_r-1)D_{50})$ keeping D_{85}/D_{15} constant is shown in Figure 5.1. Although preliminary analyses showed that variations in T_p and GF did not affect L/D_{50}, all values of L/D_{50} for different T_p and GF were used in order to obtain as large a data set as possible. Different fits were tried for all four gradations including straight line fit, exponential curve fit and power curve fit. The curve that consistently fit the four gradations was chosen as the form for use in the multi-regression analysis. For example, in the case of the relationship between L/D_{50} and $H_s/((S_r-1)D_{50})$, a power curve was found to give the best fit overall based on minimization of errors.

Similarly, the form of relationships between L/D_{50}, A/D_{50}^2 and B/D_{50} and other independent parameters were also derived.

All relationships were carefully tested and then utilized to arrive at a best-fit equation using minimization techniques.

It was found that the dimensionless toe width after the attack of 3000 waves, L/D_{50}, was dependent on the stability number, the gradation of stones (characterized by the ratio of D_{85}/D_{15}), and the duration of storm (characterized by the relative number of waves, N_R).

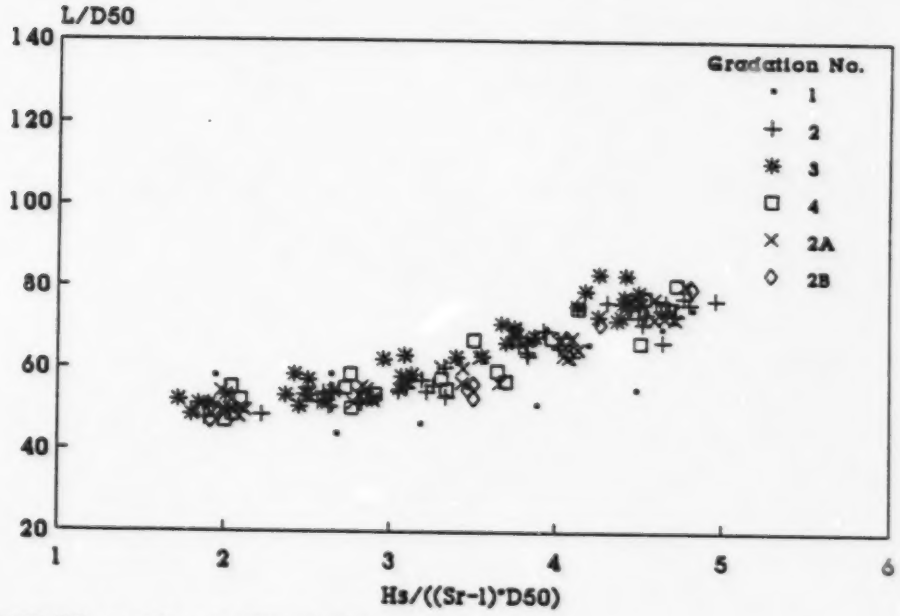

FIGURE 5.1 L/D50 vs Hs/((Sr-1)*D50)

From figure 5.1, it can be seen that L/D_{50} has a non-linear relationship with $H_s/((S_r-1)D_{50})$. Various fits including the straight line fit, the exponential fit and the power curve fit were tried to establish the relationship between the two expressions. In general it was found that a relationship of the form

$$\frac{L}{D_{50}} = a_1\left[\frac{H_s}{(S_r-1)D_{50}}\right]^{a_2} \qquad [5.1]$$

fits the data best, where a_1 and a_2 are regression coefficients to be determined.

This relationship is transformable into a linear form by taking the logarithm on both sides of equation 5.1 so that

$$ln\ \frac{L}{D_{50}} = ln\ a_1 + a_2\ ln\ \frac{H_s}{(S_r-1)D_{50}} \qquad [5.2]$$

Thus a plot of $ln(L/D_{50})$ against $lnH_s/(S_r-1)D_{50})$ gives a linear relationship with a_2 as the slope of the straight line and $ln(a_1)$, as the y-intercept.

The relationship between L/D_{50} and D_{85}/D_{15} was found to fit a second degree polynomial best, i.e.,

$$\frac{L}{D_{50}} = a_6 + a_7\frac{D_{85}}{D_{15}} + a_8\left(\frac{D_{85}}{D_{15}}\right)^2 \qquad [5.3]$$

where a_6, a_7, and a_8 are regression coefficients to be determined.

The relationship between $(L/D_{50})_R$ and N_R was also found to fit a power curve best (see figure 3.80). The exponential curve fit is much worse; and a semi-logarithmic plot as shown in figure 5.2 fails to produce a straight line; the form of the best fit curve is

$$(\frac{L}{D_{50}})_R = a_9 N_R^{a_{10}} \qquad [5.4]$$

where a_9 and a_{10} are regression coefficients, and

$$(\frac{L}{D_{50}})_R = \frac{(\frac{L}{D_{50}})_N}{\frac{L}{D_{50}}} \qquad [5.5]$$

$(L/D_{50})_R$ is the relative dimensionless toe width and $(L/D_{50})_N$ is the dimensionless toe width formed after N waves attack the structure.

The relationship in equation 5.5 is transformable to a linear form by taking the logarithm of both sides so that

$$ln(\frac{L}{D_{50}})_R = ln\ a_9 + a_{10}\ ln\ N_R \qquad [5.6]$$

Thus a plot of $ln(L/D_{50})_R$ against $ln(N_R)$ gives a linear relationship with a_{10} as the slope of the straight line and $ln(a_9)$ as the y-intercept.

To find a relationship between the dependent parameter $(L/D_{50})_N$ and the independent parameters $H_s/((S_r-1)D_{50})$, D_{85}/D_{15} and N_R, firstly a linear multiple regression was attempted. Equations 5.2, 5.3 and 5.7 are rewritten in a linear form as follows,

$$ln\frac{L}{D_{50}} = a_{11} + a_{12}\ ln\frac{H_s}{(S_r-1)D_{50}} \qquad [5.7]$$

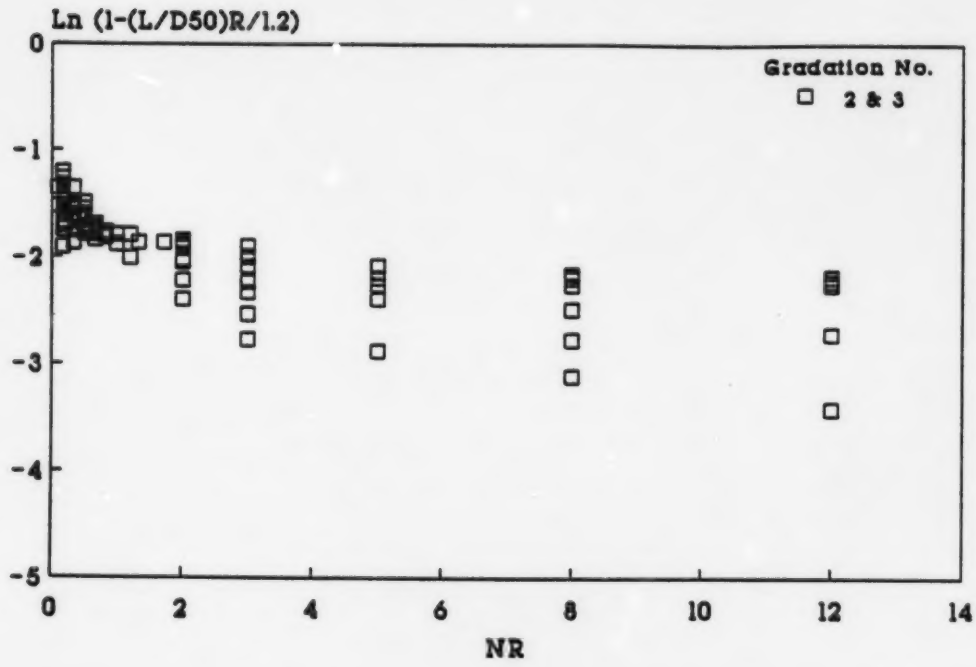

Figure 5.2 Relative toe width versus relative number of waves (semi-logarithmic plot)

$$\frac{L}{D_{50}} = a_{13} + a_{14}\frac{D_{85}}{D_{15}} + a_{15}\left(\frac{D_{85}}{D_{15}}\right)^2 \qquad [5.8]$$

$$ln\left(\frac{L}{D_{50}}\right)_R = a_{16} + a_{17}\, ln\, N_R \qquad [5.9]$$

where a $_{11}$ to a_{17} are regression coefficients to be determined. It can be seen that since the dependent parameters in equations 5.7, 5.8 and 5.9 are different, it is not possible to obtain a linear equation (i.e. linear in the regression coefficients) of the form

$$ln\left(\frac{L}{D_{50}}\right)_N = a_{18} + a_{19}\, ln\frac{H_s}{(S_r-1)D_{50}} + a_{20} ln N_R + a_{21}\frac{D_{85}}{D_{15}} + a_{22}\left(\frac{D_{85}}{D_{15}}\right)^2 \qquad [5.10]$$

or of the form

$$\left(\frac{L}{D_{50}}\right)_N = a_{23} + a_{24}\, ln\frac{H_s}{(S_r-1)D_{50}} + a_{25} ln\, N_R + a_{26}\frac{D_{85}}{D_{15}} + a_{27}\left(\frac{D_{85}}{D_{15}}\right)^2 \qquad [5.11]$$

where a_{18} to a_{27} are regression coefficients. Therefore a non-linear regression was undertaken firstly by combining equations 5.7 and 5.8. The form on non-linear regressions is

$$\frac{L}{D_{50}} = a_{28} + a_{29}\left[\frac{H_s}{(S_r-1)D_{50}}\right]^{a_{30}} + a_{31}\frac{D_{85}}{D_{15}} + a_{32}\left(\frac{D_{85}}{D_{15}}\right)^2 \qquad [5.12]$$

where a_{28} to a_{32} are regression coefficients to be determined.

By regression, the coefficients were found to be

$$a_{28} = 26$$
$$a_{29} = 1.2$$
$$a_{30} = 2.2$$
$$a_{31} = 11$$
$$a_{32} = -1.5$$

therefore, the model is

$$\frac{L}{D_{50}} = 26 + 1.2\left[\frac{H_s}{(S_r-1)D_{50}}\right]^{2.2} + 11\frac{D_{85}}{D_{15}} - 1.5\left(\frac{D_{85}}{D_{15}}\right)^2 \qquad [5.13]$$

In the above model the value of L/D_{50} is given only for a structure subjected to the attack of 3000 waves. To obtain the corresponding value for any number of waves attack, the relative dimensionless toe width after reshaping, $(L/D_{50})_R$ was regressed against the relative number of waves, N_R, using equation 5.9 and performing a linear regression of $1n(L/D_{50})_R$ against $1n(N_R)$ gives,

$$1n\left(\frac{L}{D_{50}}\right)_R = 0.042\ 1n\ N_R \qquad [5.14]$$

The adjusted square multiple R for this model is 0.75, meaning that 75% of the results are explained by this relationship. Combining equations 5.5 and 5.14, the dimensionless toe width after reshaping by N waves is given by

$$\left(\frac{L}{D_{50}}\right)_N = \frac{L}{D_{50}}\ N_R^{0.042} \qquad [5.15]$$

where L/D_{50} is given in equation 5.13

or

$$(\frac{L}{D_{50}})_N = [26 + 1.2(\frac{H_s}{(S_r-1)D_{50}})^{2.2} + 11\frac{D_{85}}{D_{15}} - 1.5(\frac{D_{85}}{D_{15}})^2]\ N_R^{0.042} \qquad [5.16]$$

The above equations were plotted with the data points obtained from this research and are shown in figure 5.3 and 5.4. Figure 5.3 shows the data points, as well as the regression curves, for all four gradations after the attack of 3000 waves. It can be seen that gradation 1, having the largest amount of voids, provided the most resistance. With the decrease in voids, gradations 2 and 3 were more easily reshaped, and the toe moved further offshore, gradation 3 being more easily reshaped than gradation 2. Gradation 4, however, is more stable than gradations 2 and 3 and does not move as far offshore, indicating that the presence of larger size stones exerting their influence in stabilizing the breakwater and retarding the reshaping process.

Figure 5.4 shows the relative dimensionless toe width plotted against the relative number of waves and in general a good fit was obtained.

5.1.1.2 Volume of stones

It was found that the dimensionless volume of stones under reshaping was dependent in the stability number and the gradation of stones. Following the same techniques discussed above a multiple non-linear regression based on minimization techniques was performed and resulted in the following expressions. The model describing the volume of reshaping A/D_{50}^2 as a function of $H_s/((S_r-1)D_{50})$, D_{85}/D_{15}, and N_R is

$$\frac{A}{D_{50}^2} = 148 + 30\left[\frac{H_s}{(S_r-1)D_{50}}\right]^{1.9} + 194\frac{D_{85}}{D_{15}} - 27\left(\frac{D_{85}}{D_{15}}\right)^2 \qquad [5.17]$$

Figure 5.5 shows the plot of dimensionless area under reshaping for gradations 1, 2, 3, and 4 after the attack of 3000 waves. It can be seen that the results for gradation 2 are almost coincident with those of gradation 4. Other than that, there is a clear trend that A is smaller with a more porous breakwater. This trend is, in general, similar to that observed for the dimensionless toe width, L/D_{50}.

In the above model, the value of A/D_{50}^2 was given only for structures subjected to the attack of 3,000 waves. To obtain the corresponding value for any number of waves $(A/D_{50}^2)_R$ was regressed against N_R giving

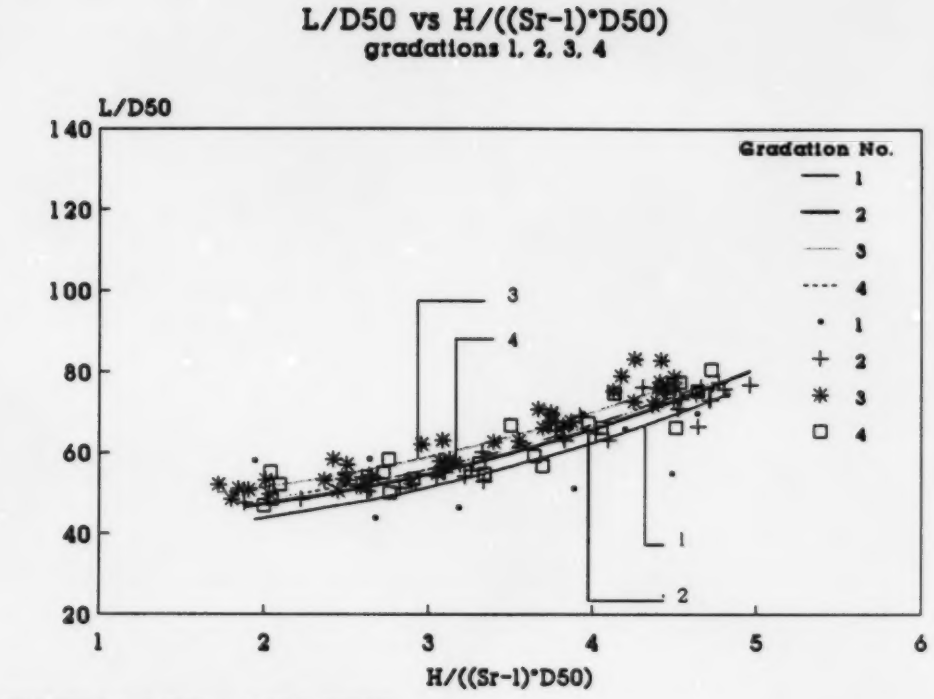

FIGURE 5.3 L/D50 vs H/((Sr-1)*D50)

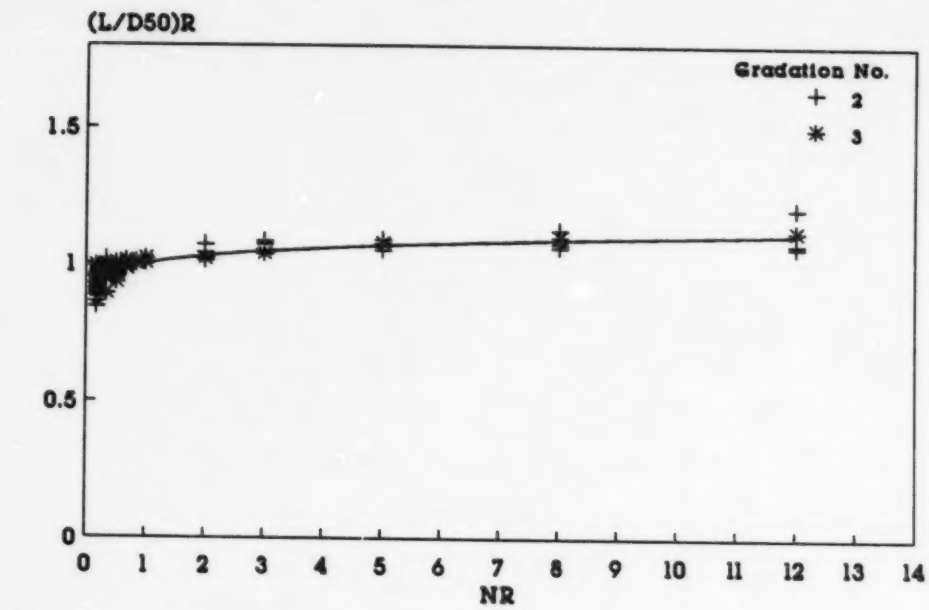

FIGURE 5.4 (L/D50)R vs NR

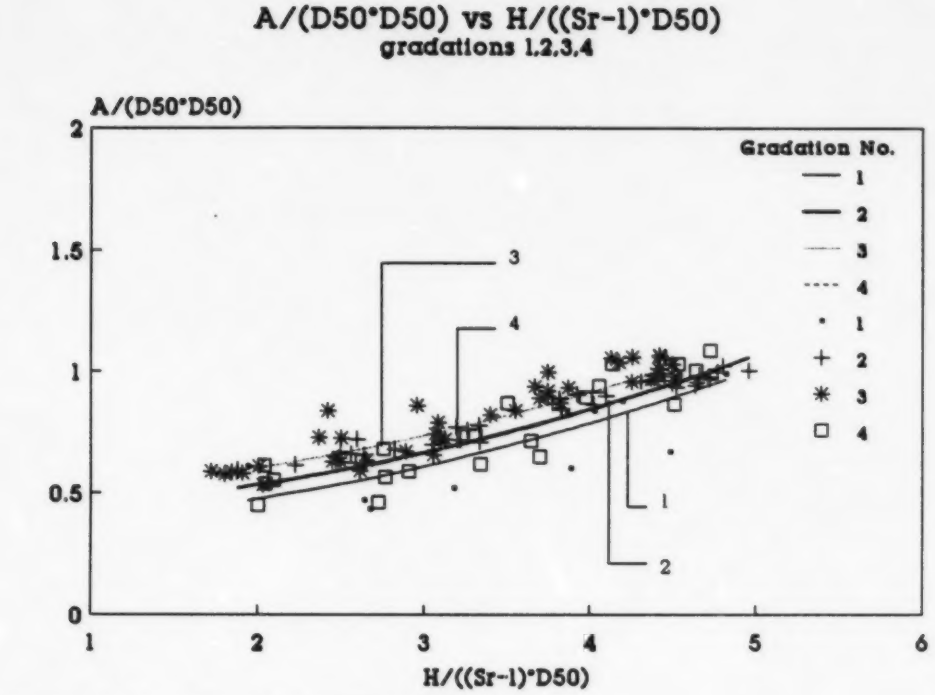

FIGURE 5.5 A/(D50*D50) vs H/((Sr-1)*D50)

$$(\frac{A}{D_{50}^2})_R = N_R^{0.043} \qquad [5.18]$$

with an adjusted square multiple R value of 0.76.

Figure 5.6 shows the regression curve and the data points for the relative area of reshaping to the relative number of waves. In general, the additional increase after 3000 waves is small.

The dimensionless volume of stones required for reshaping after N waves is give by

$$(\frac{A}{D_{50}^2})_N = [148 + 30(\frac{H}{(S_r-1)D_{50}})^{1.9} + 194\frac{D_{85}}{D_{15}} - 27(\frac{D_{85}}{D_{15}})^2]\ N_R^{0.043} \qquad [5.19]$$

5.1.1.3 Width of berm eroded

It was found that the dimensionless width of berm eroded, was dependent on the stability number, the gradation of stones, the percentage of rounded stones in the armour and the number of waves attacking the structure. Following procedures outlined earlier it was found that the model to predict the value of B/D_{50} as a function of $H_s/((S_r-1)D_{50})$, D_{85}/D_{15} and P_R is

$$\frac{B}{D_{50}} = [-10 + 0.51[\frac{H_s}{(S_r-1)D_{50}}]^{2.5} + 7.5\frac{D_{85}}{D_{15}} - 1.1(\frac{D_{85}}{D_{15}})^2] + 6.1P_R \qquad [5.20]$$

Figure 5.7 shows a comparison of the model with measured data for all four gradations plotted on the same graph. Figure 5.7 shows that porous breakwaters are in general more stable. The exception to this rule occurs when there is a substantial amount of large stones present which exert their influence and reverse the trend.

Figure 5.8 shows the data points for 3 gradations with different percentage of rounded stones. The angular stones (gradation 2A) were found to be more stable than gradation 2B (15% rounded stones) which were in turn more stable than gradation 2 (30% rounded stones).

In the above model the value of the dimensionless width of berm eroded was given for structures subjected to the attack of 3000 waves. To obtain the corresponding value for any number of waves attacking the structure, the relative dimensionless width of berm eroded $(B/D_{50})_R$ was regressed against N_R giving:

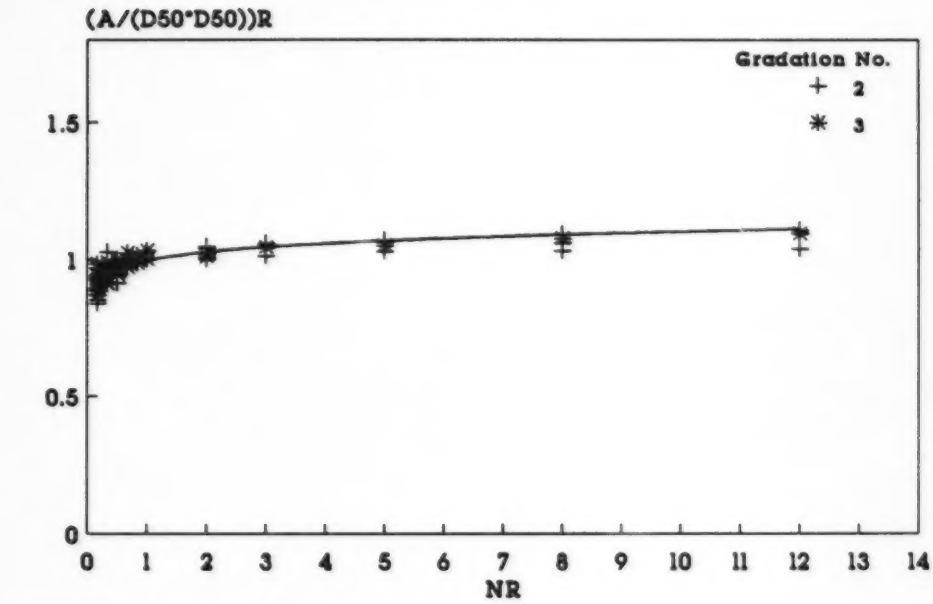

FIGURE 5.6 (A/(D50*D50))R vs NR

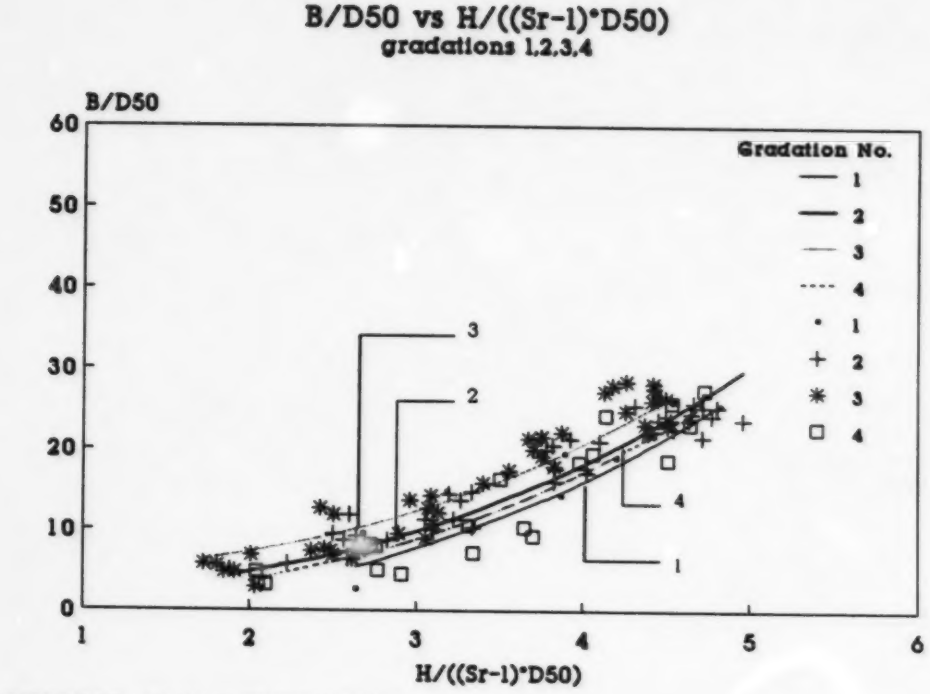

FIGURE 5.7 B/D50 vs H/((Sr-1)*D50)

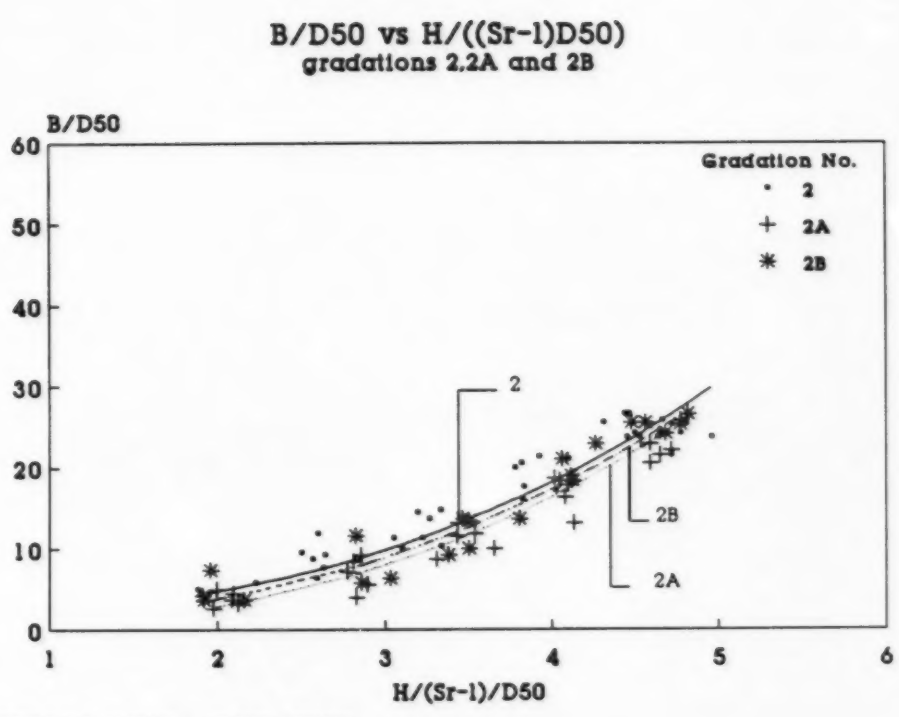

FIGURE 5.8 B/D50 vs H/((Sr-1)D50)

$$(\frac{B}{D_{50}})_R = 1 + 1n\ N_R^{0.11} \qquad [5.21]$$

which was found to fit the relationship best with an adjusted square multiple R value of 0.70. It should be noted that this relationship is different from those for the relative toe width and relative area under reshaping. If the same power curve fit is attempted, an adjusted square multiple R value of only 0.61 is obtained, indicating that the power fit is less satisfactory.

A plot of the fitted curve (equation 5.21) and the data points is shown in figure 5.9. The width of berm eroded by N waves is given by

$$(\frac{B}{D_{50}})_N = [-10 + 0.51(\frac{H}{(S_r-1)D_{50}})^{2.5} + 7.5\frac{D_{85}}{D_{15}} - 1.1(\frac{D_{85}}{D_{15}})^2 + 6.1P_B].[1 + 1n\ N_R^{0.11}] \qquad [5.22]$$

5.1.2 Sensitivity of the Model

A sensitivity analysis of equation 5.16 was carried out for gradation 4, (D_{85}/D_{15} = 5.4), under the attack of 1500 waves and for stability numbers from 2 to 5.

The effect of +10% variation of each regressor in equation 5.16: 26 (par1), 1.2 (par2), 2.2 (par3), 11(par4), 1.5(par5) and 0.042(par6) on L/D_{50} is plotted on figure 5.10. It can be seen that the exponent to the stability number (par3) is most sensitive; small variations of it produced relatively large variations in L/D_{50}, especially at high stability numbers.

A sensitivity analysis of equation 5.19 was carried out for gradation4, (D_{85}/D_{15} = 5.4), under the attack of 1500 waves and for stability numbers from 2 to 5.

The effect of +10% variation of each of the regressors: 148(par1), 30(par2), 1.9(par3), 194(par4) and 27(par5) and 0.043(par6) on A/D_{50}^2 is plotted on figure 5.11. It can be seen that the exponent to the stability number (par3) is the most sensitive; small variations of it produced relatively large variations in A/D_{50}^2, especially at high stability numbers.

A sensitivity analysis of equation 5.22 was carried out for gradation 4, (D_{85}/D_{15} = 5.4), containing 30% rounded stones, under the attack of 1500 waves and for stability numbers from 2 to 5.

The effect of +10% variation of each of the regressors: -10(par1), 0.51(par2), 2.5(par3,

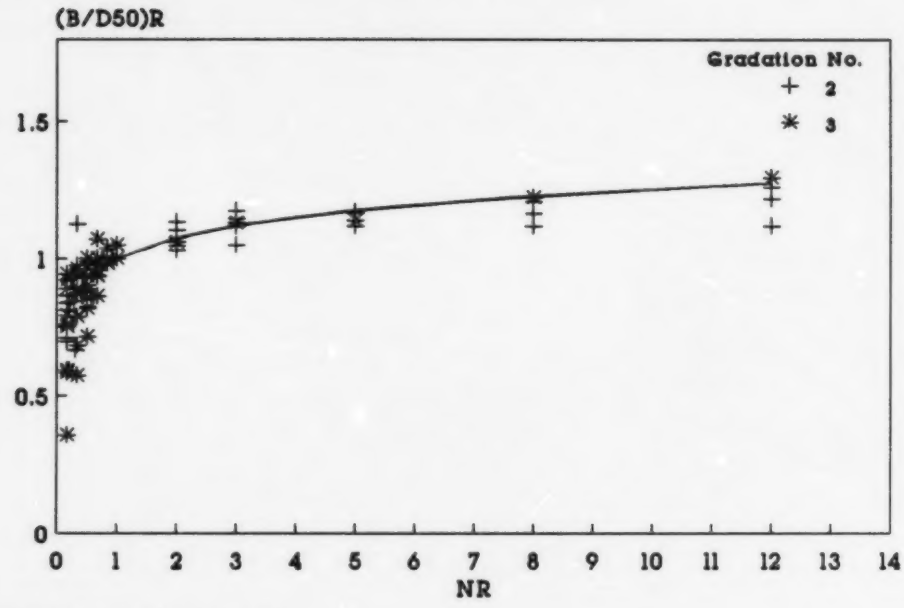

FIGURE 5.9 (B/D50)R vs NR

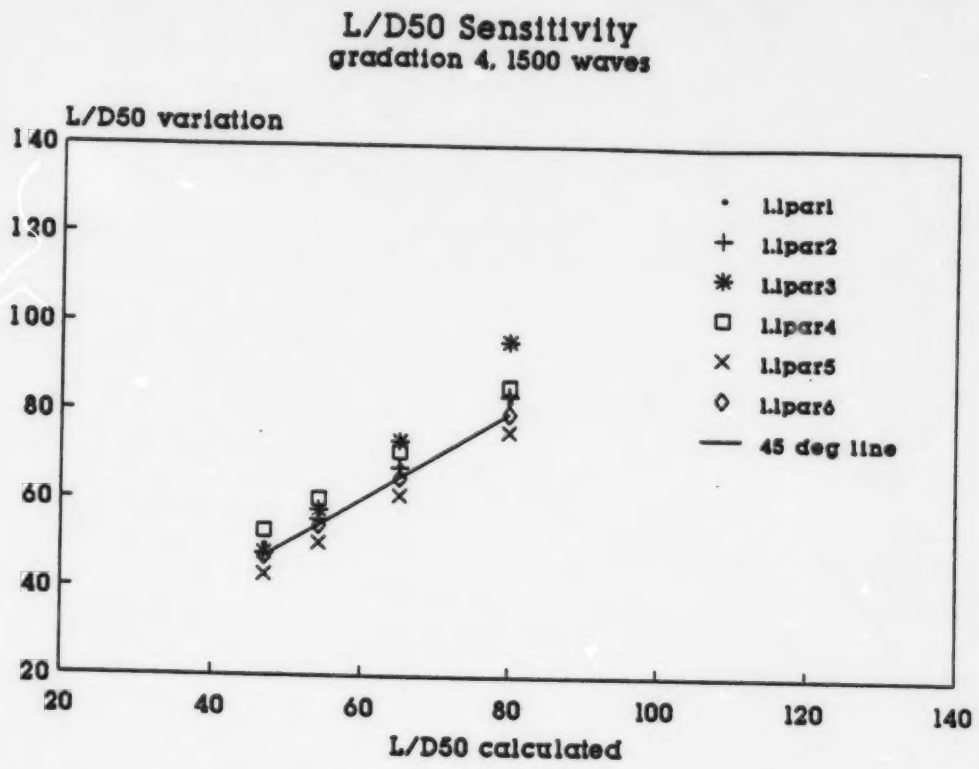

Figure 5.10 Sensitivity of dimensionless toe width to variations in regressors

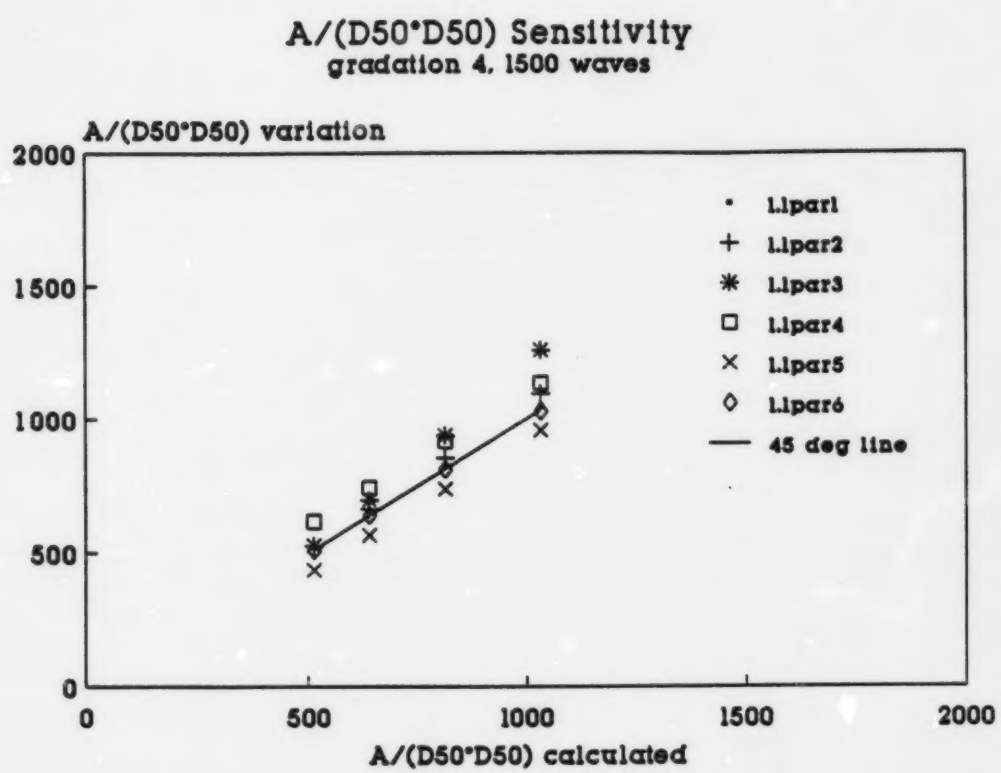

Figure 5.11 Sensitivity of dimensionless reshaping area to variations in regressors

7.5(par4), -1.1(par5) and 6.1(par6) on B/D_{50} is plotted on figure 5.12. It can be seen that the exponent to the stability number (par3) is the most sensitive, small variations of it produces relatively large variations in B/D_{50}, especially at high stability number. The exponent of N_R was not studies as the sensitivity of it is known to be low from previous knowledge with L/D_{50} and A/D_{50}^2.

Overall, it was observed that the exponent to the stability number have the largest influence on the reshaping process. All other effects are secondary.

5.1.3 Comparison with Model Results

The model was compared with the results of a hydraulic model study for a breakwater at Kelflavik, Iceland, (Baird and Woodrow, 1987)), which has the following parameters:

P_R	=	0.1(assumed)
D_{50}	=	1.0m
D_{85}/D_{15}	=	1.9(assumed)
N_R	=	1(3000 waves)
H_S	=	5.8m
S_r	=	2.65

Based on hydraulic model studies, a berm breakwater was designed having B = 14m, L = 60m and A = $730M^2/m$.

Based on the predictive model and using the above parameters, the calculated values of the dynamically stable breakwater should have the following configuration:

B	=	12m
L	=	60m
A	=	$750m^2/m$

These values compares relatively well with the results of the hydraulic model investigation. In fact the berm designed in the model studies had considerable "reserve" stability, indicating that a berm width of less than 14 would have remained stable.

5.1.4 Comparison with Prototype Results

A comparison was made between the parameters calculated using the present model and the profiles measured on a dynamically stable breakwater built at North Bay, Ontario, Canada, which was surveyed after being in service for 5 years (Baird and Associates (1989)). The breakwater consisted of a trapezoidal cross-section without a core. The diameter of stone, used varied from approximately 0.1m to 0.45 m. A wave hindcast was carried out and indicated the highest significant wave that occurred since the breakwater was built was about 1.38m with spectral peak period of 4 seconds and lasted about 1 hour. Surveys of the reshaped profile were carried out in June, 1985 and October, 1988. The latter survey showed more reshaping. The profiles measured in this latter survey were used as a basic for comparison with present predictive model.

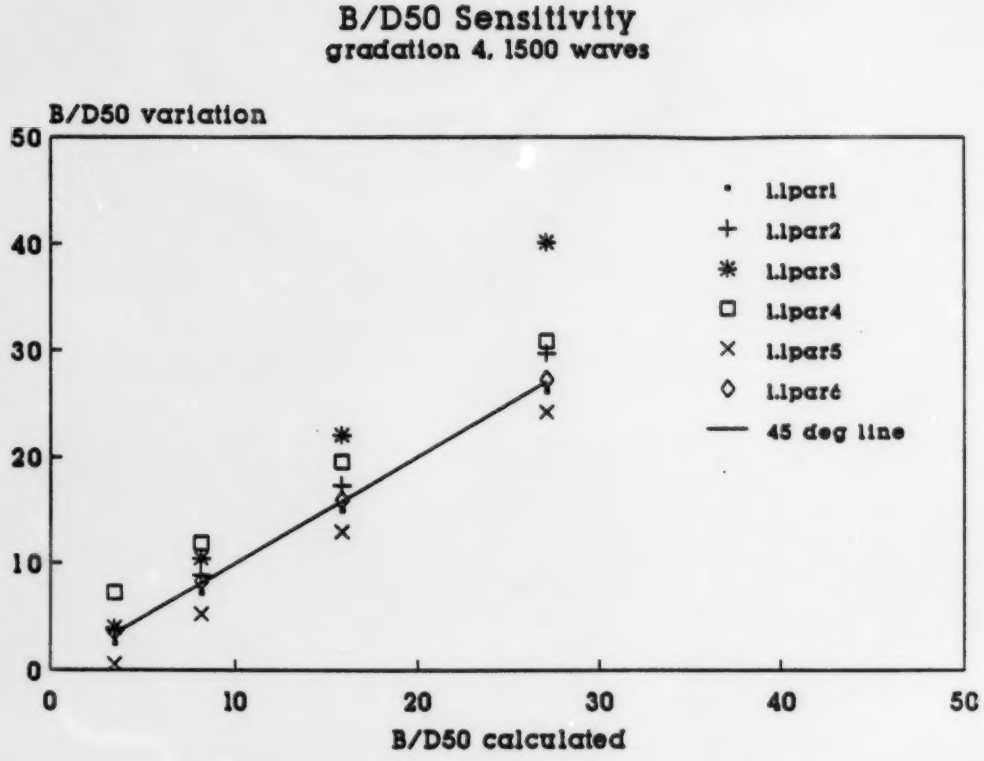

Figure 5.12 Sensitivity of dimensionless width of berm eroded to variations in regressors

The following parameters were used to characterize the breakwater for use in the predictive model:

P_R	=	30%
N_R	=	0.3(900 waves)
D_{50}	=	0.275m
D_{85}/D_{15}	=	3(allowing for contamination by fines)
H_s	=	1.38m

The results are tabulated in Table 5.1. It can be seen that this model under predicts L/D_{50} by approximately 10%, B/D_{50} by about 30%, but over predicts A/D_{50}^2 by about 10%. However it should be borne in mind that there is suspicion that the breakwater at North Bay was contaminated with fines (Baird, (1989)) and the attacking waves were found to approach the breakwater at an oblique angle and thus the deviation between prototype and model may be considered reasonable.

Table 1

Comparison of Predicted Results with Prototype Results
at North Bay, Ontario, Canada

	Predicted by Present Model	North Bay Station 0+80	North Bay Station 1+00	North Bay Station 1+20	North Bay Station 1+40	North Bay Average
L/D_{50}	56	63	64	60	56	61
A/D_{50}^2	700	640	650	580	600	620
B/D_{50}	11	17	18	15	11	15

6.0 CONCLUSIONS

6.1 TWO DIMENSIONAL TESTS

1. The series of tests carried out indicated that wave height is the most important factor governing the reshaping of the dynamically stable breakwaters.

2. The volume of stones required for reshaping was found to be dependent on the wave height, the gradation of stones and the number of waves attacking the structure.

3. The toe width extending offshore was found to be dependent on the wave height, the gradation of stones, and the number of waves attacking the structure.

4. The width of berm eroded was found to be dependent on the wave height, the gradation of stones, the number of waves attacking the structure and the percentage of rounded stones.

5. The effect of groupiness factor, spectral peak wave period and average wave period was found to have little or no influence on either A, B or L.

6. The influence of grouped waves appeared to be important only during or shortly after the stage of incipient motion of the armour units, which originally are in static equilibrium. Once motion is initiated, the armour units start to move "en masse", and wave groupiness is no longer of primary importance. The overall wave energy in the sea state, characterized by wave height dominanes.

7. Gradations 2 and 3, the two intermediate gradations were found to give more consistent results than the narrowest and the widest gradations (gradations 1 and 4).

8. It was found that D_{50} and a parameter representing the spread of the armour stone (for example, D_{85}/D_{15}) were needed to account for the influence of the armour stone gradation of reshaping of dynamically stable breakwaters.

9. The toe width, volume of stones required for reshaping and width of berm eroded after N waves attacking the structure are given by the following equations:

$$\left(\frac{L}{D_{50}}\right)_N = \left[26 + 1.2\left(\frac{H_s}{(S_r - 1)D_{50}}\right)^{2.2} + 11\frac{D_{85}}{D_{15}} - 1.5\left(\frac{D_{85}}{D_{15}}\right)^2\right] N_R^{0.042} \quad [6.1]$$

$$\left(\frac{A}{D_{50}^2}\right)_N = \left[148 + 30\left(\frac{H_s}{(S_r - 1)D_{50}}\right)^{1.9} + 194\frac{D_{85}}{D_{15}} - 27\left(\frac{D_{85}}{D_{15}}\right)^2\right] N_R^{0.043} \quad [6.2]$$

$$\left(\frac{B}{D_{50}}\right)_N = \left[-10 + 0.51\left(\frac{H_s}{(S_r - 1)D_{50}}\right)^{2.5} + 7.5\frac{D_{85}}{D_{15}} - 1.1\left(\frac{D_{85}}{D_{15}}\right)^2 + 6.1P_B\right].[1 + 1n \; N_R^{0.11}] \quad [6.3]$$

6.2 THREE DIMENSIONAL TESTS

(To be completed).

7. REFERENCES

1. Ahrens, J.P., "Large wave tank tests of riprap stability". CERC Tech. Memorandum No. 51, May 1975.

2. Ahrens, J.P. "Reef type breakwaters", 20th Int. Conf. on Coastal Eng., Houston 1984, pp. 2648-2662.

3. Baird, W.F. and Hall, K.R. "The design of armour systems for rubblemound breakwaters", Specialty Conf. on Rubblemound Breakwaters, I.C.E., London 1983.

4. Baird, W.F. and Hall, K.R. "The design of breakwaters using quarried stone, 19th Int. Conf. on Coastal Engineering, Houston 1984, pp. 1024-1031.

5. Burcharth, H.F., and Frigaard, P., "Reshaping Breakwaters, On the Stability of Roundheads and Truck Erosion in Oblique Waves", Proceedings of workshop on Unconventional Rubble-mound Breakwaters, Ottawa 1987 pp. 55-72.

6. Burcarth, H.F. and Thompson, A.C. "Stability of armour units in oscillatory flow", Coastal Structures 83, Washington, March 1983, pp 71-83.

7. Foster, D.N. "Investigation of quarry run breakwater, Little Grassy, King Island", Univ. of New South Wales, Water Research Lab. Tech. Rept. 69/20, 1969 (17p).

8. Graveson, H., Jensen, O.J. and Sorensen, T. "Stability of rubblemound breakwaters II. Danish Hydraulic Inst., 1980.

9. Gourlay, M.R. "Beaches: profiles, processes and permeability", Dept. of Civil Engineering, Univ. of Queensland, Australia, 1980.

10. Hall, K.R., "Experimental and Historical Verification of the performance of naturally armouring breakwaters", Proceedings of Workshop on Unconventional rubblemound breakwaters, Ottawa, 1987 pp. 104-137.

11. Hall, K.R. and Rauw, C.I. and Baird, W.F. "Development of a wave protection scheme for a proposed offshore runway extension", Coastal Structures 83, Washington, 1983, pp 157-170.

12. Kemp, P.H. "The relationship between wave action and beach profile characteristics", Proc. 7th Int. Conf. on Coastal Engineering, The Hague, 1960, pp 262-278.

13. Kogami, Y. "Researches on stability of rubblemound breakwaters." Coastal Engineering in Japan, Vol 21, December 1978, pp 75 - 93.

14. Moutzoris, C. "A profile of a sloping breakwater based on recent results concerning wave propagation and breaking", 7th Int. Harbour Congress, Antwerp, 1978, pp 2.04/1 - 2.04/7.

15. Naheer, E., and Buslov, V. "On rubblemound breakwaters of composite slope", Coastal Engineering, Vol 7, 1983, pp. 253-270.

16. Popov, I.J. "Experimental research on formation by waves of stable profiles of upstream faces of earth dams and reservoir shores", 7th Int. Conf. on Coastal Engineering, The Hague, 1960. pp 282-293.

17. Priest, M.S., Pugh, J.W. and Singh, R. "Seaward profile for rubblemound breakwaters", 9th Int. Conf. on Coastal Engineering, Lisbon, 1964. pp 553-559.

18. Rennie, J. "An historical, practical and theoretical account of the breakwater of Plymouth Sound". Weale, London, 1948.

19. van Hijum, E. "Equilibrium profiles and longshore transport of coarse material under oblique wave attack", Proceedings 15th International Conference on Coastal Engineering, Honolulu, Hawaii, 1976, pp. 1258-1276.

20. van Hijum, E., and Pilarczyk, K.W. "Gravel Beaches, Equilibrium profile and longshore transport of coarse material under regular and irregular wave attack", publication no. 274, Delft Hydraulics Laboratory, Delft, 1982.

21. Watts, G.M. "Laboratory study of effects of varying wave periods on beach profiles," Technical Memorandum No. 53, US Army Waterways Experiment Station, September 1964.